Autogenous Healing of Lime-Soil Mixtures

M. R. THOMPSON and B. J. DEMPSEY, University of Illinois

Autogenous healing characteristics of 2 lime-reactive soils were evaluated. Freeze-thaw testing with intermittent curing periods and initial "stress flawing" with intermittent curing were used to study the magnitude and significance of autogenous healing effects in lime-soil mixtures. Data from the study indicated that autogenous healing (strength gain in a flawed material) does occur following stress flawing or cyclic freezing and thawing of lime-soil mixtures. In fact, the terminal strengths of cured mixtures sequentially subjected to cyclic freezing and thawing, additional curing, and additional freezing and thawing were greater than the original cured strengths.

This limited study of two lime-reactive soils indicated that autogenous healing does occur in lime-soil mixtures under favorable curing conditions. It would be expected, based on past laboratory and field experience, that the conclusion is generally applicable to most lime-soil mixtures that display a substantial initial strength increase. The residual strength philosophy for establishing quality requirements for lime-soil mixtures to be used for various purposes (modified subgrade, subbase-base) is a valid concept. With favorable curing conditions, deterioration produced by various factors during critical portions of the materials service life will likely be restored by the autogenous healing process.

•IN recent years lime has emerged as one of the most effective additives for improving the engineering properties of fine-grained soils. Numerous studies have shown that when lime is added to a fine-grained soil, plasticity is reduced, workability improved, shrinkage decreased, and with reactive soils, substantial strength increases are obtained and durable (freeze-thaw resistant) materials are produced.

When lime-stabilized soils are used as pavement layers, it is apparent that the structural integrity and load carrying capacity of the layer will be reduced as a result of cyclic freeze-thaw (Fig. 1), shrinkage and swell, weathering, fatigue, and stresses caused by overloading. However, if the stabilized soil has the ability to regain strength or heal with time, the distress produced will not be cumulative since autogenous healing during favorable curing conditions would serve to restore the stability of the material.

Autogenous healing studies of lime-fly ash aggregate mixtures by Callahan and Ahlberg (2) and published (3) and unpublished data for lime-soil mixtures have indicated that autogenous healing may occur with these types of mixtures.

The purpose of this study was to determine whether lime-soil mixtures, whose structural integrity had been reduced by initial overloading or cyclic freezing and thawing, would regain strength or "autogenously heal" with time.

PREPARATION OF TEST SPECIMENS

Materials

Two typical Illinois soils which react well with lime, Illinoian till (Sangamon County) and Bryce B, were used in the study. Properties of the soils and lime-soil mixtures

Paper sponsored by Committee on Lime and Lime-Fly Ash Stabilization and presented at the 48th Annual Meeting.

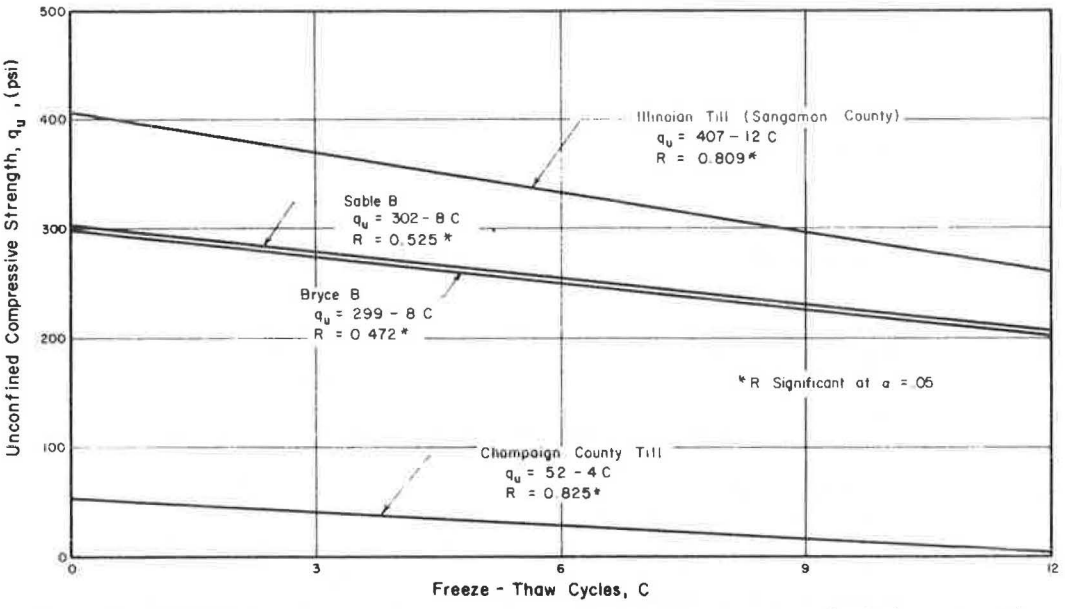

Figure 1. Influence of freeze-thaw cycles on unconfined compressive strength, 48-hr curing (1).

are given in Table 1. A hydrated high calcium lime containing 96 percent available $Ca(OH)_2$ with 95 percent passing the No. 325 sieve was used in all of the test mixtures.

Mixture Design and Preparation

Only that portion of the soil which passed the No. 4 sieve was used in the test mixtures. The amount of lime added to the soil consisted of the optimum percentage (dry weight basis) determined from previous strength studies by Thompson (4). The required amounts of soil and lime were initially dry mixed with a Lancaster mortar mixer to insure uniform distribution of the lime. After dry mixing, enough water was added to the mixture to bring it to optimum moisture content and mixing continued for approximately three minutes. After mixing, the lime-soil mixture was tightly covered to prevent moisture loss and allowed to mellow for one hour before compaction.

TABLE 1

NATURAL SOIL AND LIME-SOIL MIXTURE PROPERTIES

Soil	Bryce B	Illinoian Till
General description	Humic-gley (B horizon) derived from thin loess over Wisconsinan drift	Typical Illinoian till
Natural soil properties:		
AASHO classification	A-7-6(18)	A-6(6)
< 2-μ clay, percent	52	14
Liquid limit, percent	53.1	25.5
Plasticity index, percent	28.8	11.0
Carbonates	Noncalcareous	18.6 percent
pH	7.4	8.3
Predominant clay mineral	Illite	Illite-chlorite
Lime-soil mixture properties:		
Lime treatment, percent	5	3
AASHO T-99 compaction		
Optimum water content, percent	25.8	13.0
Maximum dry density, pcf	97.3	121
Compaction, blows/layer[a]	45-30-15[b]	60-35-10[b]

[a] Number of blows per layer used in compacting 2-in. diameter by 4-in. specimens.
[b] Top-middle-bottom.

Compaction Procedures

The specimens for the study were prepared by compacting the lime-soil mixtures into 2-in. diameter by 4-in. high circular steel molds in three equal layers. Each layer was scarified before placing the next layer to insure bonding. Compaction was accomplished by means of a hammer with a 2-in. diameter base which fits inside the mold. The compactive effort was applied by a 4-lb weight falling through a distance of 12 in. Pilot studies indicated that when equal compactive effort was applied to each layer, nonuniform densities would occur in the 2- by 4-in. specimens. The compactive effort was greatest on the top layer and least on the bottom layer. This method of compaction produced a uniform density throughout the specimen height. The average density was equivalent to that obtained from AASHO T-99. The water content and density of each specimen were carefully controlled in order to obtain nearly identical specimens.

Curing Procedure

Immediately after compaction, the lime-soil specimens were removed from the molds, marked, weighed, placed in plastic bags, and sealed. The plastic bags provided an effective means of maintaining the optimum moisture content in the compacted specimens during the curing period. The test specimens were placed on rigid boards after removal from the molds in order to prevent handling damage. An accelerated initial curing period of 48 hours at 120 F was used.

LABORATORY METHODS

Initial Overloading

The split tensile strength test as described by Thompson (5) was used for measuring the strength recovery in lime-soil mixtures with time. For each lime-soil mixture, 24 specimens were cured for 48 hours at 120 F in enclosed containers. After initial curing, 12 of the specimens were flawed by loading in unconfined compression (0.05 in./min). The load was reversed immediately after the ultimate load had been reached. Four flawed specimens and four unflawed specimens were tested immediately in split tension. The remaining specimens were placed in plastic bags and recured for periods of 28 or 56 days at 77 F. Four flawed and four unflawed specimens were tested in split tension after each of the recuring periods. Test results are given in Table 2.

Cyclic Freeze-Thaw

For each lime-soil mixture, 16 specimens were prepared and initially cured. Following curing all specimens were subjected to a 24-hr water soaking period. After the soak period, 4 specimens were tested in unconfined compression (0.05 in./min).

The remaining 12 specimens were subjected to 9 cycles of freezing and thawing. The freeze-thaw test was a directional freezing test (top-bottom) with a free water table at the bottom of the specimen. Each cycle consisted of 16 hr of freezing (22 F) followed

TABLE 2

INITIAL OVERLOADING STUDY DATA

Lime-Soil Mixtures	Initial Curing	Unconfined Compressive Strength[a] (psi)	Split Tensile Strength[b] (psi)		
			Additional Curing (days at 77 F)		
			0	28	56
Illinoian till, 3 percent lime	(1) 48 hr at 120 F	529	51	88	94
	(2) 48 hr at 120 F	Unflawed	69	106	118
Bryce B, 5 percent lime	(3) 48 hr at 120 F	240	32	36	41
	(4) 48 hr at 120 F	Unflawed	33	45	49

[a] Average of 12 specimens.

[b] Average of 4 specimens; split tensile strength is approximately 13 percent of the unconfined compressive strength (5).

TABLE 3

CYCLIC FREEZE-THAW DATA

Lime-Soil Mixture	Curing and Exposure Conditions	Unconfined Compressive Strength[a] (psi)
Illinoian till, 3 percent lime	(a) 48 hr at 120 F + 24-hr soak	341
	(b) a + 9 F-T cycles	280
	(c) b + 48 hr at 120 F	481
	(d) c + 9 F-T cycles	466
Bryce B, 5 percent lime	Same as (a) above	178
	Same as (b) above	137
	Same as (c) above	298
	Same as (d) above	196

[a]Average of 4 specimens.

by an 8-hr thawing period at ambient room temperature. Details of the procedure are given elswhere (1).

After 9 F-T cycles, 4 of the specimens (randomly selected) were tested in compression. The 8 remaining specimens were cured in sealed containers for an additional 48 hr at 120 F. Following the second curing period, which would represent a summer condition following a severe winter of several F-T cycles, 4 of the specimens were tested in unconfined compression and the remaining 4 were subjected to an additional 9 freeze-thaw cycles before tested in unconfined compression. Test results are given in Table 3.

ANALYSIS AND DISCUSSION OF AUTOGENOUS HEALING DATA

Initial Overloading

The effects of additional curing on the split-tensile strengths of the flawed and unflawed lime-soil mixtures are shown in Figures 2 and 3. For both the Illinoian till and Bryce B mixtures, the flawed and unflawed strengths increased with additional curing at 77 F.

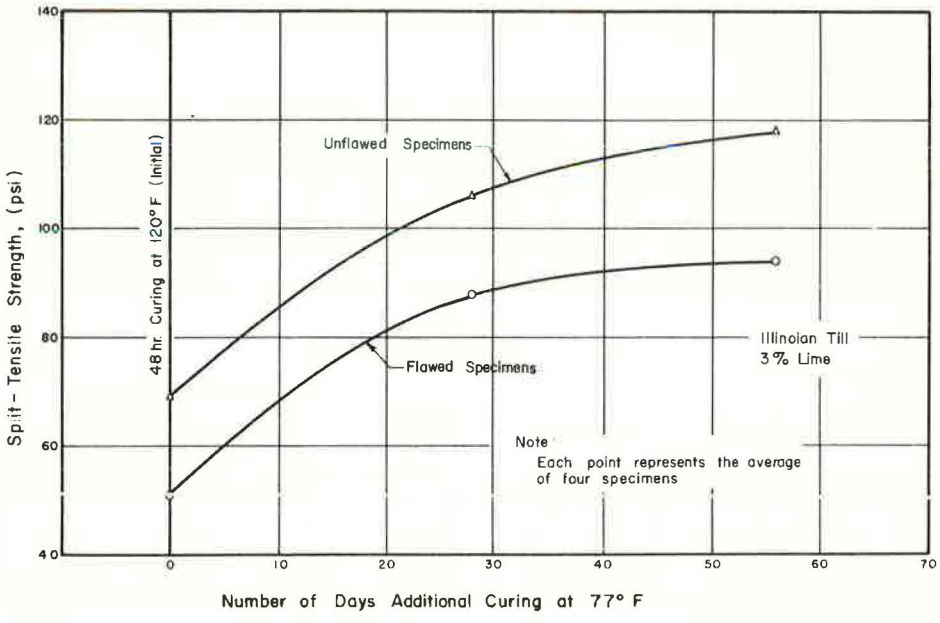

Figure 2. Influence of curing time on split-tensile strength increase.

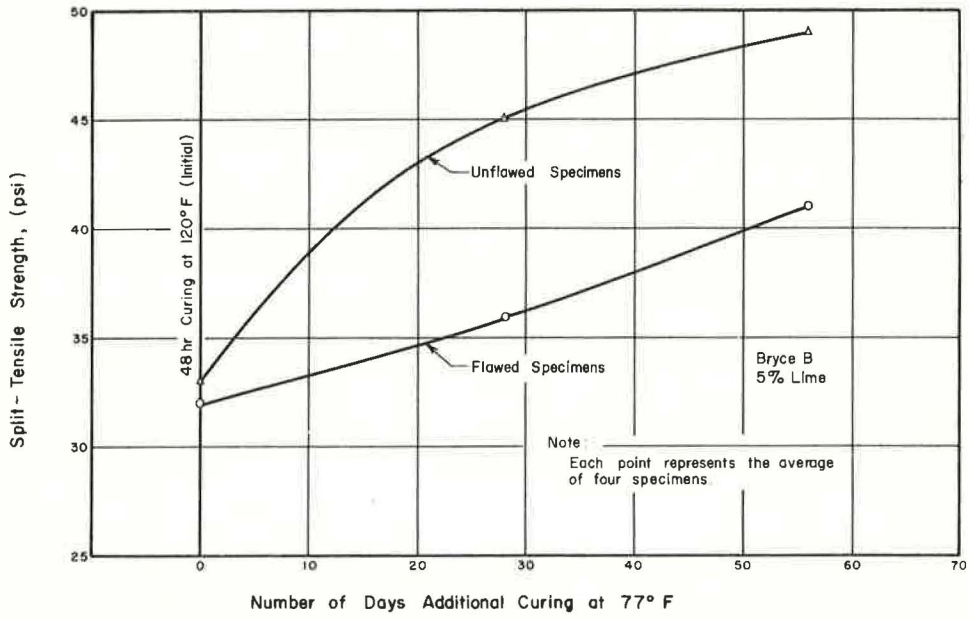

Figure 3. Influence of curing time on split-tensile strength increase.

The average strength differences between the Illinoian till flawed and unflawed specimens were 18 psi after initial curing and 24 psi after 56 days additional curing at 77 F.

The flawed strength of the Bryce B mixture did not vary greatly from the unflawed strength after initial curing, but a difference of 8 psi was noted after 56 days additional curing at 77 F. The flawed specimens gained 9 psi and the unflawed specimens gained 16 psi during the additional curing periods.

A randomized complete block factorial analysis of the data (Table 4) indicated that there was a significant influence ($\alpha = 0.05$) of curing time on strength. The interaction between flaw condition and curing time was not significant ($\alpha = 0.05$) indicating that strength increase with time occurred regardless of whether the specimens were initially flawed. This phenomenon, strength gain in flawed material, is more commonly known as "autogenous healing."

TABLE 4

INITIAL OVERLOADING STUDY: ANALYSIS OF VARIANCE

Source of Variation	Degrees of Freedom	Variance	Calculated F
Total	47		
Replicates	3	15.35	
Soil type	1	28,275	496.9*
Flaw condition[a]	1	2,015	35.4*
Curing[b]	2	3,748	65.8*
Interactions:			
Soil type-flaw condition	1	609	10.7*
Soil type-curing	2	1,386	24.3*
Flaw condition-curing	2	42.8	0.75
Soil type-flaw condition-curing	2	23.7	0.42
Error	33	56.9	

[a](a) No initial loading or (b) initial loading to ultimate compressive strength.
[b]Curing: 0, 28, or 56 days at 77 F following initial cure of 48 hr at 120 F.
*Significant F, $\alpha = 0.05$.

Cyclic Freeze-Thaw

The effect of cyclic freezing and thawing, subsequent curing, and additional cyclic freezing-thawing is shown in Figure 4. It is apparent that autogenous healing has occurred to a substantial extent for both soils. In fact, the terminal strengths of both mixtures, following 18 freeze-thaw cycles, are equal to or greater (α = 0.05) than the initial strengths.

The general trend of strength versus number of freeze-thaw cycles indicates that if freeze-thaw damage is cumulative from year to year, a low strength material would eventually be produced. However, damage is not cumulative (Fig. 4) and autogenous healing tends to restore the quality of the mixtures.

Since many field projects have been providing satisfactory service for several years in some locations, this would also indicate that cyclic freeze-thaw deterioration is not cumulative. If a mixture satisfactorily survives the first winter of service, the strength of the material will increase, due to a sustained lime-soil reaction, to the extent that subsequent freezing and thawing will not reduce the mixture strength to a critical level. The above concept was initially hypothesized in a study by Dempsey and Thompson (1), and the data of this study substantiate the position.

General

Callahan et al (2) have indicated that autogenous healing in lime-pozzolan-aggregate mixtures was significant, especially at early ages (after a small amount of initial cure). They further stated that the amount of healing depended on the curing conditions, degree of contact of the fractured surfaces, and age at which initial fracture occurred.

The effects of variable initial curing were not analyzed in this study since only one initial curing period (48 hr at 120 F) was used. This curing is approximately equivalent to 30 to 60 days of summer curing in Illinois. The pozzolanic reaction in lime-soil mixtures (a reaction between soil silica and/or alumina and lime to form various types of cementing agents, primarily calcium silicates and/or calcium aluminates) which is responsible for the strength increase will continue as long as free lime is available in the

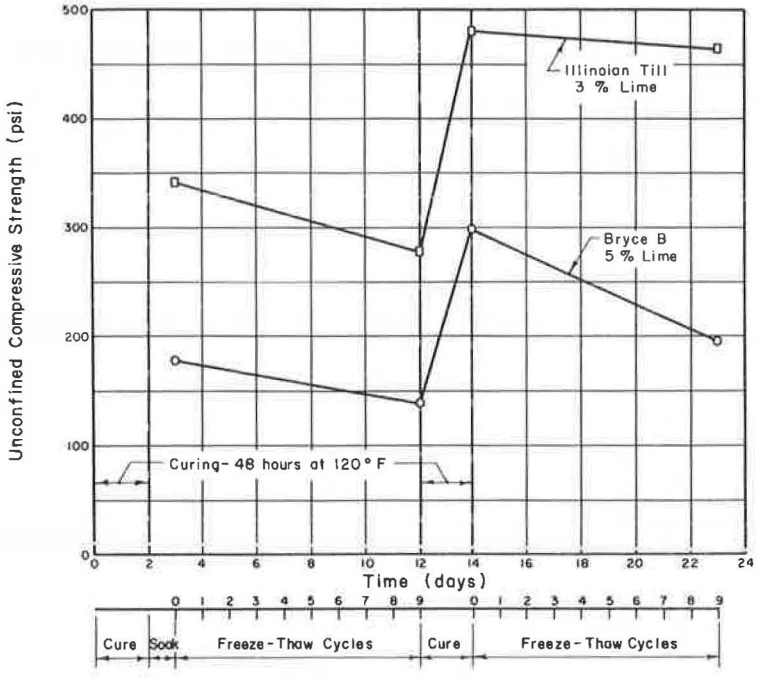

Figure 4. Influence of cyclic freeze-thaw and intermediate curing on unconfined compressive strength.

soil and reactive soil constituents are present. Since the pozzolanic reaction in lime-soil mixtures occurs over a period of many years, it is apparent that strength loss caused by excessive load stresses, shrinkage and swell, or durability deterioration may be partially or completely recovered under appropriate curing conditions.

It is possible that the formation of flaws in a lime-soil mixture may create new reaction surfaces which may expedite strength recovery. The method (unconfined compressive test) used in this study to introduce flaws into the lime-soil specimens caused some of the flaws to open up rather widely. Autogenous healing probably did not occur along some fractures since there was no contact between the flawed surfaces.

The autogenous healing process has several practical implications. If a soil will initially react with lime to produce a substantial strength increase, the results of this study suggest that subsequent lime-soil reactions may repair flaws produced in the material by various factors and may, in fact, produce a higher quality material than the one obtained following initial curing.

Fatigue damage will be offset or minimized since during the summer months flexural stresses in the lime-soil layer will be reduced (due to stiffer subgrade support) and strength increases will be produced by the autogenous healing process. The preceding factors produce a combined effect of reducing the applied stress level when expressed as a percentage of ultimate flexural strength.

Based on the above concepts one can justify basing initial strength requirements for various lime-soil mixture applications on the philosophy of residual strength. If the residual strength following the first winter of service is sufficient for the mixture usage (base-subbase-modified subgrade), subsequent deterioration probably will not be of any major consequence since autogenous healing processes will tend to restore the quality of the mixture prior to additional freezing and thawing. The "residual strength concept" has been used by Thompson (6) for establishing general quality requirements for various lime-soil mixture applications.

SUMMARY AND CONCLUSIONS

This limited study of two lime reactive soils indicated that autogenous healing does occur in lime-soil mixtures under favorable curing conditions. It would be expected, based on past laboratory and field experience, that the conclusion is generally applicable to most lime-soil mixtures that display a substantial initial strength increase.

The residual strength philosophy for establishing quality requirements for lime-soil mixtures to be used for various purposes (modified subgrade, subbase-base) is a valid concept. With favorable curing conditions, deterioration produced by various factors during critical portions of the materials service life will likely be restored by the autogenous healing process.

REFERENCES

1. Dempsey, B. J., and Thompson, M. R. Durability Properties of Lime-Soil Mixtures. Highway Research Record 235, p. 61-75, 1968.
2. Callahan, J. P., Morrow, J., and Ahlberg, H. L. Autogenous Healing in Lime-Pozzolan-Aggregate Mixtures. T.A.M. Report No. 631, Univ. of Illinois, 1962.
3. McDowell, C. Evaluation of Soil-Lime Stabilization Mixtures. Highway Research Record 139, p. 15-24, 1966.
4. Thompson, M. R. Factors Influencing the Plasticity and Strength of Lime-Soil Mixtures. Bull. 492, Eng. Exp. Sta., Univ. of Illinois, 1967.
5. Thompson, M. R. Split-Tensile Strength of Lime-Stabilized Soils. Highway Research Record 92, p. 69-80, 1965.
6. Thompson, M. R. Lime-Treated Soils for Pavement Construction. Jour., Highway Division, ASCE, Vol. 94, No. HW2, Nov. 1968.

Experimental Lime Stabilization in Nebraska

W. J. RAMSEY and O. L. LUND, Nebraska Department of Roads

In 1956, the Nebraska Department of Roads constructed an experimental project using hydrated lime in the stabilization of plastic subgrade soils, and in the upgrading of inferior base course materials. A previous report (1) gave early details of this project. This paper reports and summarizes the tests and observations made since construction. From the 10-year study conducted on this experimental project it was concluded that hydrated lime is a suitable material to improve plastic subgrade soils and to use as an admixture to upgrade inferior base course materials.

IN 1956, Nebraska became interested in hydrated lime for use in the stabilization of soils and base materials. As a result of laboratory studies, an experimental project, including a lime-treated subgrade soil section and a lime-treated base course section, was constructed that summer. The project, a part of US 136, is located west of Tecumseh, in Johnson County about 60 miles south and east of Lincoln.

In 1959, a paper was published (1) giving details of the preliminary field investigation, the laboratory study, design, location of the two test sites within each subdivision, preconstruction sampling, construction procedures, cost data, post-construction sampling and testing, and discussion of results.

Since construction the following observations have been made:

1. Field sampling and laboratory testing—intermittent basis.
2. Benkelman beam deflection tests—spring and fall of each year, 9-kip wheel load.
3. Cracking survey—fall of each year.
4. Wheel path depression survey—fall of each year. Measurements obtained by measuring the amount of space between a 7-ft metal straightedge and the surface of the asphaltic concrete on 1-ft intervals; final measurements were taken with a level.
5. General condition survey—fall of each year.

In this report, the results of this study are summarized in two main sections:

1. Lime-treated subgrade soil—design of the four 1500-ft subdivisions is given in Table 1. The treated subgrade soils were glacial clays having an AASHO soil classification range of A-6 (11) to A-7-6 (17).
2. Lime-treated base course—Table 1 gives the design of each subdivision. The granular material was a local coarse sand. Aftonian silt is an interglacial wind-blown layer deposited between the Nebraskan and Kansan glacial stages.

LIME-TREATED SUBGRADE SOIL

Laboratory Soils Tests on Field Samples

During the field investigation, the plan had been to run unconfined compressive strength and routine soil tests on undisturbed cores. However, attempts to obtain cores using diamond and carbide-tungsten tipped core barrels in combination with wet and dry drilling techniques proved unsuccessful. In the 3 percent lime-treated subdivision undisturbed samples were taken by pushing a 3- by 4-in. sampling tube

Paper sponsored by Committee on Lime and Lime-Fly Ash Stabilization and presented at the 48th Annual Meeting.

TABLE 1

DESIGN OF EXPERIMENTAL SECTIONS

Lime-Treated Subgrade Soil Section				
Subdivision Number	1	2	3	4
Station to station	1047 to 1062	1062 to 1077	1077 to 1092	1092 to 1107
AC surface course, in.	3	3	3	3
Soil-agg. base co., in.	4	4	4	4
Granular subbase co., in.	7	None	None	None
Subgrade treatment, in.	None	7	7	7
Lime, %	None	3	6	10
Remarks	Standard design	—	—	—
Lime-Treated Base Course Section				
Subdivision Number	5	6	7	8
Station to station	1048 to 1061	1161 to 1174	1174 to 1187	1187 to 1200
AC surface course, in.	3	3	3	3
Soil-agg. base co., in.	4	None	None	None
Lime-Aftonian silt base co., in.	None	6	6	6
Aftonian silt, %	None	15	20	20
Lime, %	None	2	4	7
Granular subbase co., in.	7	5	5	5
Remarks	Standard design	—	—	—

into the treated material. Since vertical cracks developed in the cores, unconfined compressive strength tests were not run. In the sections containing higher precentages of lime, the material was too hard to obtain samples in this manner; therefore, all testing was confined to disturbed samples.

The preliminary laboratory phase indicated that lime treatment apparently causes the agglomeration of some of the silt and clay-size particles with the net result that the soil is somewhat coarsened. However, it should be pointed out that the particles were weakly bonded and that by varying the mechanical mixer agitation period the results of the tests could be changed. For this reason, a standard 5-min agitation period was established. More than usual grinding and crushing was required during sample preparation because of the hardness of the field samples. This extra manipulation probably resulted in further breakdown of the particle bonds. Therefore, it is believed that the soil tests performed on the lime-treated samples should be considered only as approximations. Some observations of the hydrometer tests, on samples taken from the subgrade (Table 2), may include: (a) all testing periods show that the most

TABLE 2

AVERAGE LABORATORY TEST RESULTS: LIME-TREATED SUBGRADE SOILS

No. Days Cure	No. of Tests	Hydrometer Tests			Plasticity Tests		Field Moisture Equiv.	Shrinkage Limit	Shrinkage Ratio	Volumetric Change	Lineal Shrinkage
		Sand +0.074 mm	Silt 0.074 to 0.005 mm	Clay -0.005 mm	LL	PI					
(a) 3 Percent Lime-Treated Subgrade Soil											
Raw soil	2	23	42	35	45	24	24.40	12.47	1.85	22.07	6.4
16	6	44	45	11	38	9	30.99	21.35	1.58	15.23	4.6
600	4	39	55	6	38	8	34.00	21.80	1.57	19.15	5.7
2600	3	26	62	12	38	13	—	—	—	—	—
3850	6	22	55	23	38	14	33.70	17.70	1.71	27.36	7.8
(b) 6 Percent Lime-Treated Subgrade Soil											
Raw soil	2	16	56	28	42	23	23.45	15.34	1.78	14.44	4.4
16	6	52	47	1	NP	NP	36.46	25.53	1.45	15.85	4.8
600	4	59	40	1	NP	NP	38.25	27.51	1.41	15.14	4.6
2600	3	49	47	4	NP	NP	—	—	—	—	—
3850	6	39	51	10	NP	NP	35.35	28.23	1.41	10.04	3.1
(c) 10 Percent Lime-Treated Subgrade Soil											
Raw soil	2	13	55	32	43	22	23.35	14.49	1.80	15.95	4.8
16	6	42	58	0	NP	NP	39.46	26.44	1.37	18.08	5.4
600	4	57	42	1	NP	NP	41.30	29.60	1.32	15.44	4.7
2600	3	—	—	—	NP	NP	—	—	—	—	—
3850	6	39	51	10	NP	NP	36.27	26.58	1.45	14.05	4.3

pronounced effect of hydrated lime is the reduction of the percentage of clay-size particles and an increase in sand, (b) in all three lime-treated subdivisions (3, 6 and 10 percent) there appears to be a loss of the bonding effect of the lime with the passage of time, and (c) all tests seem to indicate that the effects of treatment with 6 and 10 percent lime are essentially the same.

One of the most publicized features of lime is its ability to reduce the plasticity index of soils. However, there has been much discussion concerning this phenomenon since some believe this reduction to be permanent while others feel that eventually there will be some increase in the plasticity index. Table 2 indicates that all tests in the 6 and 10 percent lime-treated subdivisions show the soils to be nonplastic following the lime treatment. The plasticity index of the soil treated with 3 percent hydrated lime was reduced from 24 to 9 in 16 days and to 8 in 600 days. However, the 2,600 and 3,850 day tests show that the plasticity index has increased to 13 and 14, respectively. This may indicate that when small percentages of lime are used in the treatment of glacial clays of the type and in the environment found on this project, early reduction in the plasticity index may be subject to a reversal with the passage of time.

The results of the field moisture equivalent and shrinkage tests are somewhat erratic (Table 2). Even though the trends are difficult to ascertain, it does appear that hydrated lime causes definite changes in the field moisture equivalent, shrinkage limit, and shrinkage ratio. However, the effect is not clear-cut on the volumetric change and lineal shrinkage characteristics.

Benkelman Beam Deflection Tests

On each test site (2 per subdivision) Benkelman beam deflection tests were made on the inside and outside wheelpaths during the spring and fall periods from December 1956 to October 1966. The seasonal Benkelman beam deflection tests fail to reveal a

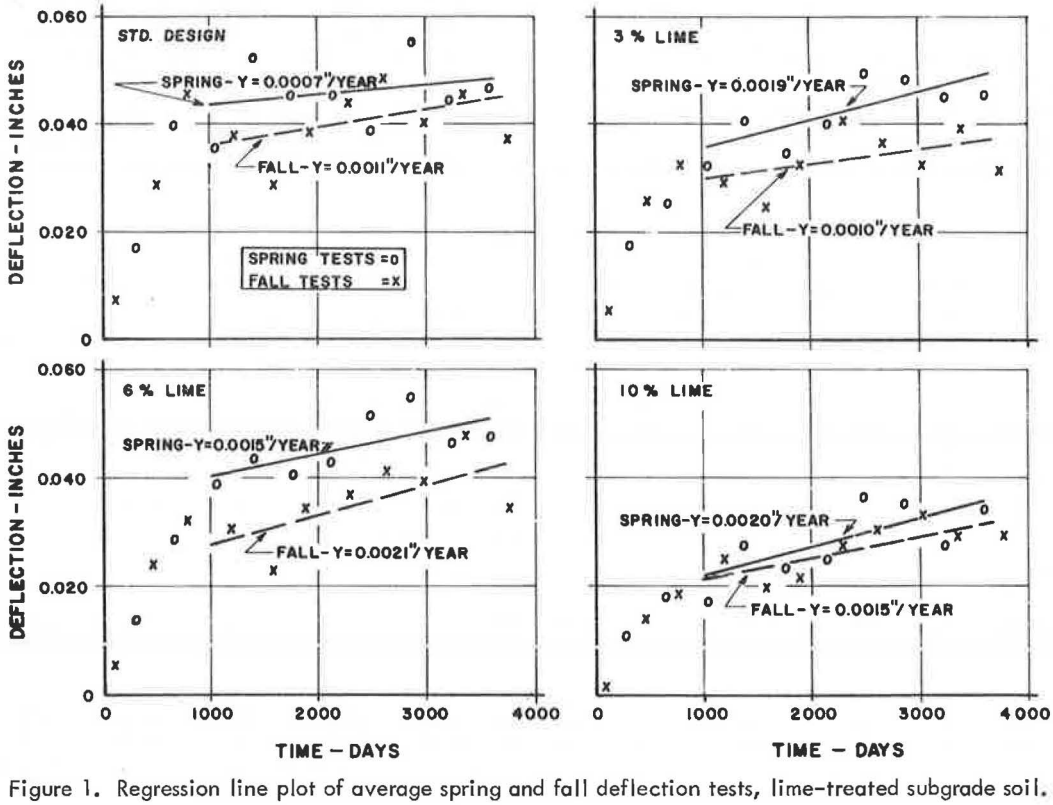

Figure 1. Regression line plot of average spring and fall deflection tests, lime-treated subgrade soil.

well-defined relationship between percentage of lime and deflection. However, the outer wheelpath (OWP) deflection values in the 10 percent lime-treated subdivision are lower than those of the other subdivisions.

To summarize the data for each design, a spring and fall deflection value was calculated, using an average value of the tests taken in both wheelpaths. Figure 1 shows that during the first five testing periods there was a decided increase in deflection. Tests taken after the fall of 1958 show a general increase but at a much slower rate. Since the subgrade was extremely dry at the time of construction, the change in slope of the deflection versus time trend may be due to the increase in the moisture content of the subgrade soil. Using the deflection values of the tests taken between spring 1959 and fall 1966, first degree polynomial curves were computed, using an IBM model 1620 computer. After study of the data (Fig. 1) some possible observations are:

1. The regression lines indicate that there is clearly an increase in deflection with the passage of time and the application of vehicular traffic for all four of the experimental subdivisions;
2. The spring regression line for the standard design subdivision (0 percent lime) is flatter than the corresponding lines developed for the lime-treated subdivisions;
3. The increase in the spring deflection values above the fall deflections for the 10 percent lime-treated subdivision is smaller than for the other subdivisions; and
4. The spring and fall regression lines for the 10 percent lime-treated subdivision plot below those developed for the other subdivisions; however, when the regression line slopes are compared, there appears to be no relation between slope and percent lime used.

Transverse and Longitudinal Cracking

During the 10 years that this project was under observation, a careful record as to the amount of yearly cracking was kept. An accumulative total of the data is shown in

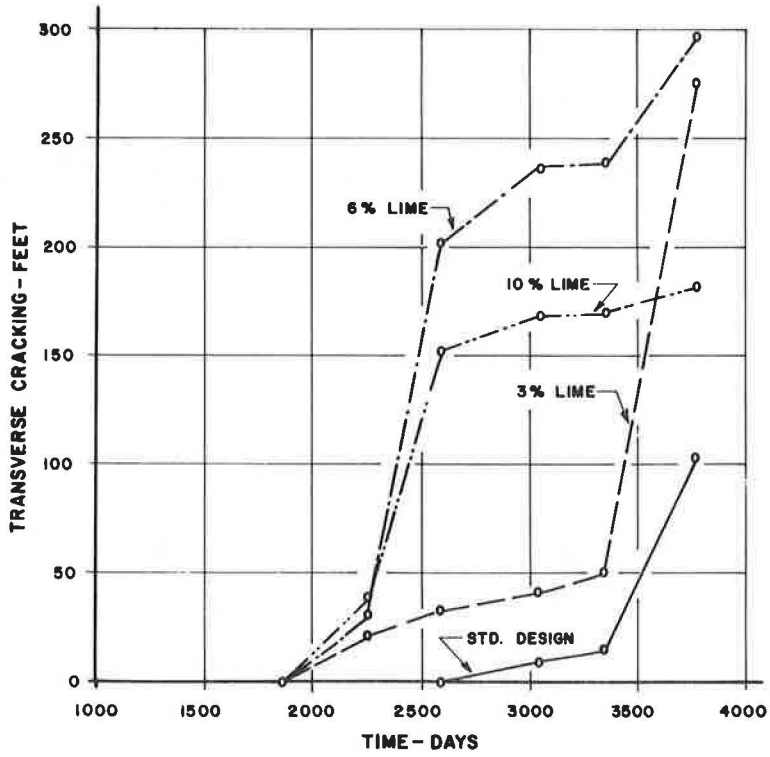

Figure 2. Yearly accumulative total of lineal feet of transverse cracking, lime-treated subgrade soil.

Figure 2. No longitudinal cracking was found in the top lift of the asphaltic concrete in any of the subdivisions.

Transverse cracking was first noted in all of the lime-treated subdivisions in the sixth year after construction. It was not until the eighth year that cracking began to occur in the standard design subdivision.

From Figure 2, some observations of the cracking pattern at the end of the 10-yr period may include:

1. There is less cracking in the standard design subdivision than in the lime-treated subdivisions;
2. Less cracking occurred in the 10 percent lime-treated subdivision than in either the 3 or 6 percent lime-treated subdivisions;
3. The accumulative total cracking in the 3 and 6 percent subdivisions is approximately the same; and
4. The crack survey data show no relationship between cracking and percent lime used.

Wheelpath Depression

To determine if rutting was in the consolidation or displacement of the asphaltic concrete, or in one of the underlying courses, or a combination of these, thickness measurements were made of each course, at 1-ft intervals, across the 22-ft surface at both test sites in each subdivision. Some difficulty was encountered in taking the measurements due to the inability to distinguish a marked difference at the contact between similar courses, e.g., soil aggregate base course and the granular subbase, lime-treated soils and untreated soils. From the average of these measurements and a surface survey a transverse cross section was plotted for each subdivision (Fig. 3). From this plot it will be noted: (a) for the standard design, some of the surface rutting is reflected in the soil aggregate base course and quite possibly in the granular

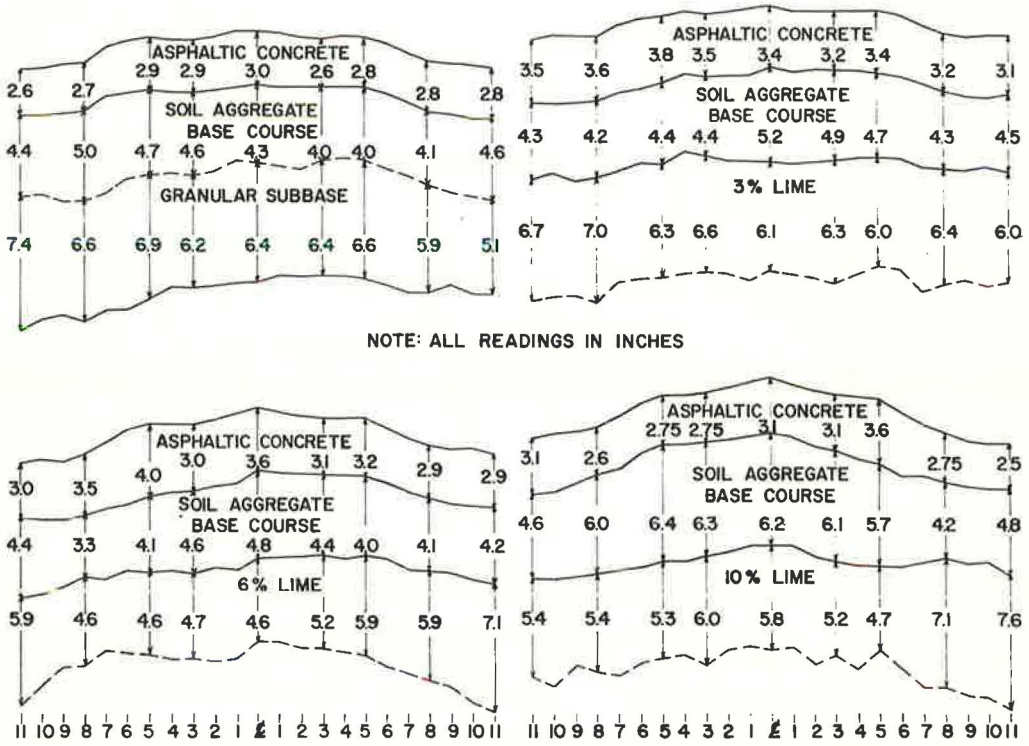

Figure 3. Average transverse cross section, lime-treated subgrade soil.

subbase; and (b) for the 3, 6 and 10 percent lime-treated soils, it appears that the surface rutting extends into the soil aggregate base course in all the lime-treated subdivisions. Since the original cross section of the lime-treated courses were not taken it is difficult to ascertain if rutting extends into this layer. However, from examination of the measured sections it appears that little if any rutting occurs in the lime-treated courses.

General Surface Condition

During the years that this project was under observation, in addition to the transverse and longitudinal cracking record, notations were made of other types of surface failure, for example, map or alligator cracking, distortion, and raveling. From completion of construction in the fall of 1956 through November 1962 no failures occurred and no maintenance other than crack filling was required.

The following is a yearly resume of failures which occurred after 1962.

1963 Failures

1. Standard design subdivision: none.
2. Lime-treated (3 percent) subdivision: 50 ft of excessive rutting in the OWP of the right lane caused by displacement of the soil aggregate base course; no movement was detected in the lime-treated subgrade soil.
3. Lime-treated (6 percent) subdivision: two areas (90 and 75 ft) of excessive rutting were found in the OWP of the right lane. Wheelpath depression measurements showed as much as 1.8 in. of rutting in both areas. Deflection measurements in both failed areas were higher than the subdivision OWP average. In one of the failed areas, a transverse trench about 18 in. wide and 24 in. deep was dug to determine the cause of the excessive rutting. From measurements and visual inspection, it was found that the rutting was caused by movement and subsequent thinning (1.8 in.) of the soil aggregate base course. No depression or movement was detected in the lime-treated subgrade soil. Holes bored in the other failed area showed a definite thinning ($1\frac{3}{4}$ in.) of the soil aggregate base course. Again no movement in the lime-treated subgrade soil was detected.
4. Lime-treated (10 percent) subdivision: none.

1964 Failures

1. Standard design subdivision: none.
2. Lime-treated (3 percent) subdivision: short failure due to fill settlement over a culvert.
3. Lime-treated (6 percent) subgrade: none.
4. Lime-treated (10 percent) subgrade: none.

1965 Failures

1. Standard design subdivision: six areas of map cracking, ranging in length of from 10 to 74 ft, were found in the OWP of the left lane. Depression measurements showed that excessive rutting was occurring in all of these areas. Benkelman beam deflection tests, taken on each side of the map cracked areas, were higher than the subdivision average. Some displacement of both the soil aggregate base course and granular subbase was noted.
2. Lime-treated (3 percent) subdivision: none.
3. Lime-treated (6 percent) subdivision: none.
4. Lime-treated (10 percent) subdivision: none.

1966 Failures

1. Standard design subdivision: two short (8 and 13 ft in length) map-cracking areas were noted in the OWP of the left lane. Investigation of these areas indicated that there was some displacement of the underlying granular base courses.

TABLE 3

UNCONFINED COMPRESSIVE STRENGTH LIME-TREATED BASE COURSE

Number Days Cure	Unconfined Compressive Strength (psi)								
	2% Lime-Treated Base			4% Lime-Treated Base			7% Lime-Treated Base		
	Min.	Max.	Avg.	Min.	Max.	Avg.	Min.	Max.	Avg.
600[a]	—	—	165 (1)[b]	430	745	587 (2)	405	795	600 (2)
1380	—	—	—	—	—	—	870	2310	1590 (2)
2580	—	—	—	—	—	—	1690	2010	1850 (2)
3810	—	—	—	559	3065	2030 (6)	1432	3249	2080 (9)

[a]2- by 2-in. cube cut from 12-in. diameter core. [b]Number in parentheses is number of tests.

2. Lime-treated (3 percent) subdivision: four map-cracked areas, varying in length of from 6 to 51 ft, were noted. Investigation showed a thinning of the soil aggregate base course. There was no indication of movement in the lime-treated subgrade soil.
3. Lime-treated (6 percent) subdivision: none.
4. Lime-treated (10 percent) subdivision: none.

LIME-TREATED BASE COURSE

Laboratory Tests on Field Samples

Due to the cementing properties of hydrated lime, when added to Aftonian silt-course sand mixtures, it was planned that the principal laboratory test to be performed on field samples would be the unconfined compressive strength test. The most successful method found to take cores was that of using a 4-in. diameter diamond tipped core barrel and wet drilling. However, this technique met with only limited success (Table 3).

Table 3 gives the minimum, maximum and average unconfined compressive strengths of the cores tested. It will be noted that: (a) the difference in the average 10-yr strength between the 4 and 7 percent lime-treated subdivisions is insignificant; (b) the lime-treated base material in the 2 percent subdivision was not cemented strongly enough to obtain cores; and (c) in the 7 percent lime-treated subdivision the average unconfined compressive strength shows an increase with each testing period.

Benkelman Beam Deflection Tests

For the 10-yr observation period Benkelman beam deflection tests were made on the inner wheelpath (IWP) and outer wheelpath during the spring and fall of each year. The deflections taken between the fall of 1956 and the spring of 1959 show more abrupt increases in deflection than those taken after this period. This change in the slope of the deflection versus time trend may be due to the increase in the moisture content of the subgrade soil. The seasonal deflection values for both the IWP and OWP show the expected relationship between lime content and deflection, that is, highest deflection for the 2 percent lime, lower deflection for the 4 percent lime, and lowest deflection for the 7 percent lime. The deflection for the standard design subdivision is sometimes higher than the 2 percent subdivision but usually falls between the values of the 2 and 4 percent lime-treated subdivisions.

The points in Figure 4 are averages of the IWP and OWP deflection values for the spring and fall. The plotted regression lines are first degree polynomial curves calculated from the tests taken between spring 1959 and fall 1966. Some observations of the data are (a) except for the spring regression lines in the standard design subdivision which show a slight downward trend, all regression lines indicate an increase in deflection with the passage of time; (b) the regression line slopes of the 2 and 4 percent lime-treated subdivisions are steeper than those of the standard design or 7 percent lime-treated subdivisions; (c) the standard design regression lines show the smallest yearly deflection increase of any of the subdivisions; (d) in the 7 percent lime-treated subdivision the fall regression lines plot above the spring lines (the yearly rate of deflection increase shows these lines to be parallel); and (e) the regression line plots do not

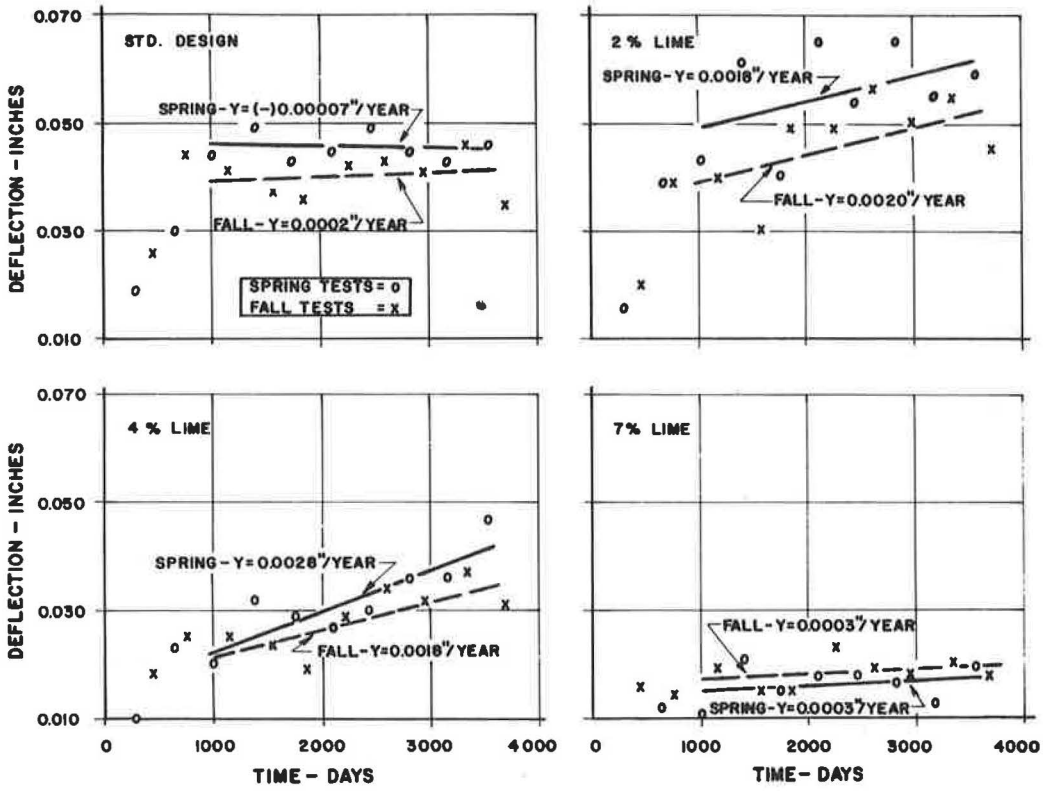

Figure 4. Regression line plot of average spring and fall deflection tests, lime-treated base course.

indicate a clear relationship between slope and percentage of lime used. However, when the 7 percent lime-treated base course deflection values and resultant regression line plots are compared with the same data obtained for the other lime-treated subdivisions a definite improvement in supporting capability is apparent.

Longitudinal and Transverse Cracking

During the 10-yr observation period only a small amount of longitudinal cracking was observed: 2 percent lime-treated base = (1961) 39 ft and (1962) 2 ft; 4 percent lime-treated base = (1961) 117 ft. In all cases the cracking occurred in the right traffic lane (eastbound), about 1 ft from the edge of the top lift of the asphaltic concrete. It is believed that the cracking which occurred in 1961 might have been due to unusually heavy loads hauled to a nearby Atlas missile site which was under construction.

The 10-yr cumulative transverse cracking total is plotted in Figure 5. Transverse cracking was first observed in the 4 percent lime-treated subdivision in 1959 and in the 2 and 7 percent subdivisions in 1961. It was not until 1966 that cracking was noted in the standard design subdivision and then only two cracks of 2 and 3 ft were found. It appears that all lime sections are equally susceptible to the cracking tendency. However, due to the more rigid nature of the lime-treated bases, it was not unexpected that more cracking occurred in them than in the standard design subdivisions.

At a number of locations in all three lime-treated subdivisions, cores were taken over the cracks. In every instance, in the 4 and 7 percent subdivisions, the cracks extended through the lime-treated base course. Since cores could not be taken in the 2 percent subdivision and examination of the core hole sides did not show any evidence of cracking it is not known if cracks extended through the base material.

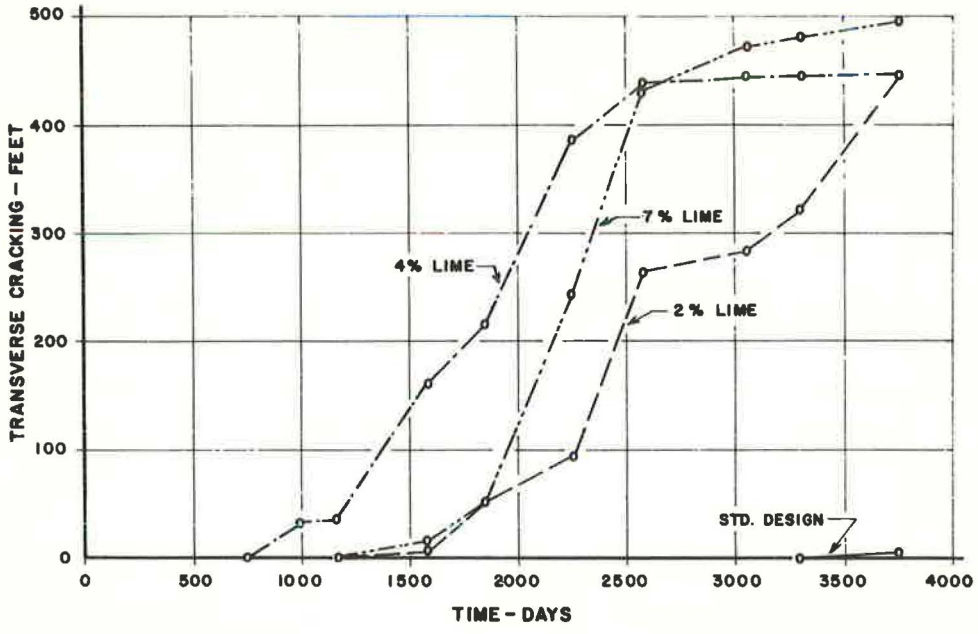

Figure 5. Yearly accumulative total of lineal feet of transverse cracking, lime-treated base course.

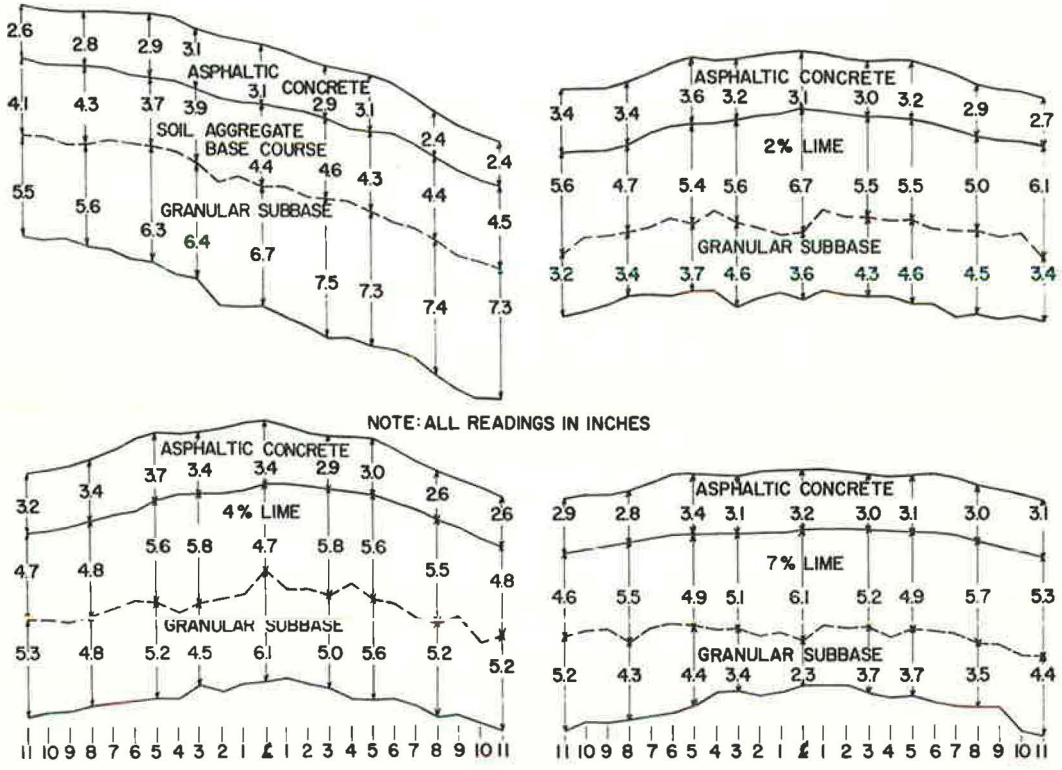

Figure 6. Avearage transverse cross section, lime-treated base course.

Wheelpath Depression

To determine the extent of displacement in each layer, thickness measurements of the asphaltic concrete and underlying courses were made at 1-ft intervals. In all of the subdivisions, some difficulty was encountered in determining the contact between the base courses. A transverse cross section was plotted for each subdivision from the averages of these measurements and data obtained with a surveyor's level. From Figure 6, it will be noted:

1. Standard design: surface rutting extends into the soil aggregate base course; it is also believed that there may be some displacement in the granular subbase course.
2. Lime-treated (2 percent) base: some of the surface rutting is reflected in the underlying lime-treated base; it is doubtful if the granular subbase is displacing.
3. Lime-treated (4 percent) base: from study of the cross section, it appears that a slight amount of the rutting in the left lane may extend into the lime-treated course. In the right lane, it is doubtful if rutting extends into this course. It is not believed that the irregularities occurring in the granular subbase are the result of the surface ruts.
4. Lime-treated (7 percent) base: only a slight amount if any of the surface rutting is reflected in the lime-treated course.

General Surface Condition

Condition surveys were made on each subdivision at least once a year. A record was kept on the amount of map cracking, distortions or other types of failures. The results of the survey in each subdivision follows.

Standard Design

None, 1956 through 1966.

2 Percent Lime-Treated Base Course

None, 1956 through 1965.

In 1966, two map-cracked areas 8 and 10 ft in length were noted in the OWP of the left lane. Deflection tests taken adjacent to these areas were the same as the subdivision average (OWP—0.058 in.). Wheelpath depression measurements in these areas were about 0.1 in. deeper than the left lane, OWP average of 0.52 in. Measurements in holes bored in these areas did not indicate any noticeable thinning of the lime-treated base material.

4 Percent Lime-Treated Base Course

None, 1956 through 1964.

In 1965, eight feet of map cracking was found in the OWP of the right lane; the cause of this failure could not be attributed to the lime-treated base course.

None, 1966.

7 Percent Lime-Treated Base Course

None, 1956 through 1966.

CONCLUSIONS

The following conclusions are based on tests and observations made during the ten-year study.

Lime-Treated Subgrade Soil

1. The results of the soil tests are somewhat inconclusive. However, it appears that more long-range benefit may be gained when 6 to 10 percent lime is added than when smaller percentages are used.

2. The Benkelman beam deflection tests fail to reveal a well-defined relationship between percentage of lime and deflection; however, from the deflection tests and regression line plots the following summarizes the best performance rating of the four experimental subdivisions: (a) deflection magnitude, 10 percent lime; (b) rate of deflection increase, standard design; (c) relationship of spring to fall deflection, 10 percent lime; and (d) projected 15-yr deflection, 10 percent lime.
3. All lime-treated subdivisions were more susceptible to transverse cracking than the standard design subdivision.
4. In the lime-treated subdivisions no failure could be attributed to the inability of the lime-treated course to perform its function.
5. As a result of this project, it was concluded that hydrated lime is a suitable stabilizing agent to improve plastic subgrade soils.

Lime-Treated Base Course

1. The difference in the average 10-yr unconfined compressive strength between the 4 and 7 percent lime-treated base course material is insignificant.
2. When only 2 percent hydrated lime is added to the base material, it appears that little if any strength is gained through the cementing properties of the lime.
3. The seasonal deflection values are inversely proportional to the percentage of lime used. The deflections in the standard design subdivision usually fall between the values of the 2 and 4 percent lime-treated subdivisions. On the basis of the deflection tests and regression line plots the following summarizes the best performance rating of the four experimental subdivisions: (a) deflection magnitude, 7 percent lime; (b) rate of deflection increase, standard design; (c) relationship of spring to fall deflection, 7 percent lime; and (d) projected 15-yr deflection, 7 percent lime.
4. The lime-treated base courses appear to be more susceptible to cracking than the untreated base course.
5. Except for a slight amount of map cracking which developed in the OWP of the 2 and 4 percent lime-treated subdivisions, no failures occurred in any of the subdivisions.
6. It appears that hydrated lime is a suitable material to use as an admixture to improve the performance of inferior base course materials. Apparently more benefit is derived when 4 to 7 percent lime is added to the base material than when lesser amounts are used.

ACKNOWLEDGMENTS

This investigation was conducted by the Division of Materials and Tests, Nebraska Department of Roads, in cooperation with the United States Department of Transportation, Bureau of Public Roads. The work was performed as Project No. HPR-1, 63-10A, Part II, Research. The authors appreciate the opportunity to summarize and report the results of this cooperative effort.

The opinions, findings, and conclusions expressed in this report are those of the authors and not necessarily those of the Bureau of Public Roads.

REFERENCES

1. Lund, O. L., and Ramsey, W. J. Experimental Lime Stabilization in Nebraska. HRB Bull. 231, p. 24-59, 1959.
2. National Lime Association. Lime Stabilization of Roads. Washington, D. C., 1954.
3. Diamond, S., and Kinter, E. B. Mechanisms of Soil-Lime Stabilization. Public Roads, Vol. 33, No. 12, p. 260-265, Feb. 1966.

Some Deformation Characteristics of A Lime-Stabilized Clay

PER E. FOSSBERG, Institute of Transportation and Traffic Engineering, University of California, Berkeley

A montmorillonitic clay was stabilized with 10 percent lime, molded at relatively high water contents, cured for 2 and 5 weeks, and tested with repeated loading in triaxial compression under various confining pressures and under drained and undrained conditions. The purpose of the test program was to investigate the effect of deviator stress and confining pressure on vertical strains and resilient modulus.

Each sample was tested at successively increasing deviator stresses. The results indicate that stress history effects have to be considered when evaluating permanent strains at low numbers of load repetitions, and also when interpreting such data in terms of fatigue behavior. Furthermore, the permanent deformations suffered under increasing repeated load stress levels depend largely upon the interplay between these stresses, the water content and the confining pressure; however, a general prediction as to the relative effect of these three factors cannot be made.

Not taking possible stress history effects into account, the tests show a relatively regular pattern of resilient strains, and conversely, resilient modulus, which invariably increases with increasing confining pressure and with decreasing deviator stress—a finding in full agreement with that obtained for other types of stabilized materials. Based on all the tests performed, reasonably good correlations exist between resilient modulus and principal stress ratio at various water contents. A convenient model for these relationships is presented.

•THE search towards rational methods in pavement design, based on elastic theory, has been intensified over the past few years. It appears that this work has mainly been concentrated in two areas: (a) development of adequate models for the theoretical analysis of layered systems, and (b) accumulation of knowledge of materials properties, particularly in regard to resilient behavior.

While model development has now advanced to a stage where multilayered systems can be analyzed fairly satisfactorily, knowledge of materials behavior necessary for the theoretical solutions is rather incomplete, particularly when dealing with stabilized materials. In the latter area, the present state of the art may be summarized as in Figure 1.

Seed et al (1) when investigating the effect of confining pressure, σ_3, and deviator stress, σ_d, on the resilient behavior of clays and clayey soils, found that the effect of confining pressure on the resilient modulus, M_R, is relatively small, while the magnitude of the applied deviator stress is all important (Fig. 1a).

Paper sponsored by Committee on Lime and Lime-Fly Ash Stabilization.

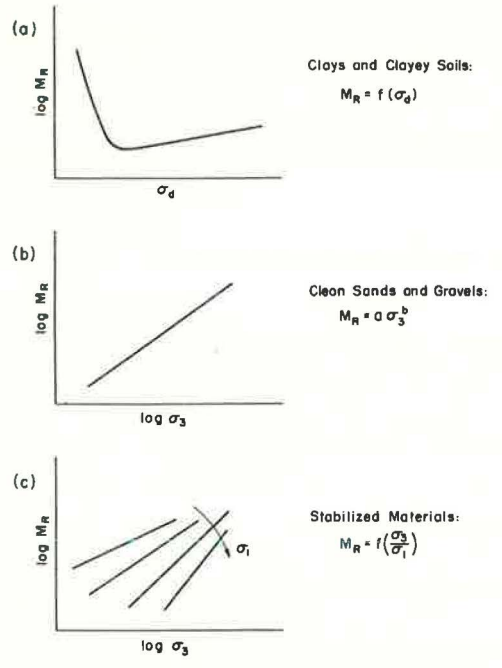

Figure 1. Resilient modulus as a function of stresses for three types of soils.

On the other hand, for cohesionless materials, as reported by Trollope et al (2) for a sand, and by Mitry (3) for a dry granular material, the resilient modulus increases with an increase in confining pressure, but is independent of the deviator stress level provided a failure condition is not reached. Mitry established a unique relationship between M_R and σ_3 (Fig. 1b).

For stablized materials having both frictional and cohesional characteristics, it is to be expected that both confining pressure and deviator stress play an important part. Thus, Gregg et al (4), testing a bitumen-stabilized windblown sand, found that M_R is markedly influenced by both confining pressure and deviator stress and is inversely related to the ratio between the major and minor principal stress. Monismith et al (5) reporting on an asphalt-emulsion-treated base arrived at essentially the same conclusion, that M_R increases with increasing confining pressure and with decreasing deviator stress. The general relationship (Fig. 1c) thus would hold true for these materials. While there is reason to believe that the same relationship holds true for cement-stabilized materials, the present paper serves to illustrate that it also applies to a lime-stabilized clay.

MATERIAL AND TEST PROCEDURES

The soil used in the present investigation was a black clay, residual from the weathering of norite, brought from Onderstepoort, Transvaal. The main mineral constituents are quartz and Ca-montmorillonite, with lesser amounts of hydrous mica, kaolinite and feldspars. Some of its relevant properties are given in Table 1. This clay was stabilized with 10 percent (by weight of dry soil) of high-calcium lime. This stabilizer content may seem high, but it is not when considering the large amount of clay present and the activity of this soil as compared to clayey gravels where a lime content of 4 to 5 percent is frequently used, but where the bulk of the material is coarse and relatively inert.

Samples to be tested in triaxial compression were prepared at two water contents, 51 and 77 percent. The clay-lime for the first set of samples was mixed for about one hour in a screw-type mixer operated under vacuum to obtain a high degree of saturation. In completion of the mixing, the samples were extruded through a 1½-in. diam. nozzle and cut in 3-in. lengths. The second set of samples was mixed for about an hour in a small pugmill, again with the application of suction. These samples were "cast" in 1½-in. diam. cylindrical molds, to a length of approximately 4 in., which was later trimmed down to 3 in. All

TABLE 1
INDICATOR PROPERTIES OF ONDERSTEPOORT CLAY

Property	Raw Soil	With 10 Percent Lime
Liquid limit, %	70	77
Plasticity index, %	42	28
Linear shrinkage, %	20	10
Material < 2 μ, %	57	
Specific gravity	2.69	
Activity	0.74	

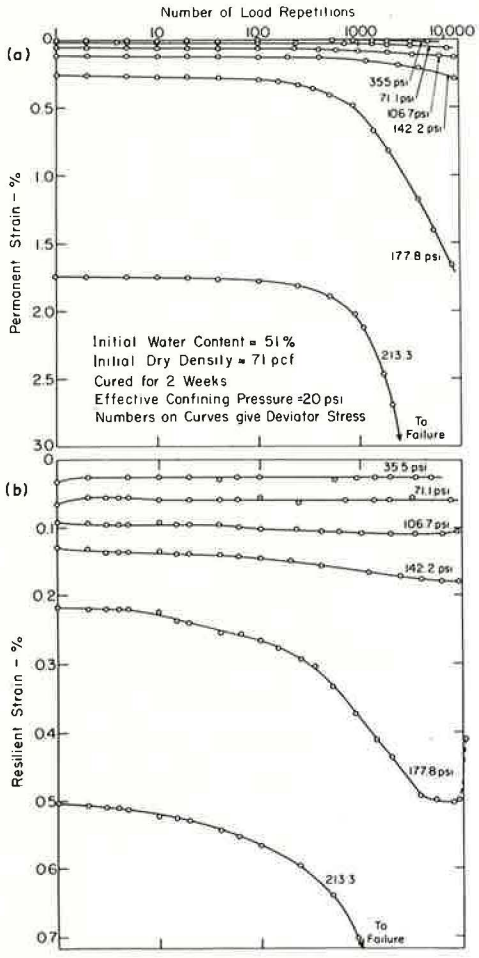

Figure 2. Permanent and resilient strains in a drained test.

samples were cured at 20 C, at a relative humidity exceeding 90 percent.

As it was desired to evaluate the test results in terms of effective stresses, full saturation of the samples was required. To achieve this, the samples upon completion of the curing period were soaked under water for four hours, with gradual application of suction at a rate of approximately 1 in. Hg per 10 min, up to 23 in. Hg, then the suction was gradually reduced over 30 min. The specimens were then mounted in triaxial cells, and isotropically consolidated overnight at pressures of 10, 20, and 40 psi. Prior to repeated load testing, an internal back pressure was gradually applied up to 30 psi, while simultaneously the cell pressures were increased to 40, 50, and 70 psi, respectively.

The samples were tested in repeated loading, using equipment basically similar to that used at the Soil Mechanics and Bituminous Materials Laboratory of the University of California, Berkeley, described by Seed et al (6). The frequency of loading was 20 per min, with a load duration of $\frac{3}{4}$ sec. Different samples were used for each confining pressure, but each sample was tested at increasing stress levels until failure. The number of stress applications at each stress level generally ranged between 5000 and 9000. Vertical deformations were measured with dial gages.

The specimens were tested under drained or undrained conditions, in the latter case with measurement of pore pressures. The term undrained is not essentially correct in this context; the system was closed during the whole test sequence at each stress level, permitting measurement to be made of the effect of repeated load applications on the "off-load" pore pressure. The equipment did not allow for pore pressures to be measured during loading; so during each stress application, temporary "drainage" took place.

TEST RESULTS

Typical patterns of permanent and resilient strains as functions of number of load repetitions at increasing stress levels are shown in Figures 2 and 3. Figure 2 represents drained test conditions at an effective confining pressure of 20 psi, for the clay-lime mixture with an initial water content of 51 percent, cured for 2 weeks prior to repeated loading. Figure 3 gives data for undrained tests on the clay-lime with an initial water content of 77 percent cured for 5 weeks, and also the variation in off-load pore pressures, starting with an effective confining pressure of 10 psi.

Permanent Strains

Each sample having been tested at increasing stress levels, the permanent strain data have been plotted in terms of cumulative values (Figs. 2a and 3a). Typically, the

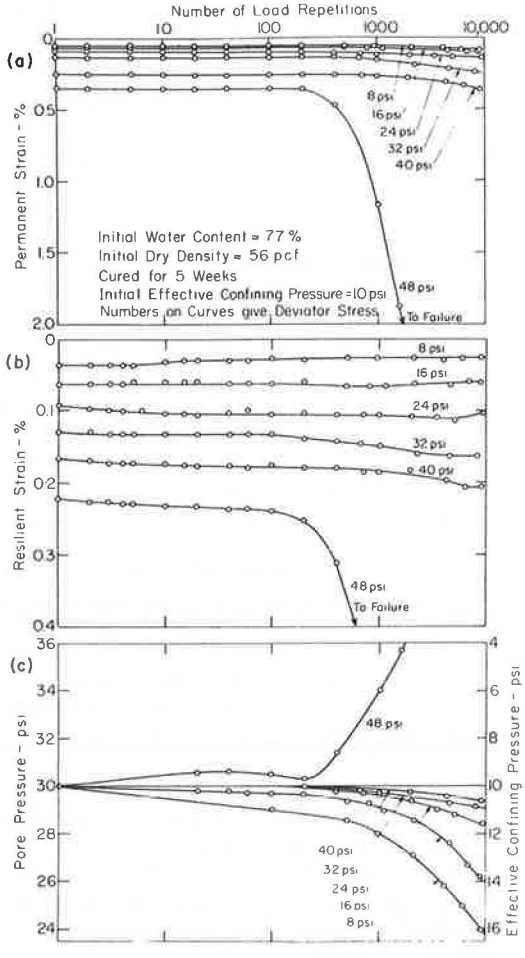

Figure 3. Permanent and resilient strains and pore pressures in an undrained test.

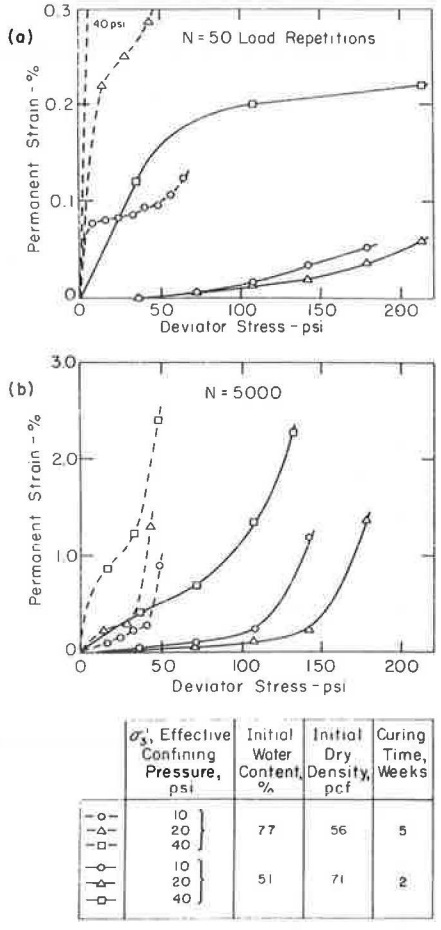

	σ_3', Effective Confining Pressure, psi	Initial Water Content, %	Initial Dry Density, pcf	Curing Time, Weeks
-o-	10	77	56	5
-Δ-	20			
-□-	40			
-o-	10	51	71	2
-Δ-	20			
-□-	40			

Figure 4. Permanent strains vs deviator stress in drained tests at various confining pressures.

curves for permanent strain show only little increase with the number of load repetitions, N, at low counts. Invariably in the present investigation, however, the slope of permanent deformation versus the logarithm of the number of load applications in this low range of N appears to be even flatter than normal, representing approximately a constant value. Part of this effect may probably be ascribed to stress history. Beyond this range of N (usually occurring around 100), the permanent strains increase markedly, indicating that the effect of stress history is less significant. This would tend to show the desirability of carrying the number of load repetitions well beyond 100 when doing tests at increasing stress levels on the same sample. On the other hand, the number of load repetitions applied at each but the last stress level was not sufficient to show whether the sample was perfectly stable (which would be indicated by the permanent strains tending towards a constant value at high numbers of load repetitions), or whether a failure condition was approached (which would be indicated by a drastic increase in permanent strains at high counts). Evaluation of fatigue life at various stress levels was not the purpose of this investigation; however, it clearly is important that such stress history effects be taken into account when interpreting fatigue test data.

Figure 4 gives the available data for permanent strains as a function of deviator stress and confining pressure under drained conditions for the two clay-limes. The

values are cumulative in the sense that Figure 4a sums up the permanent strains suffered during the first 50 load applications at each stress level, disregarding deformations occurring thereafter; in Figure 4b the same is true at 5000 load applications. The slope of the curves thus represents the rate at which permanent strains increase with deviator stress.

For the clay-lime with an initial water content of 51 percent, the tests carried out at 10-psi and 20-psi confining pressure show a progressive increase in permanent strains with increasing deviator stress, indicating a gradual weakening of the sample—the effect of which is more pronounced the lower the confining pressure. In all the other samples, however, permanent strains increase relatively rapidly during the application of the lowest deviator stresses. The reason for this effect, which is more pronounced the higher the confining pressure, is not clear, but it would appear that consolidation of the sample cannot be the cause as the observed drainage (or, at the lower confining pressures, water absorption) during this first phase was relatively small. This conclusion is corroborated by the insignificant change in pore pressures that took place in the undrained samples during this first phase. In the second phase, the permanent strains again increase progressively with the deviator stress.

The data in Figure 4 show that the effect of confining pressure on permanent strains cannot always be predicted, particularly when dealing with materials at high water contents or relatively low dry densities. The aspect of fatigue behavior, being highly related to imposed strains, also cannot be uniquely related to confining pressures.

Pore Pressures

Figure 3c shows a typical pore pressure development in an undrained test under an initial confining pressure of 10 psi. At low and intermediate levels of deviator stress, repeated stress applications are accompanied by a decrease in off-load pore pressures, indicating dilatancy of the soil skeleton. Other tests in this series, carried out at an initially high confining pressure (40 psi), consistently show an increase in pore pressures (serving to reduce the effective confining pressure) indicative of compression

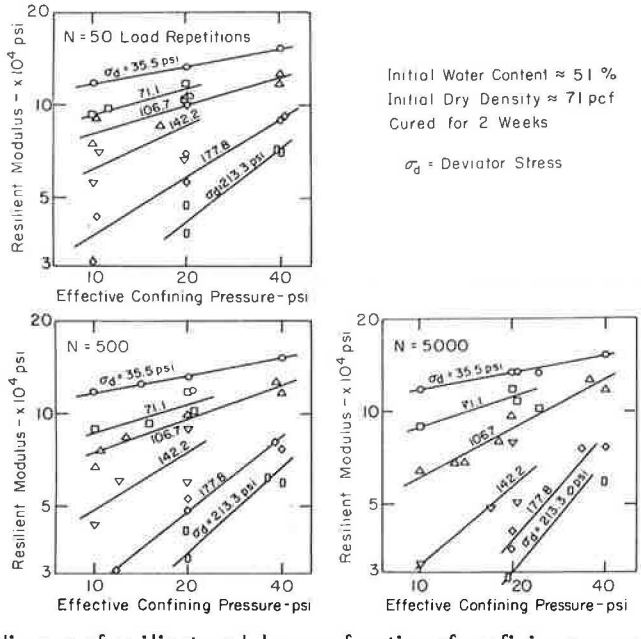

Figure 5. Typical diagram of resilient modulus as a function of confining pressure and deviator stress.

of the soil skeleton during repeated loading. These findings would indicate that the concept of a critical relationship between void ratio and confining pressure may, at least qualitatively, be valid also for stabilized soils.

At high levels of deviator stresses, a tendency towards compression is indicated (and more so, the higher the initial confining pressure) in that the pore water pressure increases, thereby reducing the effective confining pressure. This effect of reduced confining pressure is accompanied by rapidly increasing permanent and resilient strains indicative of incipient failure.

In this context an opposite effect observed in undrained tests on an asphalt-stabilized sand (7) is of interest. At fairly low initial confining pressures, but even at stress levels close to failure, pore pressures were found to fall with increasing number of load applications, which would indicate that at this confining pressure the void ratio of the sample was below the "critical." In this dilatant state close to failure, a remarkable reduction in resilient strains took place, probably due to the increased effective confining pressure.

Resilient Strains

In Figures 2b and 3b, resilient strains increase progressively with increasing deviator stress. At low and intermediate stress levels, there is relatively little variation of resilient strain with number of load repetitions. Whether this behavior is a typical feature of this material or is due to stress history effects has not been established. In accordance with expectations, a comparison of test results obtained at various confining pressures shows that resilient strains decrease with increasing effective confining pressure.

Resilient Modulus

The resilient modulus (deviator stress divided by resilient strain) increases with increasing confining pressure and with decreasing deviator stress. This is well illustrated in Figure 5, which gives data for the clay-lime mixture with an initial water content of 51 percent and cured 2 weeks prior to repeated loading. In accordance with

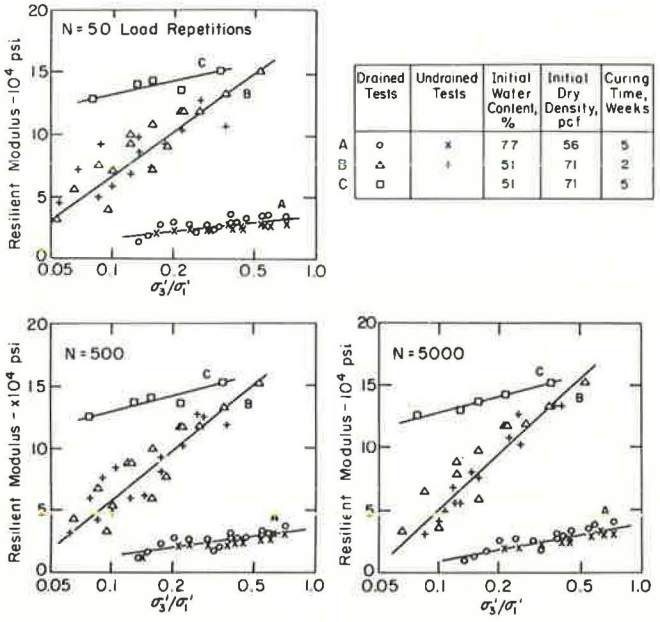

	Drained Tests	Undrained Tests	Initial Water Content, %	Initial Dry Density, pcf	Curing Time, Weeks
A	o	x	77	56	5
B	Δ	+	51	71	2
C	□		51	71	5

Figure 6. Model for the relationship between resilient modulus and principal stress ratio.

the findings for resilient strains, there is relatively little variation in resilient modulus with number of stress applications, except at high deviator stresses where the resilient modulus is markedly reduced at high numbers of load repetitions.

An analogous diagram to that in Figure 5, although somewhat less consistent, is obtained for the clay-lime mixture molded at 77 percent water content. The data in Figure 5 do not strictly comply with the concept of the resilient modulus being a simple function of the principal stress ratio, but do indicate that such a relationship is a reasonable approximation. Various models can be devised to establish the desired relationship; the best representation found is given in Figure 6, based on data from both drained and undrained tests and involving the major and minor principal effective stresses, σ_1' and σ_3', respectively. This semilogarithmic representation yields a relatively small spread of the data points and allows for a linear relationship to be drawn. Thus, for the clay-lime molded at a water content of 51 percent and cured for 2 weeks, this line can, at 5000 load repetitions, reasonably well be expressed by

$$M_R = 200.000\ (1 + 0.75 \log \sigma_3'/\sigma_1')\ \text{psi}$$

at least within the range of data here available.

For the same clay-lime mixture, but cured for 5 weeks, a limited amount of data based on undrained tests, were produced. As shown in Figure 6, the increased curing time causes an increase in the resilient modulus but it appears that the modulus for this longer cured sample is less affected by the principal stress ratio. This is reasonable, in that the cohesional component of resistance, being essentially independent of confining pressure, is proportionately larger the longer the curing time. In support of this, reference can be made to shear strength tests on this clay-lime as reported by Fossberg (8), showing that the lime has an immediate effect in increasing the true angle of internal friction, but that long-term gain in strength is mainly achieved through increase in true cohesion.

Figure 6 also gives the resilient modulus of the clay-lime mixture molded at a water content of 77 percent and cured for 5 weeks. Again we note the practically linear correlation with the logarithm of the principal stress ratio. As is to be expected, the resilient modulus at any one stress condition is considerably lower for this material than for the same molded at 51 percent water content.

CONCLUSIONS

The present investigation has shown that the resilient properties of a lime-stabilized clay, possessing pronounced cohesional and frictional characteristics, are strongly influenced by both deviator stress and confining pressure. This is in full agreement with the reported behavior of asphalt-stabilized sands and asphalt-treated granular bases. Furthermore, similar behavior can be expected for cement-stabilized materials, as also for natural "intermediate" soils, such as certain silts and clayey gravels.

A reasonable relationship has been established between resilient modulus and principal stress ratio at various water contents. If the same kind of relationship can be obtained for other types of stabilized materials and for intermediate soils, the full range of combinations of cohesional and frictional properties will be covered.

ACKNOWLEDGMENTS

The investigations described in this paper were conducted in 1964, when the author was employed by the National Institute for Road Research, Pretoria, South Africa. The laboratory tests were carried out with great skill and patience by Eric David.

REFERENCES

1. Seed, H. B., Chan, C. K., and Lee, C. E. Resilience Characteristics of Subgrade Soils and Their Relation to Fatigue Failure in Asphalt Pavements. Proc., Conf. on Structural Design of Asphalt Pavements, Ann Arbor, Mich., 1962.

2. Trollope, D. H., Lee, I. K., and Morris, J. Stresses and Deformations in Two-Layer Pavement Structures Under Slow Repeated Loading. Proc., Australian Road Research Board, Vol. I, Part II, 1962.
3. Mitry, F. C. Determination of the Modulus of Resilient Deformation of Untreated Basecourse Materials. Ph.D. Thesis, University of California, Berkeley, 1964.
4. Gregg, J. S., Dehlen, G. L., and Rigden, P. J. On the Properties, Behavior and Design of Bituminous Stabilized Sand Bases. Proc., Conf. on Structural Design of Asphalt Pavements, Ann Arbor, Mich., 1967.
5. Monismith, C. L., Terrel, R. L., and Chan, C. K. Load Transmission Characteristics of Asphalt-Treated Base Courses. Proc., Conf. on Structural Design of Asphalt Pavements, Ann Arbor, Mich., 1967.
6. Seed, H. B. and Fead, J. W. N. Apparatus for Repeated Load Tests on Soils. ASTM Spec. Tech. Publ. No. 254, 1959.
7. Fossberg, P. E. Unpublished Test Results. National Institute for Road Research, Pretoria, South Africa, 1964.
8. Fossberg, P. E. Some Fundamental Engineering Properties of a Lime-Stabilized Clay. Proc., Sixth International Conf. on Soil Mechanics and Foundation Engineering, Montreal, Canada, Vol. I, p. 221-225, 1965.

Freeze-Thaw Durability of Lime-Stabilized Clay Soils

ERKAN ESMER, West Virginia Institute of Technology; and
RICHARD D. WALKER and ROBERT D. KREBS, Virginia Polytechnic Institute

• ADDITION of lime greatly enhances the strength of many fine-grained soils. Lack of information about the permanence of these strength gains has prevented engineers from properly utilizing the improved strengths in pavement design procedures.

Effects of various forces of nature that cause strength losses in lime-stabilized soils in the field such as adverse moisture conditions and freezing and thawing have been subjects of a continuing investigation at Virginia Polytechnic Institute since 1964. Walker and Karabulut (1) in 1964 investigated the effects of closed-system freezing and thawing on strength and stiffness of a lime-stabilized clay soil. It was reported that the stabilized clay specimens lost considerable strength and these strength losses were theorized to be in part due to hydraulic pressures similar to those described by Powers (2) for concrete.

Continuation of that study which showed the importance of initial moisture conditions prior to freezing and thawing on the magnitude of strength loss of a lime-stabilized clay soil was reported by Walker et at (3) in 1967.

This study led to the work described here which is concerned with the effects of open- and closed-system freeze-thaw durability of lime-stabilized soils. Effects of lime stabilization and freezing and thawing on the soil pore structure and permeability were also studied in an effort to gain a better insight into freeze-thaw mechanisms.

MATERIALS

The soils selected for this study represented a wide range of materials used with lime in road construction in Virginia. These soils were: (a) a montmorillonitic clay (Iredell), (b) a kaolinitic fine sandy loam (Cecil), and (c) a residual limestone soil of mixed mineralogy but more illite than anything else (Lodi). Table 1 summarizes the properties of these soils.

A high-calcium hydrated lime, which was kept tightly sealed in plastic bags to minimize carbonation, was used. Typical calcium carbonate contents averaged about 4 percent as determined by heating in an oven at 900 C.

PROCEDURES

Sample Preparation

The soil was air dried and moist cured near optimum moisture content in sealed containers for 24 hours; then lime and additional moisture were added. The soil-lime mixture was allowed to cure for an additional 3 hours before compaction into 4-in. diameter molds by a hydraulic compactor producing densities approximately equivalent to those obtained under standard AASHO procedures. The soil samples were quartered along their longitudinal axis with a band saw and then were trimmed to cylindrical specimens approximately 33-mm diameter by 71. 5 mm in length with a soil lathe.

The specimens were then wrapped in Saran Wrap and dipped in Thermocote, a strippable coating, at room temperature to form an airtight seal. They were then sealed in

Paper sponsored by Committee on Lime and Lime-Fly Ash Stabilization.

TABLE 1
ATTERBERG LIMITS AND COMPACTION PROPERTIES OF LODI, CECIL, AND IREDELL SOILS

Soil	Clay L2μ (%)	LL	PL	PI	0% Lime		4% Lime		8% Lime	
					Max. Dry Density (pcf)	Opt. Moisture (%)	Max. Dry Density (pcf)	Opt. Moisture (%)	Max. Dry Density (pcf)	Opt. Moisture (%)
Lodi	55	59	45	14	94.2	25.5	90.0	27.5	89.0	28.0
Cecil	55	62	44	18	90.5	29.5	86.6	31.5	85.0	32.5
Iredell	48	69	28	41	100.5	24.0	91.3	27.0	88.8	29.5

plastic containers and placed in an oven at 120 F for 48-hr curing. This curing procedure is similar to that suggested by Anday (4), who showed that it produced results similar to 40 to 45 days of field curing at Charlottesville, Va., in the summer of 1961.

After curing, the samples were placed in a refrigerator at 40 F to arrest the curing process and to facilitate the scheduling of tests.

Freezing-and-Thawing Tests

An inexpensive testing apparatus, utilizing two styrofoam picnic boxes placed in a home-type deep-freeze unit, was used for freeze-thaw testing. A fan placed between the boxes, facing toward the top of the freezer, encouraged increased air flow at the top of the specimens. The boxes contained a styrofoam holder which held 16 specimens resting on a layer of water-saturated sand. Copper constantan thermocouples were placed at the top, middle, and bottom of a control specimen to record the temperature gradients. Thermocouples were placed at the interface of the sand-water layer, inside the sand-water layer, and outside the boxes to record the ambient temperature inside the deep-freeze unit. Figure 1 shows the setup used.

For closed-system freeze-thaw testing, sealed specimens were placed in the styrofoam boxes, whereas the bottom seals of the specimens were removed prior to their

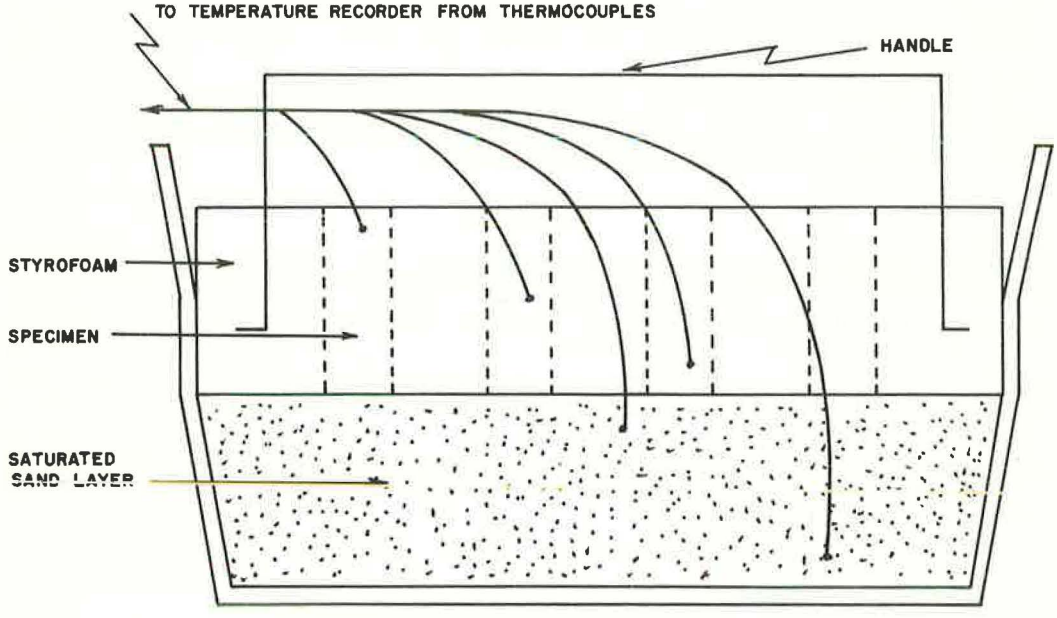

Figure 1. Diagram of freeze-and-thaw box.

placement in the boxes for open-system testing. The insulating properties of the styrofoam box and the layers prevented the saturated sand layer from freezing; this supplied the water source for the open-system specimens thus simulating a groundwater supply in nature.

The freezing of the specimens for the closed system was from top to bottom with slowly depressed temperatures, at a rate of 2.75 F/hr at the top of the specimens, at 2.45 F/hr at the middle of the specimens, and at 2.15 F/hr at the bottom of the specimens. For the open system, the rates of temperature depression were as follows: at the top of the specimens 2.65 F/hr, at the middle of the specimens 2.35 F/hr, and at the bottom of the specimens 2.05 F/hr. The rate of depression of temperature was less in the open system because there was more water present in the soil specimens.

Typical temperature gradients during the 20-hr freezing phase were as follows:

1. Top of specimen, 60 F to 5 F closed system, 60 F to 7 F open system;
2. Middle of specimen, 59 F to 10 F, closed system, 59 F to 12 F open system;
3. Bottom of specimen, 57 F to 14 F closed system, 57 F to 17 F open system;
4. Water near top of sand layer, 55 F to 32 F for both open and closed systems.

The deep-freeze unit maintained a temperature ranging from -20 F to -10 F.

Thawing was accomplished by placing the styrofoam boxes in a 70 F, 100 percent relative humidity environment to bring the specimens to their beginning temperature before again exposing them to freezing.

The closed-system specimens were subjected to 0, 5, 10 and 15 cycles and the open-system specimens to 0, 1, 3, and 5 cycles of freezing and thawing.

Unconfined Compressive Strength

Fifty-four specimens were tested for unconfined compressive strength immediately after curing, and 159 specimens were tested after various cycles of open- or closed-system freeze-thaw treatment. Testing was by loading at 0.05 in./min with loads recorded at intervals of 0.005-in. deformation to failure.

Pore Characteristic Studies

Total porosities of all specimens were determined from their measured weight, volume, and moisture content before and after freeze-thaw treatment. One specimen out of four was air dried and small chunks broken off for determination of effective porosity, mean pore radius, and pore modulus using mercury intrusion techniques with a 15,000-psi Aminco-Winslow mercury intrusion porosimeter. Using the porosimeter pores larger than 0.000012 mm (0.012 μ) in diameter could be penetrated.

Effective porosity is the ratio of the volume of the interconnected pores intruded by mercury to the total volume of the soil sample.

Mean pore radius was determined by assuming that all the pores in a soil specimen were cylindrical. Since the radius of the pores is a function of the interconnected pore volume:

$$r = f(v) \tag{1}$$

$$V = \int dV = \int y\,(r)\ \pi r^2\ dr \tag{2}$$

$$S = \int dS = 2\int y\,(r)\ \pi r\ dr \tag{3}$$

where

V = volume of pores,
S = surface area of pores,
y = number of pores, and
r = radius of pores

By definition mean pore radius, $\bar{r}$, is given by

$$\bar{r} = \frac{2V}{S} \tag{4}$$

$$\bar{r} = \frac{\int_{r_1}^{r_2} y\,(r)\,\pi r^2\,dr}{\int_{r_1}^{r_2} y\,(r)\,\pi r\,dr} \tag{5}$$

$$\bar{r} = \frac{\int_{0}^{V} r\,dV}{V} \tag{6}$$

The pore modulus, which is analogous to fineness modulus used in describing grain-size characteristics of sand, has been calculated by the summation of the pore volume intruded by mercury over a predetermined range of diameters. The diameters chosen for pore modulus determination were 60, 40, 20, 10, 5, 2.5, 1.0, 0.5, 0.10, 0.05, 0.025, and 0.012 μ.

Permeability

After the various cycles of freezing and thawing, the fourth specimen from each mold was used for a permeability determination. Following four days of air drying, the specimen ends were broken off and used for pore characteristic study. The middle or remaining portion was measured for average length and placed in the permeameter, as shown in Figure 2. A water aspirator was used to create a vacuum of about 24 in. of mercury below atmospheric pressure. Water was allowed to pass through the sample from containers ranging from 10-ml burette to a 4500-ml cylinder. The drop in elevation head and volume of water passing through the sample over 12-hr periods were recorded. The permeabilities were calculated from this information after obtaining constant readings.

RESULTS AND DISCUSSION

Examination of the unconfined compressive strength data shown in Table 2 brings out some interesting ideas, some of which are supported by pore characteristic and permeability data to be presented later.

Effect of Lime on Zero Cycle Strength

The differences in lime capacity are well exhibited. The kaolinitic (Cecil) and illitic (Lodi) soils showed an optimum strength at 4 percent lime and a distinct drop off in strength at 8 percent. The montmorillonitic (Iredell) soil showed only a minor increase at 4 percent and a large increase at 8 percent. Thus, it can be assumed that the Cecil and Lodi soils, with 8 percent lime, had excess lime available.

Effect of Freezing-and-Thawing Cycles

The information provided by the zero strength data is interesting when examined in the light of strength results after cycles of freezing and thawing. The soils with the

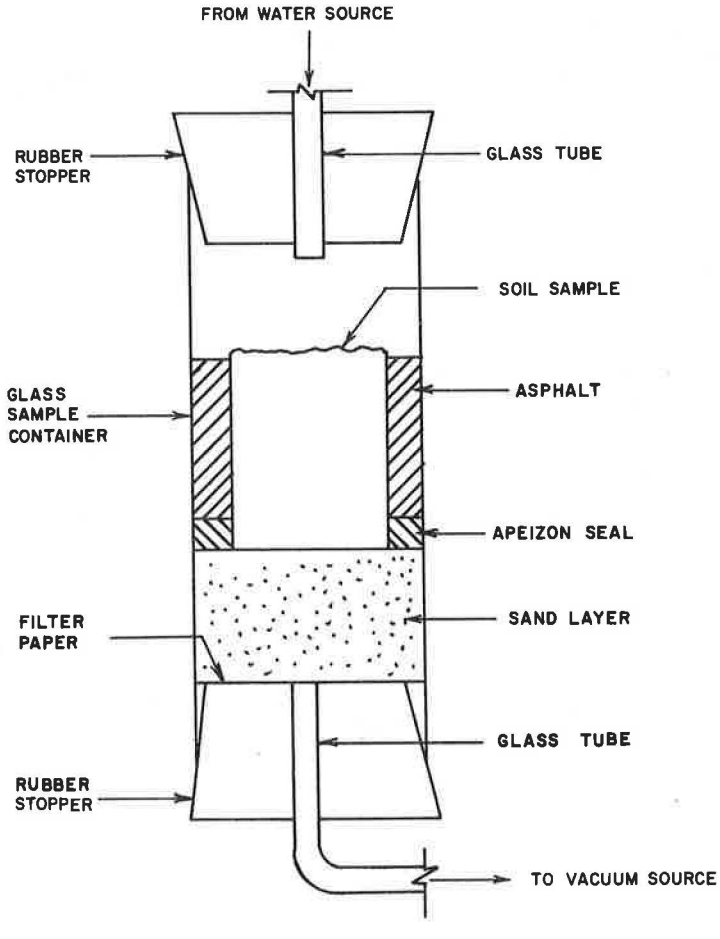

Figure 2. Diagram of permeameter.

TABLE 2

EFFECT OF LIME STABILIZATION AND FREEZING AND THAWING ON UNCONFINED COMPRESSIVE STRENGTH

Percent Lime	No. Cycles		Unconfined Compressive Strength (psi)[a]					
			Lodi		Cecil		Iredell	
	Open	Closed	Open	Closed	Open	Closed	Open	Closed
0	0	0	83	76	65	61	69	60
	1	5	21	28	17	29	0	30
	3	10	5	13	33	12	4	13
	5	15	6	5	0	13	1	7
4	0	0	211	208	155	169	76	76
	1	5	96	76	68	94	22	34
	3	10	28	25	26	68	16	17
	5	15	41	44	28	47	10	27
8	0	0	175	157	143	180	124	124
	1	5	58	68	107	121	44	32
	3	10	60	69	89	79	6	42
	5	15	105	148	107	107	21	37

[a]Each strength value represents an average of values obtained from 4 specimens, with a variance of ± 5 percent.

excess lime (Cecil and Lodi), whether open or closed during freezing and thawing, showed dramatic strength recoveries after severe losses had occurred in earlier cycles. Apparently the freezing-and-thawing damage mechanism was not operative in later cycles, thus permitting a form of self-healing to take place with the help of the excess lime. Why the freezing-and-thawing damage mechanism was not working in these later cycles will be discussed later.

The Iredell soil, perhaps not having excess lime, did not show significant recovery from initial strength loss.

Pore Characteristics

An examination of some of the pore characteristics of the three soils, before and after freeze-thaw treatment, may be helpful. Figures 3 through 6 illustrate the data obtained, and the reader should be reminded that it was necessary to dry the specimens before testing them in the mercury intrusion porosimeter. The effects of this drying were perhaps nominal in Cecil and Lodi soils but caused marked shrinkage in the Iredell soil. This is illustrated in Figure 4 when total porosity (obtained by conventional techniques) is compared to effective porosity (obtained by the porosimeter).

Except for porosity, there is some evidence of a trend of increased values for the other characteristics measured (mean pore radii and pore modulus) with increased cycles of freezing and thawing. All three characteristics seem to increase with percent lime.

The amounts of increase in porosity due to lime addition seem to depend on the soil structure. The Iredell soil which has a naturally dispersed structure experienced the greatest structural change.

The ameliorative action of the lime may have transformed its structure from a dispersed to a flocculant state resulting in an enlargment of its pores. The ameliorative effects of lime did not seem to be as pronounced in Cecil and Lodi soils because they have more of a naturally flocculant structure; thus they experience smaller enlargements in their pore structure.

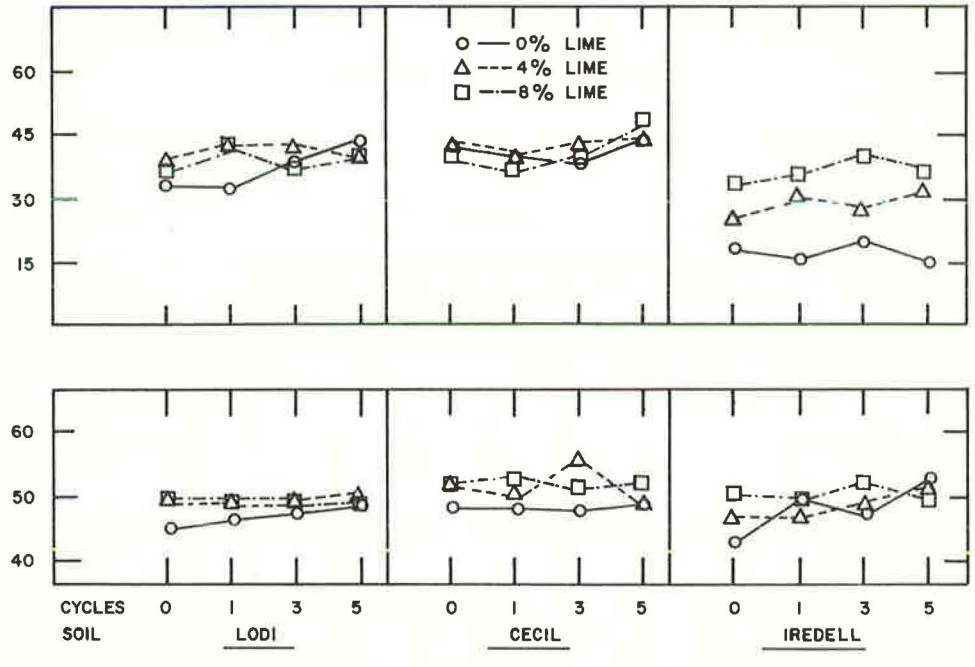

Figure 3. Effects of open-system freezing and thawing on total porosity and effective porosity of three lime-stabilized clay soils.

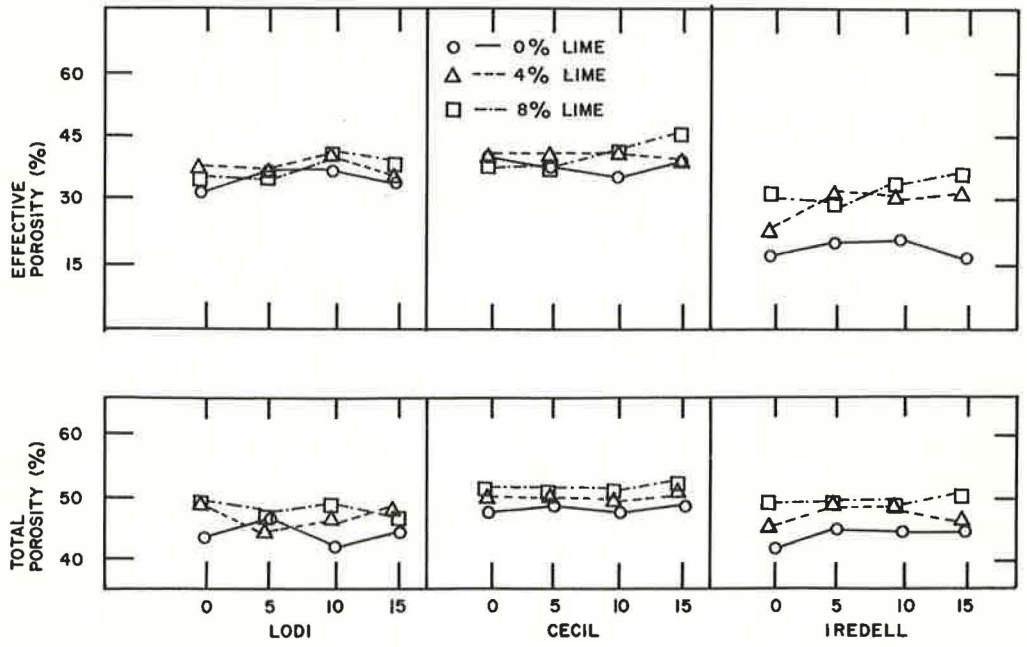

Figure 4. Effects of closed-system freezing and thawing on total and effective porosity of three lime-stabilized clay soils.

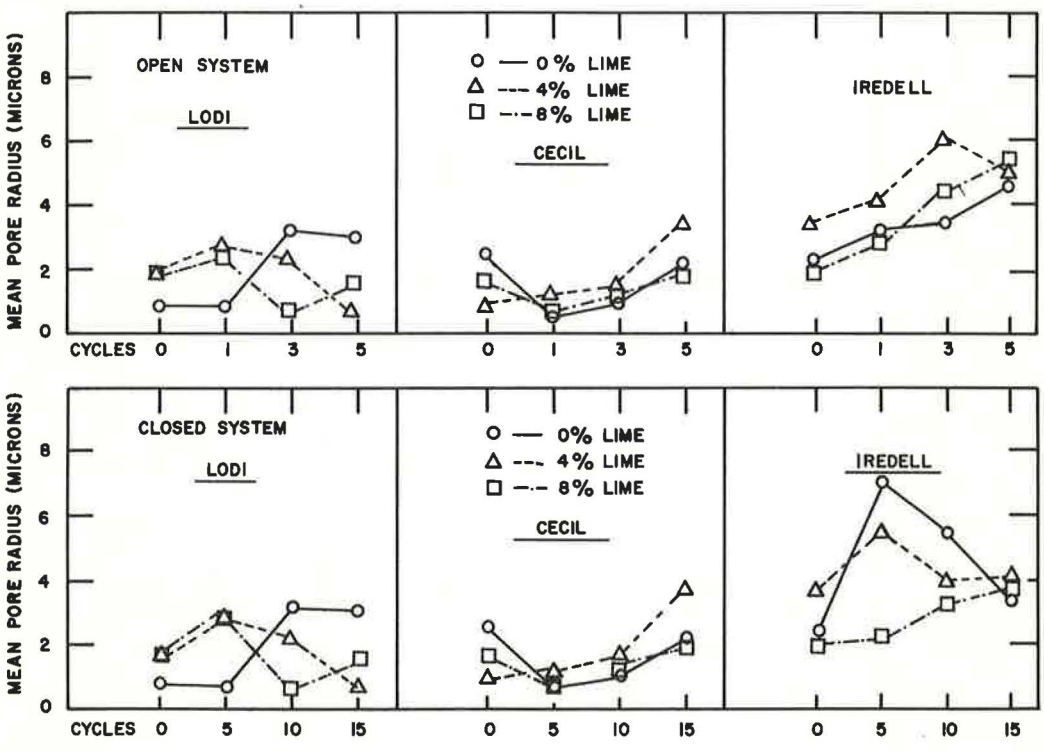

Figure 5. Effects of open- and closed-system freezing and thawing on mean pore radii of three stabilized soils.

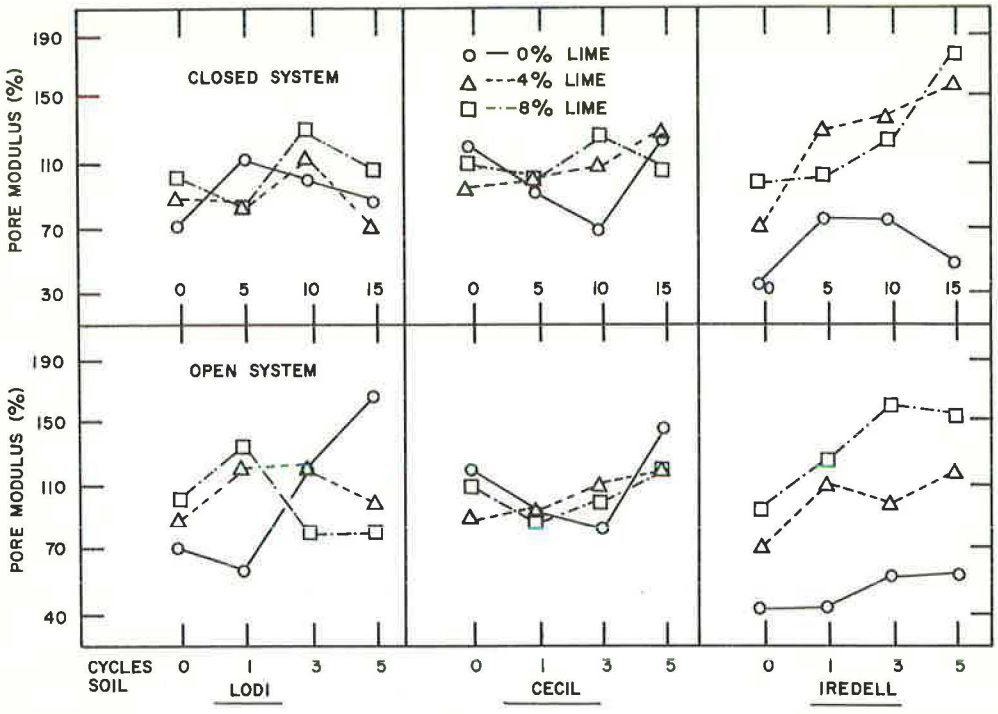

Figure 6. Effects of open- and closed-system freezing and thawing on pore modulus of three stabilized clay soils.

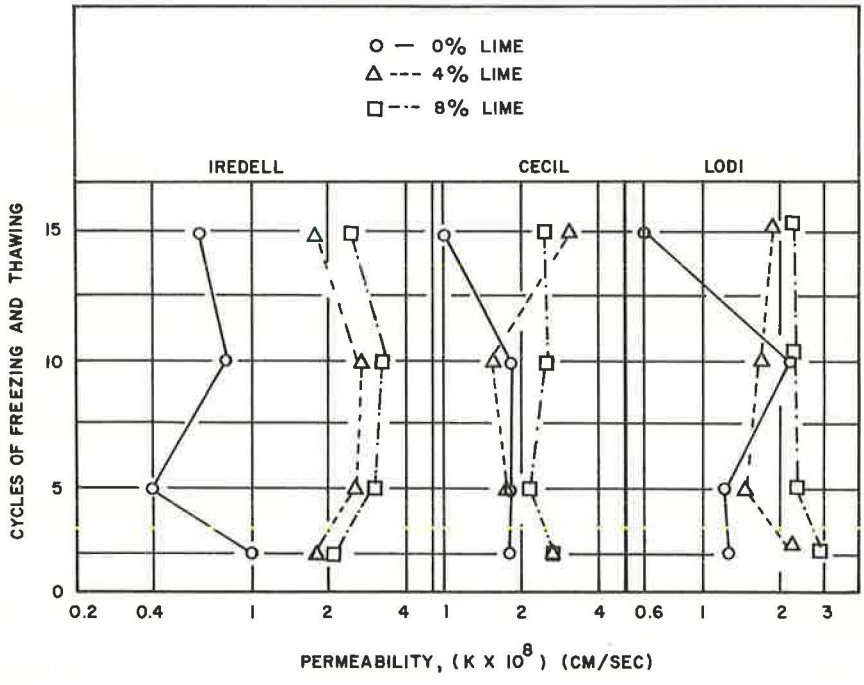

Figure 7. Effects of closed-system freezing and thawing on permeability of three stabilized soils.

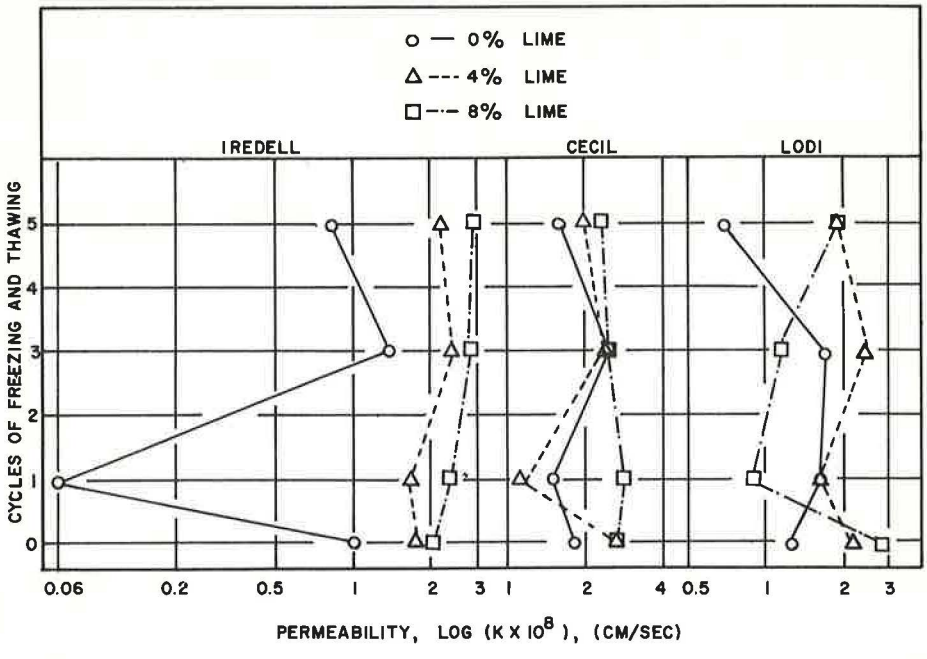

Figure 8. Effects of open-system freezing and thawing permeability of three stabilized soils.

A possible explanation of the strength regain phenomenon in the lime-stabilized specimens can be shown by further study of the pore characteristic data. Hydraulic pressures created during the freezing process may exceed the tensile strength of the pore structure of the stabilized soil specimens resulting in a general enlargement of the pores. With the larger pores present, the hydraulic pressures were minimized thus permitting healing of the Cecil and Lodi soils, which may have had excess lime available for continued curing to take place. However, this hypothesis cannot be proved by the data shown because the data are somewhat erratic and only show a general trend.

Permeability

The permeability data are also erratic, but Figures 7 and 8 show some evidence of permeability increases when lime is added to the soil, particularly with the Lodi soil. Also, for the stabilized soils, some small increase in permeability occurred with increased cycles of freezing and thawing.

SUMMARY

The results of this study can best be summarized by focusing attention on the strength data. Freezing and thawing initially sharply decreased the strength of all specimens, but the Lodi and Cecil soils recovered much of the strength loss in later cycles. It is possible that unused lime in these soils permitted fairly rapid self-healing. The Iredell soil, which did not show strength recovery, still had greater strength than its unstabilized companion specimens.

Pore characteristic and permeability data, although somewhat erratic, showed certain trends that indicated that freezing and thawing opened up the pores, reducing the damaging effects of later freeze-thaw cycles. Additions of lime clearly increased pore size and permeability.

REFERENCES

1. Walker, R. D., and Karabulut, Cetin. Effect of Freezing and Thawing on Unconfined Compressive Strength of Lime-Stabilized soils. Highway Research Record 92, p. 1-11, 1965.

2. Powers, T. C. A Working Hypothesis for Further Studies of Frost Resistance of Concrete. Proc. ACI, Vol. 41, p. 245-276, 1945.
3. Walker, R. D., Esmer, Erkan, and Krebs, R. D. Strength Loss in Lime-Stabilized Clay Soils When Moistened and Exposed to Freezing and Thawing. Highway Research Record 198, p. 1-8, 1967.
4. Anday, M. C. Curing Lime-Stabilized Soils. Highway Research Record 29, p. 13-26, 1963.
5. Lewis, D. W., Dolch, D. R., and Woods, K. B. Porosity Determinations and the Significance of Pore Characteristics of Aggregates. Proc., ASTM, Vol. 53, 1953.

Rhode Island 214—Soil-Cement Test Section

G. L. RODERICK, University of Wisconsin—Milwaukee; and
M. T. HUSTON, University of Rhode Island

An 0.8-mile test road with two control sections and five test sections with cement modified subbases, soil-cement bases with and without Na_2SO_4, and rock base, was constructed the summer of 1967. Moisture-temperature cells were installed at selected sites. Final cement contents were greater than the design because of difficulty in attaining full-depth processing. Benkelman beam deflections were less on control sections and greater on other sections in the spring than in the fall. Pavement roughness improved in the same period. Base courses had primary influence on plate bearing deflections; sections with Na_2SO_4 in the base were less rigid than those without. Surface cracks developed, due to temperature contraction of bases, in all sections with soil-cement bases; the amount of cracking was related to pavement rigidity. Sections with rock bases did not crack. No frost heave occurred. The maximum depth of frost penetration was 19 in. on two brief occasions. Subgrade moisture varied by 2 to 6 percent with lows in fall and highs in spring. Cement-treated subbase moisture was low in fall and high in spring, whereas gravel borrow subbase moisture remained constant. The overall condition of the road is good. Observations are to be continued.

•IN 1963 a laboratory study was initiated to determine the best practical method of stabilizing the abundant silty soils of Rhode Island. Study of various trace chemicals with portland cement led to the conclusion that Na_2SO_4 was the most beneficial. The results of the study have been detailed by Nacci, Moultrop and Huston (1). To confirm or modify the conclusions of the laboratory study, and to determine the feasibility of using soil-cement road construction in Rhode Island, an experimental test road was constructed and is being evaluated. This paper presents some of the results obtained to date.

DESCRIPTION OF THE TEST ROAD

The test road is an approximately 0.8-mile section of R. I. 214, a state secondary road, in Middletown, Newport County. This area normally has considerable frost action. The roadway is 44 ft wide, consisting of two 12-ft traffic lanes and two 10-ft shoulders of the same structural design. Figure 1 shows a schematic presentation of the base and subbase composition of each of the seven sections; each is surfaced with 3 in. of bituminous concrete. The control sections are of the normal state design; the test sections were designed to be of like capacity. Cement contents of the base courses were determined by Portland Cement Association test methods (2).

During construction, soil moisture cells (Soiltest MC-310A) were installed beneath the centerline and 11 ft either side of centerline at stations 16 + 00, 22 + 00 and 26 + 00 (sections 3, 4 and 5). In sections 3 and 5, the cells were installed at depths of 6, 11, 15, 19 and 24 in. beneath the surface; in section 4 the depths were 11, 15, 19 and 24 in. Periodic

Paper sponsored by Committee on Soil-Portland Cement Stabilization and presented at the 48th Annual Meeting.

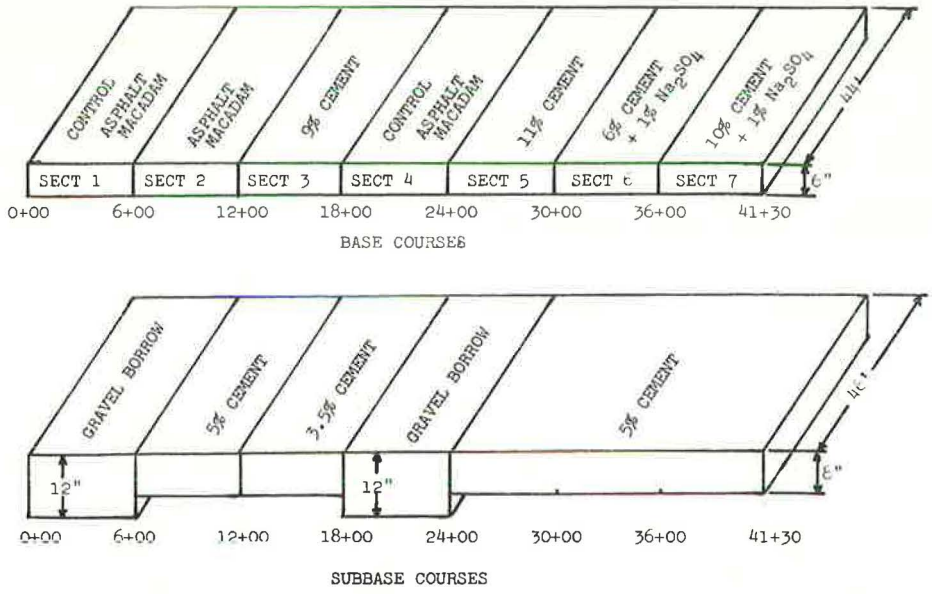

Figure 1. Composition and sequence of test and control sections.

resistance readings of the cells are converted to temperature and moisture contents. Well points were installed at each side of the road at the instrumented sites for observation of water table fluctuations.

Only the C horizon material at the site was used for construction of cement-treated bases and subbases; the B horizon soil contained organic material detrimental to cement reactions. The glacial till was quite stoney; stone sizes ranged from boulders with maximum dimension of about 2 ft to gravel. The maximum stone sizes allowed in the finished cement-treated courses were 4 in. in the subbases and 3 in. in the bases. Table 1 gives the properties of a typical soil of the group. Classifications ranged from A-2-4 to A-4(3), predominantly A-4.

Type 1 portland cement was used throughout. Sodium sulfate was supplied in granular form.

CONSTRUCTION

Specifications for construction of test sections were modified from PCA suggestions (3); detailed specifications were included in the initial-preconstruction report (4).

TABLE 1

PHYSICAL PROPERTIES OF TYPICAL SOIL

Textural composition:	
Gravel (3 in.-2.00 mm), %	20.5
Sand (2.00-0.074 mm), %	29.5
Silt (0.074-0.005 mm), %	46.0
Clay (0.005 mm), %	4.0
Consistency limits:	
Liquid limit, %	21.2
Plastic limit, %	NP
Classification	
Textural	Gravelly silt-loam
AASHO	A-4(3)
Optimum moisture (with 9% cement), %	12.0
Maximum dry density, pcf	125

Since only C horizon material was to be used in cement treatment, it was removed and stockpiled in the fall of 1966. The B material was placed in the subgrade. After a rainy spring, construction of subbases began in late June 1967. Because of the stoney nature of the material it was necessary to screen it before replacing it on the area from which it was taken.

Pulverization and mixing of the materials was done in place with a Trav-L-Plant multiple-pass rotary mixer. A bulk cement truck with a compressed air distributing system and a pressure distributor truck were used for applying cement and water to the roadway. Normally, one section (600 ft) of subbase or base was constructed

TABLE 2

CEMENT CONTENTS OF SUBBASES AND BASES

Section	Station	Cement (% dry wt soil)		
		By ASTM	Field Estimate	Design
Subbase				
Sect 2	7 + 50	7.5	5.5	5
	10 + 50	7.5		
Sect 3	13 + 50	—	3.5	3.5
	16 + 50	4.0		
Sect 5	25 + 50	8.9	5.2	5
	28 + 50	10.6		
Sect 6	31 + 50	6.8	5.4	5
	34 + 50	11.2		
Sect 7	37 + 50	6.8	5.3	5
	39 + 50	5.8		
Base				
Sect 3	13 + 50	21.0	9.5	9
	16 + 50	15.8		
Sect 5	25 + 50	20.5	10.8	11
	28 + 50	11.5		
Sect 6	31 + 50	—	6.5	6
	34 + 50	7.6		
Sect 7	37 + 50	12.2	10.3	10
	39 + 50	9.6		

per day. Each section was processed in 5 or 6 strips, 8 to 9 ft wide; compaction of one strip was concurrent with processing of the adjacent one. Na_2SO_4 was added to the bases of sections 6 and 7 with the mix water. The water in the distributor was heated to 120 F, bagged Na_2SO_4 dumped in to give a 20 percent solution, and the material kept circulating in the tank. No difficulty was encountered in keeping the Na_2SO_4 in solution.

Cement-treated subbases were finished on July 5, bases on July 10, rock bases on July 13 and the surface on July 27, 1967. Rain hampered construction on occasion. In particular, the last soil-cement base strip to be processed, the right shoulder of section 6, was drenched by a downpour after mixing. Compaction was delayed for several hours and was inadequate; however, the section was left in that condition.

No difficulty was met in meeting the pulverization requirements. Two passes of the truck per processing strip were usually required to spread the cement. Cement spread was checked on each pass by weighing the amount caught on a canvas of known area. Samples were taken, over the full depth, from the processed material for subsequent cement content determinations by the ASTM method (D806-57). Table 2 gives determined cement contents and the average of field checks. Determined cement contents are consistently higher (and in some cases considerably higher) than field estimates. Although this may be partly due to the inadequacy of the cement content test, the larger discrepancies were apparently caused by failure to obtain mixing to the full depth intended. Cores taken after construction showed in many cases that the bottom inch or more was more weakly cemented. The rotor blades of the mixer should have been replaced more frequently.

In applying water with Na_2SO_4 in the bases of sections 6 and 7 it was found that less water (solution) was required to obtain optimum compaction moisture. Therefore, the amount of Na_2SO_4, based on field application, was about 0.8 percent rather than the 1 percent design.

A light steel-wheeled roller was used on the initial compaction pass to push down stones; subsequent compaction was with a pneumatic roller. In all cases compaction was above the specified 95 percent, with an average of 99 percent of maximum density attained.

The moist base course soil was used as curing material for completed subbases. Completed bases were covered with a bituminous seal. A thin layer of sand prevented pick up of the seal by construction equipment. Sections with Na_2SO_4 appeared to harden more rapidly than those without.

POSTCONSTRUCTION FIELD TESTS

The test road will be under observation for a number of years. A program of periodic field tests and condition studies will be conducted. The following is a discussion of the results through June 30, 1968.

Traffic Count

During the week of January 11-17, 1968, an automatic traffic counter was used. The WADT was 4182 vehicles; 71 percent of the traffic was between 7:00 a. m. and 6:00

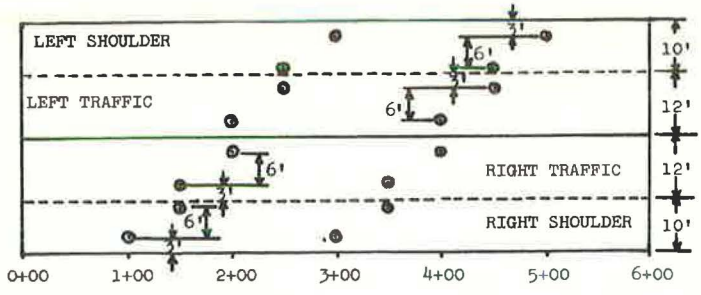

Figure 2. Layout of Benkelman beam deflection test sites.

p. m. On May 2, a visual count of traffic and vehicle types was made between 7:00 and 6:00. The total was 3365 vehicles of which less than 3 percent were trucks with dual wheels.

Benkelman Beam Deflection Test

Benkelman beam deflections were obtained at permanently marked sites August 9-11, 1967, and again April 4, 1968. Figure 2 shows the location of the 16 test sites of section 1; all other sections were tested at like points.

A modified Canadian Good Roads Association test procedure was used. Rebound surface deflections were measured with the dual wheels over the beam probe and at 2, 4, 6, 8.83 and 50 ft ahead of it. The truck had 11-in. x 20-in. 12 PR dual tires at 13.5 in. center-to-center spacing and 72 in. between centers of duals. Tire pressures were maintained at 80 psi; the rear axle load was an evenly distributed 18,000 lb. During testing the air temperature varied from 64 to 89 F in the fall and 59 to 73 F in the spring; pavement temperature varied from 72 to 103 F in the fall and 57 to 95 F in the spring. Table 3 gives the results for both series of tests. Figure 3 shows mean deflection data.

The two control sections gave smaller average deflections under a 9000-lb wheel load in the spring than in the fall. All other sections gave larger deflections, including section 2 with a rock base over cement-treated subbase. This suggests the difference in deflection behavior is due to the subbase; decreased deflection in control sections may be due to densification of the subbase under traffic. The moisture of the gravel borrow subbase remained nearly constant while that of cement-treated subbase was greater in the spring.

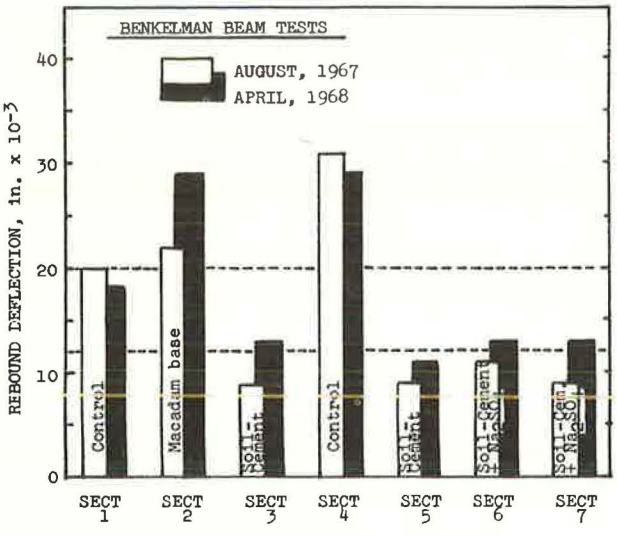

Figure 3. Mean Benkelman beam deflections.

Reasonable allowable deflections of 0.020 in. for sections with granular bases and 0.012 in. for sections with soil-cement bases were assumed on the basis of suggestions elsewhere (5). The dashed lines in Figure 3 represent these allowable values. In August, only sections 2 and 4 exceeded the allowable, but in April mean deflections were greater than allowable for all but sections 1 and 5. More detailed study of the data revealed that, in all cases, the April deflections were greater than allowable in the outer

TABLE 3

BENKELMAN BEAM DEFLECTION TEST RESULTS

Section	Mean Max. Defl, $\bar{D}$ (in. × 10^{-3})		Standard Deviation, σ (in. × 10^{-3})		Coeff. of Variation, V (%)	
	Aug 67	Apr 68	Aug 67	Apr 68	Aug 67	Apr 68
1	20	18	7	7	34	37
2	22	29	14	11	64	36
3	9	13	4	6	49	49
4	31	29	6	8	20	29
5	9	11	3	6	40	54
6	11	13	5	4	44	34
7	9	13	3	5	32	40

wheelpath of the shoulders; however, deflections were less than the allowable in the inner wheelpath and traffic lanes of sections 1, 3, 5 and 6 and in the traffic lanes of section 7. Sections 2 and 4 had greater than allowable deflections in all lanes, both fall and spring; again, the largest values were in the outer wheelpaths of the shoulders.

Roughometer Tests

Roughometer tests, with a BPR-type roughometer, were conducted on August 16-17, 1967, and again on May 14, 1968. Figure 4 shows the results in terms of the roughness index, RI, for the traffic lanes. Each RI value is the average of several runs. The riding quality of the pavement improved, with the exception of section 7. The reason for the increased roughness of section 7 is not apparent; however, the event marker of the roughometer was inoperative during the May test and a portion of the accumulated deflection assigned to section 7 may belong to section 6. The sum of RI values for the two sections is less in May in the southbound lane and only slightly higher in the northbound.

The improvement in riding quality is probably due to smoothing of surface irregularities by traffic. One run on each shoulder in May showed that these lanes, with less traffic, had a higher RI than traffic lanes in most cases.

Studies in Illinois (6) relate RI to the riding quality of flexible pavements as:

RI< 60—very good, smooth
60<RI<105—good, smooth to slightly rough
105<RI<145—fair, rough

On this basis section 7 rates fair while all other sections are good.

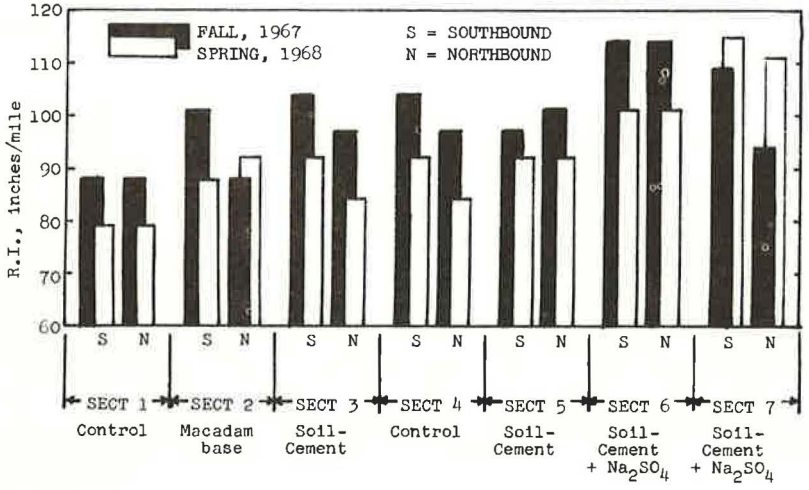

Figure 4. Roughometer test results.

Plate Bearing Test

Nonrepetitive plate bearing tests were conducted on the pavement surface of all sections between March 14 and April 4, 1968. During this period the moisture in the subgrade remained fairly uniform and there was no frost in the road. Air temperatures during testing varied from 24 to 58 F.

Tests were made at two sites on each section on the line dividing shoulders and traffic lanes, 150 ft from each end of the section, once on the right and once on the left. Loads were applied to a 12-in. diameter rigid plate by means of a hydraulic jack reacting against a large dump truck filled with sand. Surface deflections were taken at two points on the circumference of the plate.

Figure 5 presents results, after correcting loads for deadload and gage calibration, for 5 load increments. Deflections for control section 4 were considerably larger than for control section 1. This is probably due to a soft subbase condition at time of completion of the base course; a portion of section 4 near station 19 + 50 was barricaded against heavy equipment at that time. Comparison of deflections for control section 1 and section 2, rock base with 5 percent cement-treated subbase, indicates the difference in subbase had little effect on deflections. Nearly the same values were obtained for the rock base over 12 in. of gravel borrow and 8 in. of cement-modified soil.

Sections 3 and 5, with soil-cement base, gave smaller deflections than sections 6 and 7, with soil-cement plus Na_2SO_4. The relatively large deflection at station 31 + 50 (section 6) was probably due to the rain and delayed compaction as mentioned earlier. No reason is apparent for the relatively large deflections of section 7; it is hoped cores scheduled to be taken from the roadway will yield an explanation. From the present data, it appears sections with Na_2SO_4 are less rigid than those without. However, this apparent lesser rigidity may be due to the temperature cracking pattern developed during the winter months. Unfortunately, plate bearing data were not obtained before winter.

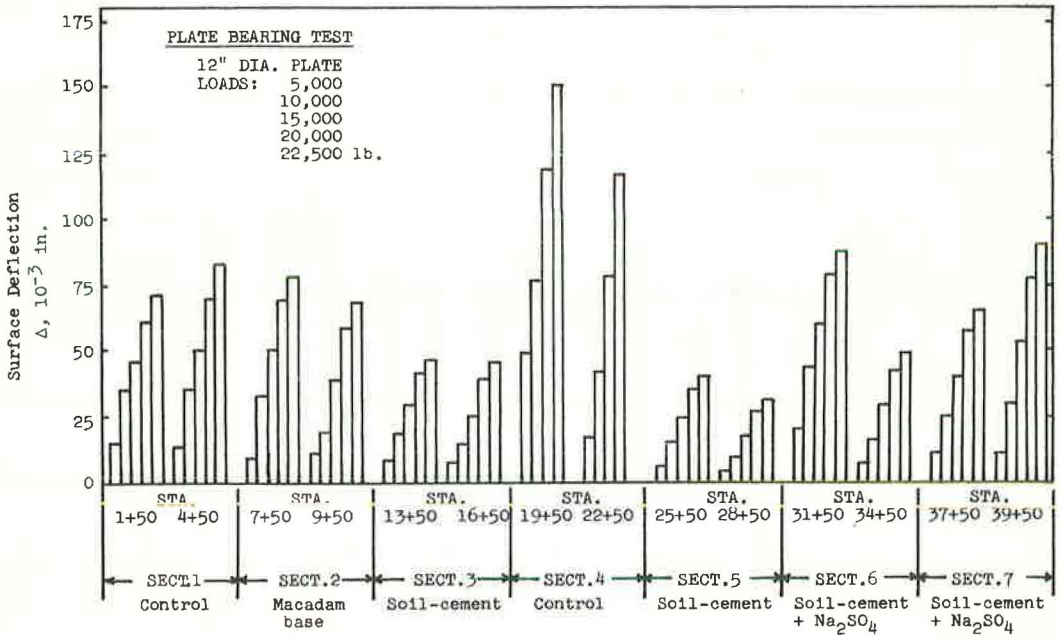

Figure 5. Plate bearing test results, spring 1968.

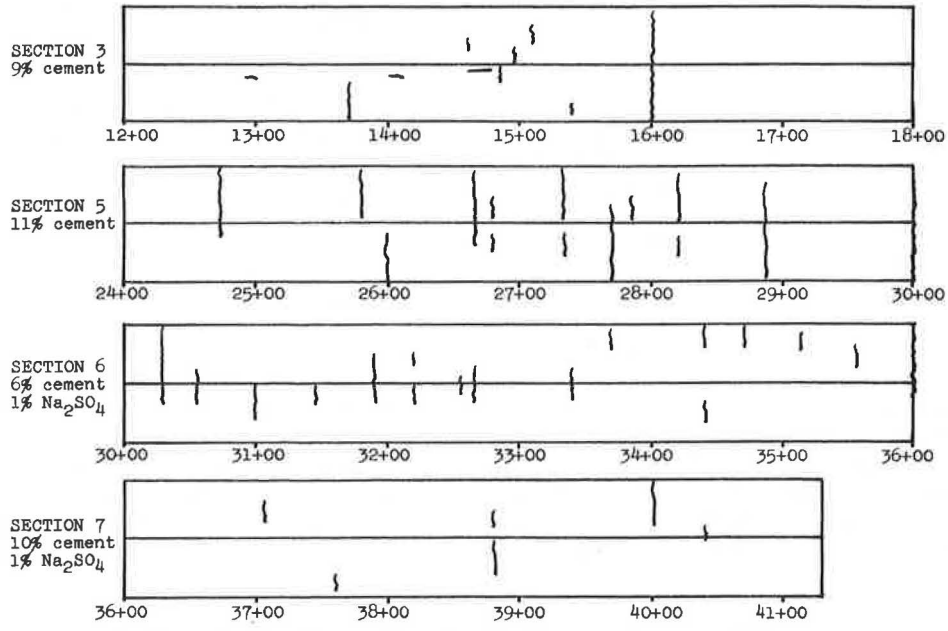

Figure 6. Location and lengths of surface cracks, spring 1968.

Crack Survey

The first cracks to develop in the pavement surface were noted on January 8 during the first cold period of the winter. Subsequent cracking occurred during the remainder of the winter, again primarily during cold periods. On April 4, a crack survey was made with width, length and position of all surface cracks recorded. Figure 6 shows the position and relative lengths of cracks in the sections affected. Table 4 summarizes results of the study. Section 3 also had 38 ft of longitudinal cracks.

All cracks were from 0 to $\frac{1}{8}$ in. wide, displayed very little or no raveling, and once developed there was no increase in width. There was no detectable differences of elevation on the two sides of cracks, i.e., they did not result from heave. Since no cracks developed in sections with rock bases, and since cracking occurred in cold weather, it was concluded the cause was temperature contraction of soil-cement bases. The first cracks developed at the instrumentation sites at stations 16 + 00 and 26 + 00, apparently due to weak zones resulting from installation of moisture cells.

There is an apparent correlation between surface cracking and plate bearing test results. Section 5, with a soil-cement base, developed the greatest amount of surface cracks and is also the most rigid as shown by plate bearing results. Section 7, with soil-cement plus Na_2SO_4 base, had the least cracking and the least apparent rigidity. Presumably, the sections with lesser amounts of surface cracking developed a greater number of small cracks which were not reflected through the wearing surface. Whether or not this cracking pattern was the result of a lesser base rigidity, the influence of Na_2SO_4, or some other factor, is not known. No plate bearing tests were made before the cracks de-

TABLE 4

TRANSVERSE CRACKS, APRIL 1968

Section	Cracks (ft)	Percent of Total
1	0	0
2	0	0
3	133	20.2
4	0	0
5	279	42.5
6	198	30.1
7	47	7.2
Total	657	100.0

TABLE 5

RANGE OF SUBGRADE MOISTURES

Station	Depth (in.)	Moisture (%)		
		Right	Center	Left
16 + 00	19	13.0-15.0	14.0-17.0	13.0-16.0
Soil-cement	24	12.0-15.0	12.5-18.5	12.5-16.0
22 + 00	24	20.5-24.0	17.5-20.5	18.0-23.0
Control				
26 + 00	19	14.5-18.5	14.5-16.5	12.5-15.5
Soil-cement	24	14.5-18.5	15.0-17.0	12.5-15.5

veloped; therefore, the apparent rigidity may be due to the cracking mechanism or vice versa.

After a period of hot weather, many of the surface cracks noted in April have closed and are no longer visible.

Frost Action

Continuous air temperature data were obtained from a weather station near the test site. Analysis of the records established a freezing index of 325 degree-days for the winter of 1967-68. The lowest temperature was -5 F on January 9, the only time below zero. Pavement temperature measurements at stations 16 + 00, 22 + 00 and 26 + 00 showed that freezing temperatures penetrated more than 6 in. for only two brief periods, January 6-15 and February 13-22. The maximum measured depth of penetration was 19 in. each time and this depth was not maintained for more than a day or two.

There was no evidence of frost heave at any time in any section. Periodic checks of surface elevation showed no change.

Subgrade Moisture

As expected, subgrade moisture fluctuated to some extent throughout the test period. Moisture cell readings were taken at least twice weekly and more often during the winter months. In general, low moisture contents occurred in late September and during the January freeze period. The higher moisture contents were in late March and early April. Table 5 gives the maximum and minimum subgrade moisture at each instrumented site.

The greater than design cement content of cement-treated subbases changed the resistance properties of the material so resistance readings could not be converted to

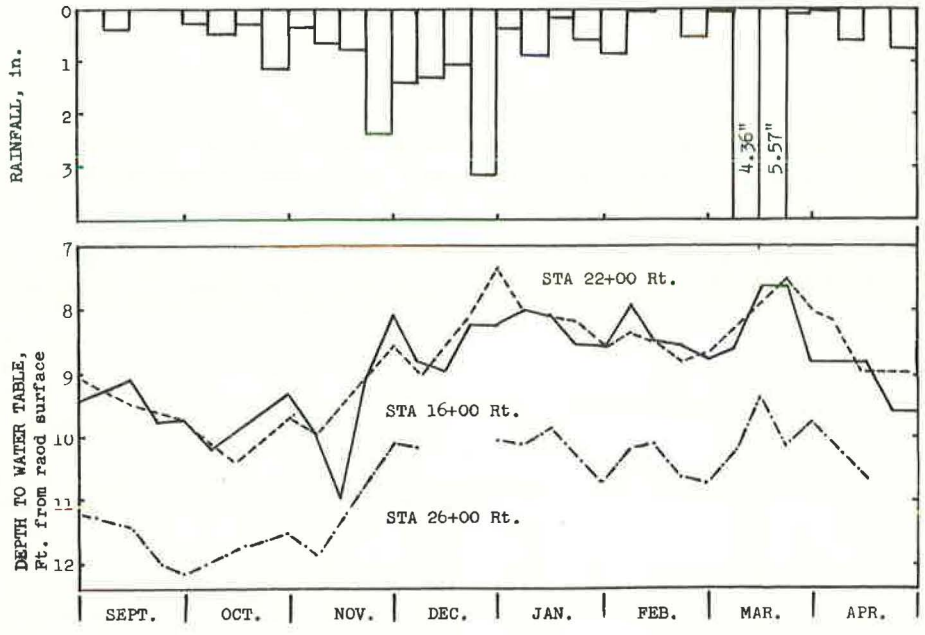

Figure 7. Water table fluctuation and rainfall.

moisture contents. Also, the gravel borrow material for control subbases was not available in time to establish moisture cell calibrations before the cells had to be installed. However, resistance readings do indicate the direction of moisture change if not magnitudes. Resistance data show that the cement-treated subbases had their lowest moisture in the fall and highest in the spring, and the gravel borrow subbase maintained a nearly constant moisture since shortly after completion of construction.

Since the first surface cracks appeared at the instrumented sites, resistance readings in the soil-cement bases reflect moisture accumulation in the cracks rather than any change in the base itself.

The depth to the water table was measured at 4 ft from each edge of the pavement at each of the instrumented sites. The lowest water table occurred in late September-early October and the highest in late December and late March. Figure 7 shows partial results. The depth of the water table on the right (downhill) side of the road and accumulated rainfall are plotted at one-fourth month intervals. Rises in the water table occurred with or shortly after periods of substantial rainfall.

SUMMARY

1. Cement Content—Determination of cement contents, by ASTM D806-57, were consistently greater than estimates from field checks during cement application. The larger discrepancies were due to insufficient depth of mixing.
2. Traffic—The WADT is 4182 vehicles, of which less than 3 percent are trucks with dual wheels.
3. Benkelman Beam—Control sections deflected less in spring than in fall while all other sections deflected more. Apparently subbases of control sections became more stable under traffic.
4. Roughometer—Pavement riding qualities improved during the test period due to smoothing of surface irregularities by traffic.
5. Plate Bearing—Base courses had primary influence on deflections. Sections with soil-cement plus Na_2SO_4 appear to be less rigid than sections with soil-cement alone.
6. Cracks—No surface cracks appeared in sections with rock bases. Cracks caused by temperature contraction of base slabs occurred in all sections with soil-cement bases. There is an apparent correlation between cracking and plate bearing deflections.
7. Frost Action—There was no evidence of frost heave. The maximum frost penetration depth was 19 in. for only two brief periods.
8. Pavement Moisture—Subgrade moistures fluctuated by 2 to 6 percent; the lows were in September and January and the highs in March-April. Cement-treated subbase moisture was low in fall and high in spring, while rock borrow subbase moisture remained nearly constant. Depth to the water table correlated well with rainfall.

CONCLUSIONS

On the basis of the partial results obtained at the time of writing, the following conclusions and observations are made:

1. Rhode Island silts of the type encountered on this project can be adequately stabilized for highway purposes by addition of cement or cement plus sodium sulfate. For the amount and type of traffic using the road, adequate stability could probably have been attained with lesser amounts of cement than were used.
2. The objective of determining the long-range effects of sodium sulfate must await further observations. Inclusion of sodium sulfate apparently accelerates the initial cement reactions leading to greater early strengths. There is some indication that sodium sulfate may influence the temperature cracking pattern of soil-cement bases; however, further testing is needed.
3. Although the anticipated costs of control and test sections were comparable, actual construction costs are not yet available. For this project, it is felt that actual construction costs for the soil-cement (and sodium sulfate) test sections may be considerably higher than those for the control sections.

ACKNOWLEDGMENTS

The research reported was done by the Division of Engineering Research and Development, University of Rhode Island. The work was sponsored and supported by the Rhode Island Department of Public Works and the United States Department of Transportation, Federal Higheay Administration, Bureau of Public Roads, under Project HPR-1(3), BPR Study No. 2, The Stabilization of Silty Soils.

The opinions, findings, and conclusions expressed in this publication are those of the authors and not necessarily those of the Bureau of Public Roads.

REFERENCES

1. Nacci, V. A., Moultrop, K., and Huston, M. T. Stabilization of Silty Soils With Portland Cement and Sodium Sulfate. Univ. of Rhode Island Eng. Bull. No. 9, Aug. 1966.
2. Soil-Cement Laboratory Handbook. PCA, 1959.
3. Suggested Specifications for Soil-Cement Base Course. PCA.
4. Initial-Preconstruction Report. Submitted to Rhode Island DPW and USBPR, Univ. of Rhode Island, June 17, 1966.
5. Carneiro, B. L. Benkelman Beam—Auxiliary Instrument of the Maintenance Engineer. Highway Research Record 129, p. 28-55, 1966.
6. Chastain, W. E., and Burke, J. E. Experience with a BRP-Type Roadometer in Illinois. HRB Bull. 328, p. 52-58, 1962.

Cracking in Pavements Influenced by Viscoelastic Properties of Soil-Cement

K. P. GEORGE, University of Mississippi

To develop a better understanding of shrinkage cracking (which is known to be time-dependent) of pavement layers, the author believes that the material should be considered to be viscoelastic rather than elastic. A step is taken in this direction when a viscoelastic model is proposed for setting up the stress-strain-time laws for soil-cement. Results of a series of constant stress creep tests indicate that the Burgers model shows the greatest promise in mechanical simulation of actual soil-cement behavior. Rheological parameters that control the soil properties are evaluated from the test data. The experimental study of creep has proved beyond doubt that creep and shrinkage are not independent phenomena. That is, the soil-cement which exhibits high shrinkage also shows generally a high creep.

The implications upon the crack spacing and crack width of the hypothesis that the stress-strain relation tends to be time-dependent are discussed. The fact that shrinkage stresses developed in a viscoelastic material are on the average about 50 percent smaller than those in a comparable elastic material is significant insofar as crack frequency is concerned. Evidence is overwhelming that rapid shrinkage favors large stresses in the material. The agreement between the observed or reported values of crack width and that computed according to the viscoelastic theory is excellent.

In predicting the behavior of pavement layers subjected to ambient conditions, the viscoelastic approach is superior to any known elastic or empirical laws. The results show convincingly that cracking of cement base can be controlled by adequate extended curing.

•THROUGH the use of stabilizing agents, locally available road materials are currently being stabilized for economical highway construction. Of the dozen or so different materials reported in the literature, those most commonly used are cement, lime, lime-fly ash, and asphalt. Although it is generally believed that under field conditions the behavior of the resulting material tends to be inelastic, all of the available methods employed to estimate the stresses in the bases and subgrades are based on the conditions of ideal elastic behavior. There is a great need, therefore, for a systematic investigation of the stress-strain-time relationships (simply known as creep) of these materials. Creep is defined as the total time-dependent deformation of the material due to load. A knowledge of the creep in stabilized soils is particularly valuable in the study of the drying shrinkage and the resulting cracking by virtue of the hypothesis that shrinkage and creep are interdependent phenomena.

The principles of viscoelasticity have been successfully used to explain the mechanical behavior of high polymers and much basic work (1) has been accomplished in this area. Mechanical models used to describe the deformation-time behavior under stress consist of combinations of elementary units of springs and dashpots in series or parallel. The relationship between stress σ and strain ϵ, respectively, for the spring

Paper sponsored by Committee on Soil-Portland Cement Stabilization and presented at the 48th Annual Meeting.

and the dashpot is $\sigma = E\epsilon$ and $\sigma = \eta(d\epsilon/dt)$ where E = Young's modulus (lb-in.$^{-2}$) and η = modulus of viscosity (lb-sec-in.$^{-2}$). The fundamental models of linear viscoelastic solids are the Maxwell model and the Kelvin model, which are comprised of spring and dashpot arranged, respectively, in a series and in parallel. The stress-strain-time behavior of these models is treated in standard references on viscoelasticity and, therefore, will not be discussed here.

In recent years, the theory of viscoelasticity has been employed to explain the mechanical behavior of asphalt mixtures (2, 3, 4) and soils (5, 6). The present investigation, however, is directed to the study of the viscoelastic behavior of soil-cement, and to the application of these concepts in developing a better understanding of cracking in pavements. Although the results and discussions are specially applicable to the rheological behavior of soil-cement, the concepts presented herein are considered to have a wider applicability.

A soil-cement base, or any pavement layer for that matter, which tends to contract because of shrinkage or ambient temperature, if fully or partially prevented from doing so, will be severely stressed in tension. When the stress exceeds the tensile strength of the material, the base cracks. Accordingly, George (7) has presented simplified solutions to the crack-spacing and crack-width problem. In this study, it is assumed that the material is perfectly elastic. The implications of a more realistic hypothesis that the stress-strain relation tends to be time-dependent are discussed in the present paper. Using information obtained from a series of constant stress creep tests, the author chooses an appropriate mechanical model for predicting the deformational behavior of soil-cement. Analytical solutions, showing the influence upon crack spacing and crack width of the rheological parameters of the material, will be presented. The predicted value of the crack width is compared with that obtained from field observations. Using the rheological model, the researcher extends the theoretical study to bring out the effect of shrinkage rate upon the ambient stress and in turn the cracking.

MATERIALS AND METHODS

Materials

The scope of the study made it necessary to restrict the laboratory investigation to tests on two soils. Table 1 gives compositional data and a brief statement of physical properties. Grain-size distribution of these soils is illustrated elsewhere (7, Fig. 3, p. 62). For convenience, each soil is identified by a one letter-two digit system, for example K03 means soil No. 3 with kaolin as the predominant clay mineral.

Type I portland cement and distilled water were used in preparing test cylinders.

Sample Preparation

The procedure for preparing the soil and blending the soil-cement mixture has been described elsewhere (8). The test cylinders, 2.8 in. in diameter and 8.4 in. high, were

TABLE 1

SOIL IDENTIFICATION AND COMPOSITIONAL DATA

Description	K03 (Tishomingo County, Miss.)	M30 (Vicksburg, Miss.)
Gradation (% finer by wt)		
2 mm	92	100
0.05 mm	20	92
0.002 mm	16	23
Liquid limit, %	31	37
Plastic limit	10	13
Shrinkage limit, %	20	22
Textural classification	Sandy	Silty clay
Engineering classification	A-2-4(0)	A-6-9
Predominant clay mineral	Kaolinite	Montmorillonite, illite
Optimum moisture, %	13.5	17.0
Proctor density, pcf	118.8	110.3
Maximum linear shrinkage on drying in 55% RH, in./in.	0.0025	0.0129

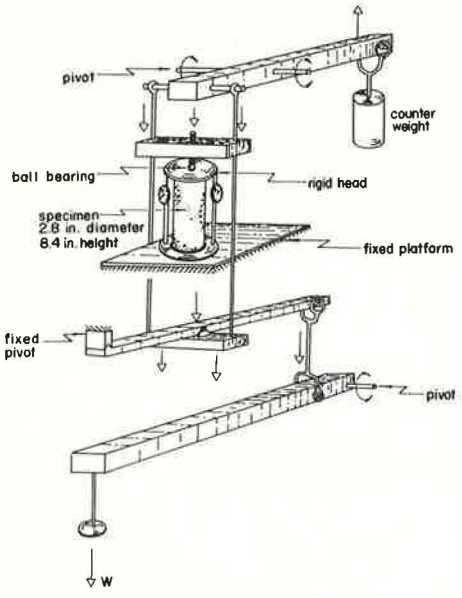

Figure 1. Schematic of loading frame to test for creep. Mechanical advantage of the lever system 40.

molded according to the ASTM Suggested Method of Making and Curing Soil-Cement Compression and Flexure Test Specimen in the Laboratory.

Apparatus and Test Procedure

The cylinders, after seven days' moist curing, were tested in a constant axial creep test in the loading frame (Fig. 1). Dial gages reading to 0.0001 in. served to measure the deformation. The sustained stress applied to the specimens approximated 50 percent of the ultimate strength.

Although creep in tension was relevant insofar as cracking in pavements was concerned, some difficulties were encountered in its experimental determination; therefore, it was decided to evaluate creep in compression. To justify this approach, the results of a 10-year study on concrete made by the U. S. Bureau of Reclamation (9) may be cited. The authors concluded that the magnitude of creep in tension and in compression was of the same order, and both were similarly affected by various factors.

DISCUSSION OF RESULTS

Although the major emphasis in this study was on evaluating the effect of creep on cracking of pavements, one important result which evolved during the experimental determination of creep warrants special mention here.

Effect of Drying Shrinkage on Creep

A brief survey of the literature on the creep of concrete revealed two prevalent points of view concerning the influence of drying shrinkage on creep. One school of thought holds that creep and shrinkage are additive. Creep is thus calculated as the difference between the total time deformation of the loaded specimen and the shrinkage of a similar unloaded specimen stored under the same conditions during the same period. The other viewpoint is that drying of moisture during a period of sustained loading influences creep. The creep results shown in Figure 2 pertain to identical soil-cement test specimens, one exposed in a 55 percent relative humidity (RH) condition (curves labeled a) and the other sealed against moisture gain or loss (curves labeled b). These results and others not reported here emphasize that creep and shrinkage are not independent phenomena.

Based on the present study, the following conclusions seem relevant. First, for a given soil-cement mixture, creep is higher the lower the relative humidity. Second, as seen from the results of soil M30, a mixture which exhibits high shrinkage generally also shows a high creep. It is hoped that more detailed results will be presented in another report (10).

In view of the finding that drying enhances creep, the author decided to perform creep tests under conditions of nearly 100 percent RH.

Influence of Creep on Shrinkage-Cracking

Shrinkage Cracking of Pavement Layers—Elastic Solution—Cracks in pavement layers may be due to the contraction caused by two factors: changes in moisture content and

ambient temperature. Since the contraction resulting from drying is more important in stabilized soils than that caused by temperature, emphasis in this study is on the cracking caused by drying shrinkage. Tension stresses can be set up in a slab as a result of linear shrinkage. If the slab is free to move (no friction between the slab and the underlying layer), stresses will not result. If friction exists between two adjacent layers, however, restraint results in the top slab from the friction forces. In long slabs the friction forces may be sufficient to cause over-stressing of the material which produces a crack. Based on these assumptions, George (7) has derived expressions for crack spacing and crack width. Respectively, these equations are

$$L_{max} = \frac{2\,\sigma_u}{\mu\gamma} \tag{1}$$

and

$$\delta_T = \epsilon_c L - \frac{\mu\gamma L^2}{4\,E_t} \tag{2}$$

where

L_{max} = slab length at which tensile stresses become critical, ft;
σ_u = ultimate tensile strength, lb-ft^{-2};
μ = coefficient of sliding friction;
γ = unit weight of material, lb-ft^{-3};
δ_T = total crack width, ft;
ϵ_c = total shrinkage, in./in.; and
E_t = modulus of elasticity of soil-cement in tension, lb-ft^{-2}.

From Eq. 1, it appears that for a specific slab placement, the crack spacing is a direct function of the tensile strength of the material; whereas from Eq. 2, it can be deduced that the crack width is primarily a function of the linear shrinkage.

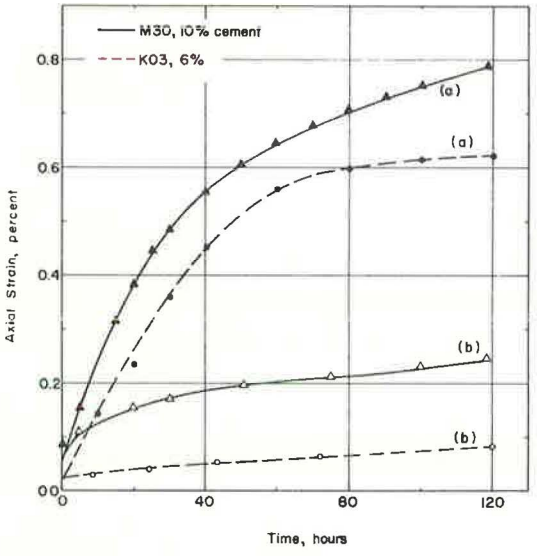

Figure 2. (a) Creep of test specimens exposed in a 55 percent RH condition; creep is calculated as the difference between the total time deformation of the loaded specimen and the shrinkage of a similar unloaded specimen. (b) Creep of test specimens sealed against moisture gain or loss—soil: silty clay (M30) at 10 percent and sand (K03) at 6 percent cement; stress level: 50 percent of ultimate, 165 and 195 psi, respectively.

Some approximate calculations for crack spacing and crack width were made with the soil properties chosen as follows: Soil K03 with 6 percent cement is calculated to have a tensile strength of 33 lb-in.$^{-2}$ (60 percent of the laboratory strength), a unit weight of 119 lb-ft^{-3}, a shrinkage of 0.0010 in./in. (8), and a modulus in tension of 66,000 lb-in.$^{-2}$. The coefficient of subgrade resistance was assumed to be 3.0 (11). Calculations show that L_{max} = 27 ft, and δ_T = 0.238 in. When the computed quantities were compared with those observed in the field, there was reasonable agreement between the predicted and observed values of crack spacing. So far as crack width was concerned, however, the agreement was extremely poor. For example, the measured crack width ranged from 0.02 in. to 0.10 in., which bracketed the average value of 0.02 in. reported by Marshall (12).

The disparity in results can be attributed to the fact that in deriving Eqs. 1 and 2, it is tacitly assumed that cement-treated soil is perfectly elastic. This assumption may not be valid. The following discussion, therefore, is an

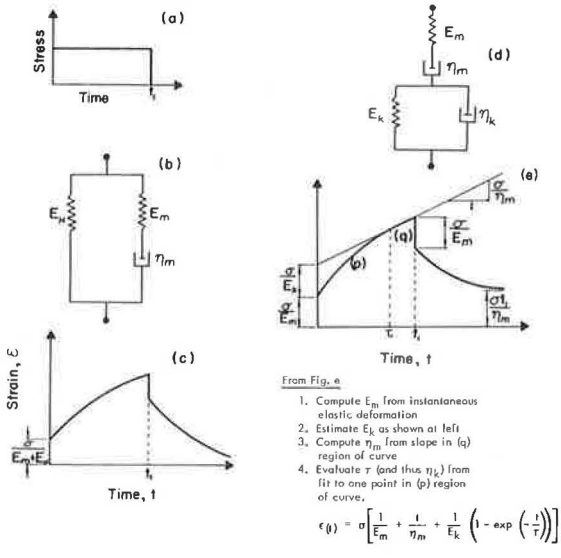

Figure 3. Strain-time relationship for the linear and the Burgers models: (a) assumed load-time relationship; (b) the linear model; (c) strain-time relationship for the linear model; (d) the Burgers model; and (e) strain-time relationship for the Burgers model.

attempt to rationalize these expressions, based on a realistic hypothesis that the material is viscoelastic.

Rheological Model for Soil-Cement—As stated previously, the theory of viscoelasticity is concerned with the relation between strain as a function of time and stress as a function of time. To illustrate this behavior conveniently, several mathematical models have been proposed. A model that is to represent accurately the mechanical properties of the material should contain certain elements that simulate the major characteristics (elastic, inelastic and/or time-dependent strain) observed in various mechanical tests. Besides the Maxwell fluid and the Kelvin solid, there are numerous ways of systematically building up more complicated models. Of these composite models, the linear model and the Burgers model have been chosen for further study and verification. To illustrate their suitability to predict the behavior of soil-cement, typical results of tests on a particular mixture are also presented.

The linear model is obtained by adding a Maxwell model to a Hookean model in parallel, as shown in Figure 3b. The behavior of this system simulates a material with a continuous skeletal structure. The coupled parallel Maxwell unit serves to transfer the load to the elastic elements in the model following the relaxation or lag time dictated by the Newtonian model. The general strain-time curve, for a constant stress applied at t = 0, is given in Figure 3c. When this curve is compared to that for a typical soil-cement mixture (Fig. 4, data points) the drawback of this model is apparent in that the removal of σ after a certain period of time, say $t = t_1$, will cause the model to regain the lost strain. This is governed by the relaxation time. The linear model, therefore, is abandoned and will not be further discussed here.

The Burgers model combines in a series the Kelvin and Maxwell models as shown in Figure 3d. In the phenomenological theory of linear isothermal viscoelasticity the constitutive law for the Burgers model is

$$\sigma + \frac{\eta_m E_k + \eta_m E_m + \eta_k E_m}{E_m E_k}\frac{d\sigma}{dt} + \frac{\eta_m \eta_k}{E_m E_k}\frac{d^2\sigma}{dt^2} = \eta_m \frac{d\epsilon}{dt} + \frac{\eta_m \eta_k}{E_k}\frac{d^2\epsilon}{dt^2} \qquad (3a)$$

where

ϵ = strain, in./in.;
σ = stress, lb-in.$^{-2}$;
t = time, sec;
E = modulus of elasticity, lb-in.$^{-2}$;
η = modulus of viscosity, lb-sec-in.$^{-2}$.

Subindices refer to model elements in Figure 3d.

This equation can be written in the normalized form:

$$\sigma + p_1\dot{\sigma} + p_2\ddot{\sigma} = q_1\dot{\epsilon} + q_2\ddot{\epsilon} \qquad (3b)$$

in which

$$p_1 = \frac{\eta_m E_k + \eta_m E_m + \eta_k E_m}{E_m E_k}; \quad p_2 = \frac{\eta_m \eta_k}{E_m E_k}; \quad q_1 = \eta_m; \quad q_2 = \frac{\eta_m \eta_k}{E_k}$$

The solution of Eq. 3a for strain ϵ for a constant stress σ acting between $t = 0(=t_0)$ and $t = t_1$ is

$$\epsilon(t) = \sigma \left[\frac{1}{E_m} + \frac{t}{\eta_m} + \frac{1}{E_k} \left(1 - \exp(-t/\tau) \right) \right] \tag{4}$$

for $t_0 \leq t \leq t_1$. The value $\tau = \frac{\eta_k}{E_k}$ is called the relaxation time. If the stress σ is released at $t = t_1$, the total strain would be governed as follows:

$$\epsilon(t_1) = \sigma \left[\frac{1}{E_m} + \frac{t_1}{\eta_m} + \frac{1}{E_k} \left(1 - \exp(-t_1/\tau) \right) \right] \tag{5}$$

The first term on the right-hand side of Eq. 5 represents the elastic deformation from the Hookean element in the Maxwell model. The permanent deformation, or set, is given by the second term on the right-hand side. The Kelvin model (third term) plays its part in the aftereffects of load or stress survival as shown in the stress-strain-time diagram shown in Figure 3e.

The few characteristic results of soil-cement, which furnished strong clues as to the suitability of the Burgers model in the investigation, are that (a) the instantaneous recovery in the specimens (Fig. 4) is nearly the same as the instantaneous elastic deformation, and (b) the specimens subjected to various amounts of creep exhibited the same amounts of elastic recovery. It is hypothesized, therefore, that Burgers model shows the greatest promise in mechanical simulation of actual soil-cement behavior.

Experimental Verification of Rheological Model—The viscoelastic constants (E_m, E_k, η_m, η_k) for the four-element model are most easily approximated from the results of a creep test described in Figure 3e.

To determine the ability of the Burgers model to reflect the characteristics of soil-cement mixture, and to determine the usefulness of the equations developed for the model, rheological constants estimated from the creep test are applied to Eqs. 4 and 5. As shown in Figure 4, the agreement between the experimental and predicted data is

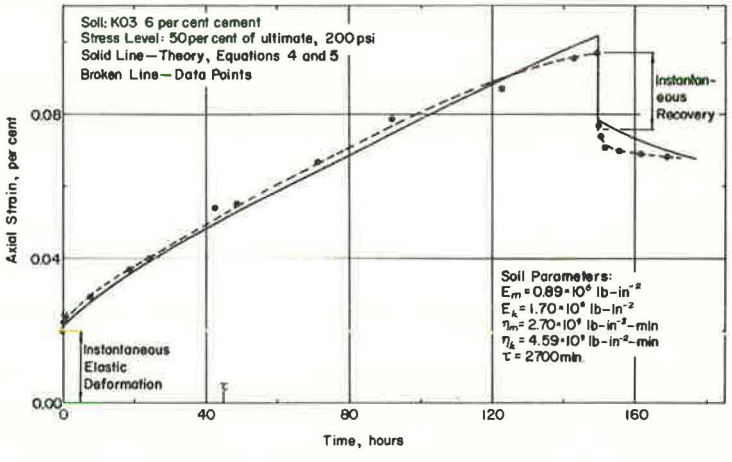

Figure 4. Comparison of creep test data with that predicted by the Burgers model.

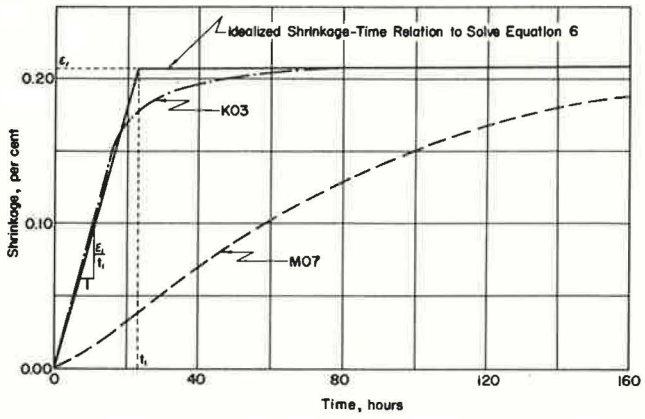

Figure 5. Time-rate of shrinkage of soil-cement mixes when air dried at 55 percent RH and 72 ± 4° F—cement content in both soils is 6 percent (8).

excellent. The model, therefore, permits a reasonable prediction of such data from those of the creep test.

Effect of Creep on Crack Spacing—The effect of creep on crack spacing seems to be only indirect, mainly insofar as the creep affects the tensile strength of the material. Eq. 1 reveals that crack spacing is strongly dependent on tensile strength. Although no study has yet been reported concerning the effect of creep on the ultimate tensile strength of soil-cement, Neville (13), in discussing the results of his creep study on concrete, reported that the influence of creep on the ultimate strength of a simply supported beam subjected to a sustained load was not significant. He also stated that the creep of plain concrete did not per se affect the strength, although under very high stresses (85 to 90 percent of the rapid ultimate load) creep hastens the approach of the limiting strain at which failure takes place. So far as soil-cement is concerned, similar arguments may lead to the conclusion that, when subjected to constant stress creep, it could fail prematurely because the maximum strain exceeded the limiting strain. This result, however, is not considered significant. The important influence on crack spacing could be in the internal stresses developed during shrinkage. Considering the material is viscoelastic, the tension stress developed as a result of the time-dependent shrinkage needs to be evaluated.

As indicated in the previous section, the behavior of soil-cement can be satisfactorily represented by that of the Burgers model. Assuming that the material undergoes a constant shrinkage rate, that is, $(d^2\epsilon/dt^2) = 0$, one can write Eq. 3b as follows:

$$\sigma + p_1\dot{\sigma} + p_2\ddot{\sigma} = q_1\dot{\epsilon} \qquad (6)$$

As shown in Figure 5 the stress developed in the material because of the imposed strain can be computed by solving the differential equation with suitable boundary conditions. The solution for the stress in terms of the rheological parameters is

$$\sigma = \left(\frac{\epsilon_1}{t_1}\right) E_m \left[\frac{\eta_m}{E_m} + \frac{1 - \frac{1}{\alpha\tau}}{(\beta-\alpha)} \exp(-\alpha t) + \frac{1 - \frac{1}{\beta\tau}}{(\alpha-\beta)} \exp(-\beta t)\right] \qquad (7)$$

where

$$\left.\begin{matrix}\alpha \\ \beta\end{matrix}\right\} = \frac{1}{2}\left(\frac{E_k + E_m}{\eta_k} + \frac{E_m}{\eta_m}\right) \pm \frac{1}{2}\sqrt{\left(\frac{E_k + E_m}{\eta_k} + \frac{E_m}{\eta_m}\right)^2 - 4\frac{E_k E_m}{\eta_k \eta_m}}$$

$\tau = \frac{\eta_k}{E_k}$, often called the retardation or delay time.

The ratio ϵ_1/t_1 signifies the shrinkage rate as shown in Figure 5.

With the appropriate rheological constants substituted in Eq. 7, the stress developed in two soils (K03 and M30), as a function of time for two values of shrinkage rates, is calculated and the result is shown in Figure 6. The stress developed in the viscoelastic material is always smaller than that in a comparable elastic material, and the difference in the behavior of the materials will be more apparent as the shrinkage rate decreases. In other words, the material exhibits stress relaxation; and the chances are that a pavement base of viscoelastic material, such as soil-cement, would exhibit even fewer cracks. Furthermore, Figure 6 reveals that the stress ratios are nearly identical in the two soils (at t_1 = 10,000 min), although the same t_1-value results in distinct shrinkage rates. This finding simply indicates that the stress ratio is independent of the shrinkage rate, but strongly dependent on the soil properties, especially η_m/E_m ratio.

Shrinkage Rate and Cracking—Eq. 7 reveals the internal stress developed in the material when a constant rate of strain caused by shrinkage or temperature change is assumed. It may be asserted that cracking takes place when,

$$\sigma_u = \left(\frac{\epsilon_1}{t_1}\right) E_m \left[\frac{\eta_m}{E_m} + \frac{1 - \frac{1}{\tau\alpha}}{\beta-\alpha} \exp(-\alpha t) + \frac{1 - \frac{1}{\tau\beta}}{\alpha-\beta} \exp(-\beta t) \right] \qquad (8)$$

where σ_u = ultimate tensile strength of soil-cement, lb-in.$^{-2}$.

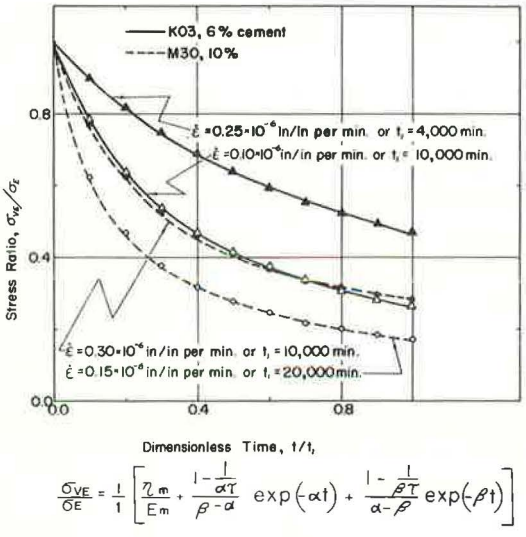

Figure 6. Time-dependent stress in viscoelastic soils due to time-dependent shrinkage. Ratio of the stress computed considering the material is viscoelastic to that considering elastic is designated stress ratio. Soil parameters from Figure 4. Parameters of soil M30 at 10 percent cement: E_m = 0.30 x 10^6; E_k = 0.33 x 10^6; η_m = 1.0 x 10^9; η_k = 1.0 x 10^9. Time taken to attain the maximum shrinkage is designated t_1.

Examining Eq. 8, it appears that the risk of cracking is determined by an interaction of the shrinkage rate, the tensile strength, the deformational properties of the soil-cement, and time. The important result, however, is that the tensile stress developed because of restraint will be a direct function of the rate of shrinkage ($\dot{\epsilon}$). In other words, if the load-deformation relationship of the material is assumed to be viscoelastic, rapid shrinkage should favor large stresses. So far as strength of the material is concerned, it may be conjectured that brittle materials could exhibit slightly increased rupture stress with the rate of loading (17). This increase, however, is considered insignificant compared to the former. The stress developed in relation to rate of shrinkage is significant in the cracking of soil-cement base, since the shrinkage rate of kaolinite soil-cement is much larger than that of montmorillonite. For example, in Figure 5, the kaolinte and montmorillonite soil-cements attain the same maximum shrinkage in 50 and 250 hours, respectively. In other words, the tension stresses and the tendency to crack will be much greater in kaolinite soil-cement than in montmorillonite soil-cement.

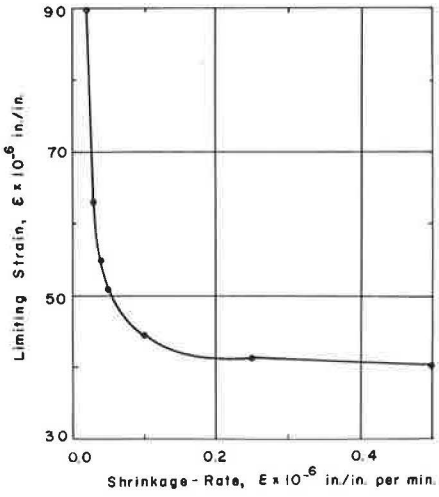

Figure 7. Limiting strain (strain at breaking) decreases with shrinkage rate according to Eq. 8. Soil parameters from Figure 4.

To substantiate this hypothesis, the crack patterns of two models, soil-cement mixtures of K03 and M07, are obtained. The model was a 24 in. by 24 in. by 1 in. deep soil-cement slab molded in a flat wooden container 27 in. by 27 in. by 6 in., inside dimensions. A short description and detailed results on model testing may be found elsewhere (18). Significantly, the accumulated crack length and crack propagation of K03 are greater than that of its counterpart M07. Application of this result to field situations would suggest that kaolinite soil-cement pavement bases warrant special attention and curing during the first few days in order to minimize serious cracking.

Eq. 8 implies that the ultimate strain at rupture depends on the whole strain history of the material before failure. When shrinkage occurs slowly, the strain capacity of soil-cement is greater than when rapid shrinkage takes place. This is exemplified by inserting the experimentally determined rheological constants of the soil-cement in the criterion of crack formation, Eq. 8, and calculating the strain at failure at different rates of shrinkage. Such data (Fig. 7) again stress the importance of proper, extended curing of soil-cement to minimize undesirable cracking.

Effect of Creep on Crack Width—The crack width (7) is influenced by two opposing factors: the tendency of the soil-cement to shrink, compensated to some extent by the elongation of the material. Accordingly, the equation for the crack width was derived:

$$\delta T = \epsilon_c L - \frac{\mu \gamma L^2}{4 E_t} = \delta_1 - \delta_2 \qquad (2)$$

The first term on the right-hand side, which accounts for the contraction caused by shrinkage, is not affected by creep. The second term, however, needs revision in view of the fact that the tensile stress resulting from the restraint below is time-dependent. The effect of shrinkage on tensile stress seems to be only indirect, mainly insofar as the shrinkage affects the slab displacement. The key factor that influences the tensile stress, however, is the coefficient of the subgrade resistance μ which, according to the tests by the Bureau of Public Roads (11), tends to increase with the slab displacement. Test results also showed that the maximum horizontal resisting force that could be developed was for an 0.10-in. displacement. Making the simplifying assumption that the subgrade resistance is linearly time-dependent and based on the hypothesis that the space variation of stress (7) is linear ($\sigma_x = \mu \gamma x$), an expression for the stress is

$$\sigma(t, x) = \mu(t)\, \gamma x = \mu \gamma x \frac{t}{t_1} = \sigma(x) \frac{t}{t_1} \qquad (9)$$

The stress function can be represented in two-dimensional space as shown in Figure 8. The problem thus reduces to evaluating the strain and thereby the deformation of a section of pavement, length L, subjected to the prescribed stress distribution.

First, the strain caused by the time-dependent stress can be computed by using the hereditary integral (14). The hereditary integral, applicable to a stress distribution where a stress σ_0 is suddenly applied at t = 0, but that σ then varies as an arbitrary function $\sigma_{(t)}$ is

$$\epsilon(t) = \sigma(0)\,J(t) + \int_0^t J(t - t')\,\frac{d\sigma'}{dt'}\,dt' \qquad (10a)$$

Where J (t) is known as the creep compliance of the material; for the Burgers model

$$J(t) = \frac{t}{q_1} + \frac{p_1 q_1 - q_2}{q_1^2}\left(1 - \exp\left(-t/\tau\right)\right) + \frac{p_2}{q_2}\left(\exp\left(-t/\tau\right)\right) \qquad (11)$$

in which p_1, p_2, q_1, and q_2 have the same interpretation as in Eq. 3b. Eq. 10a shows how the strain at any given time depends on all that has happened before. This is quite different from what happens in an elastic material, whose strain depends at any time solely on the stress acting at that time only. Through integration by parts, Eq. 10a may be brought into another, often more useful, form:

$$\epsilon(t) = \sigma(t)\,J(0) + \int_0^t \sigma(t')\,\frac{dJ(t - t')}{d(t - t')}\,dt' \qquad (10b)$$

Second, the total elongation can be obtained as follows:

$$\delta_2 = 2\int_0^{L/2} \epsilon(t, x)\,dx \qquad (12)$$

Substituting for $\sigma(t)$, $j(0)$, and $\frac{dJ(t - t')}{d(t - t')}$ in Eq. 10b and the resulting equation in turn in Eq. 12, and performing the required integration and simplification, the following expression for δ_2 in the range $t < t_1$, is obtained:

$$\delta_2 = \frac{\mu\gamma L^2}{4}\left\{\left[\frac{1}{E_m} + \frac{1}{E_k} + \frac{t}{2\eta_m}\right]\frac{t}{t_1} + \frac{1}{E_k}\,\frac{\tau}{t_1}\left[\exp\left(-\frac{t}{\tau}\right) - 1\right]\right\} \qquad (13)$$

For $t > t_1$ the expression becomes

$$\delta_2 = \frac{\mu\gamma L^2}{4}\left\{\frac{1}{E_m} + \frac{1}{E_k} + \frac{1}{\eta_m}\left[t - \frac{t_1}{2}\right] + \frac{1}{E_k}\,\frac{\tau}{t_1}\left[\exp\left(-\frac{t}{\tau}\right) - \exp\left(-\frac{t - t_1}{\tau}\right)\right]\right\} \qquad (14)$$

To emphasize the significance of the elongation (δ_2), it might be well to note that the crack width decreases with the increase in δ_2.

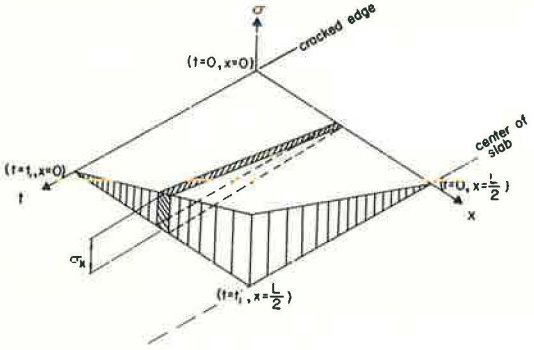

Figure 8. Stress variation in two-dimensional space. Stress linearly varies: (i) from crack-edge to center of slab and (ii) from $t = 0$ to $t = t_1$. Subgrade resistance and in turn the stress reaches maximum in time t_1.

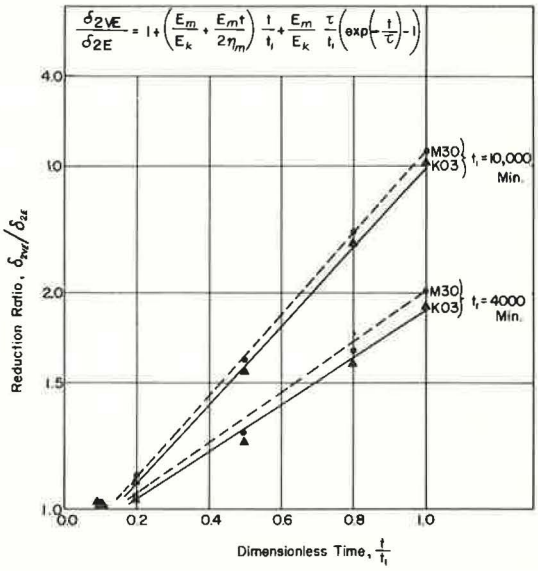

Figure 9. Reduction ratio plotted against time. Ratio of the elongation for a viscoelastic material to that for an elastic is designated reduction ratio.

In order to investigate the influence of the viscous properties of the material on crack width, Eq. 13 is evaluated in soils K03 and M30, respectively, at two values of shrinkage rates, and the resulting data in dimensionless form are shown in Figure 9. In these computations, the subgrade resistance and the linear shrinkage were assumed to attain their respective maximum in the same time interval (t_1). The fact that the reduction ratio ($\delta 2VE/\delta 2E$), elongation of viscoelastic material to that of elastic, increases with time signifies the importance of viscous properties of soil-cement in reducing crack width.

The material properties presented earlier in the report in conjunction with the data in Figure 9 (reduction ratio = 3) were again used to predict the crack width. The agreement between the actual and the predicted data (0.06 in. compared to 0.08 in.) is excellent, showing that the rheological model reflects the characteristics of the material to a marked degree.

When the plots for the two soils K03 and M30 are examined, the soil parameters between soils do not seem to have significant influence on the reduction ratio. Insofar as the relative significance of the parameters of a mix is concerned, the modulus of viscosity η_m exerts the most influence on crack width in that a smaller η_m contributes to narrower cracks.

By comparing the plots for different values of shrinkage rates in Figure 9, one may infer that by decreasing the shrinkage rate the crack width could be controlled. In other words, prolonged curing of the base should favor narrower cracks.

RESULTS AND CONCLUSIONS

In this paper, limitations imposed by purely elastic analysis of the cracking problem are reviewed. In order to take the time-dependent material properties into account, the Burgers model has been proposed. To validate the predictability of the model and to approximate the rheological parameters, a series of constant stress creep tests was performed in the laboratory. The theoretical study, making use of the Burgers model, resulted in the following observations:

1. Creep and shrinkage are not independent phenomena; for any mixture, creep is higher the lower the relative humidity.
2. The Burgers model shows the greatest promise in mechanical simulation of actual soil-cement behavior.

3. Stress computed according to viscoelastic theory is on the average 50 percent smaller than that computed by the elastic theory.
4. Insofar as the rate of shrinkage is concerned, rapid shrinkage favors large stresses.
5. The crack width computed according to the viscoelastic theory is within practical limits and is in excellent agreement with that observed in the field.

This paper concludes that in predicting the behavior of pavement layers subjected to ambient conditions, the viscoelastic approach is superior to any known elastic or empirical laws. The results, although largely qualitative, suggest the possibility of controlling the crack intensity by enhancing the viscous properties of the material. The findings of this study are conclusive in showing that cracking of cement base can be minimized by adequate extended curing.

ACKNOWLEDGMENTS

This report is part of the research conducted in connection with Project 5666 of the Engineering Experiment Station, University of Mississippi, under the sponsorship of the Mississippi State Highway Department and the U. S. Department of Transportation, Bureau of Public Roads. This support is gratefully acknowledged.

The opinions, findings, and conclusions expressed in this publication are those of the author and not necessarily those of the State or the Bureau of Public Roads.

Frank C. Yao, Graduate Assistant in Soil Mechanics, assisted in the testing and analysis of data.

REFERENCES

1. Alfrey, T., Jr. Mechanical Behavior of High Polymers. Interscience Publishers, New York, 1948.
2. Secor, K. E., and Monismith, C. L. Viscoelastic Properties of Asphalt Concrete. HRB Proc., Vol. 41, p. 299-320, 1962
3. Pister, K. S., and Monismith, C. L. Analysis of Viscoelastic Flexible Pavements. HRB Bull. 269, p. 1-15, 1960.
4. Monismith, C. L. Temperature Induced Stresses and Deformations in Asphalt Concrete. Proc., AAPT, 1965.
5. Singh, A., and Mitchell, J. K. General Stress-Strain-Time Function for Soils. Jour. Soil Mech. and Found. Div., ASCE, Vol. 94, No. SM1, p. 21-46, 1968.
6. Mitchell, J. K., Campanella, R. G., and Singh, A. Soil Creep as a Rate Process. Jour. Soil Mech. and Found. Div., ASCE, Vol. 94, No. SM1, p. 231-254, 1968.
7. George, K. P. Cracking in Cement-Treated Bases and Means for Minimizing It. Highway Research Record 255, p. 59-71, 1968.
8. George, K. P. Shrinkage Characteristics of Soil-Cement Mixtures. Highway Research Record 255, p. 42-58, 1968.
9. U. S. Bureau of Reclamation. A 10-Year Study of Creep Properties of Concrete. Concrete Laboratory Report No. SP-38, Denver, Colo., 1953.
10. Yao, F. C. Creep on Cracking of Soil-Cement Base. Univ. of Mississippi, Library, Oxford, 1969.
11. Kelly, E. F. Application of the Results of Research to the Structural Design of Concrete Pavements. Public Roads, Vol. 20, 1939.
12. Marshall, T. J. Some Properties of Soil Treated With Portland Cement. Symposium on Soil Stabilization, Council of Scientific and Industrial Research, Australia, 1954.
13. Neville, A. M. Theories of Creep in Concrete. Proc., ACI, Vol. 52, p. 47-60, 1955.
14. Flügge, W. Viscoelasticity. Blasidell Publishing Co., Waltham, Mass., 1967.
15. Abdel-Hady, M., and Herrin, M. Characteristics of Soil-Asphalt as a Rate Process. Jour. of Highway Div., ASCE, Vol. 92, No. HW1, p. 49-69, 1966.

16. Hansen, T. C. On Rheology of Hardened Concrete. Proc., Swedish Cement and Concrete Research Inst., Vol. 37, Stockholm, 1962.
17. Goldstein, M. N., Misumsky, V. A., and Lapidus, L. S. The Theory of Probability and Statistics in Relation to Rheology of Soils. Proc., Inter. Conf. on Soil Mech. and Found. Eng., p. 123, Paris, 1961.
18. George, K. P. Mechanics of Fracture and Cracks in Soil-Cement Pavement Base. Offered for publication in Proc., ASCE, 1969.

Cement Content of Soil-Cement By X-Ray Fluorescence

RODNEY J. W. HUANG, Iowa State University; and
GILBERT L. RODERICK, University of Wisconsin—Milwaukee

•THE increasing use of soil-cement in highway construction emphasizes the need for a simple, fast, and accurate method of determining cement contents. This paper describes the development and evaluation of an x-ray spectrographic analysis for determining content of soil-cement.

Several investigators have used x-ray spectroscopy for studying raw cements. Among these are Croke and Kiley (1), Frank (2), Schloemer (3), Bens (4), Uchikawa, Inomata and Inoue (5), Rabot and Alegre (6), and Andermann and Allen (7). Handy and Rosauer (8) and Handy and Demirel (9) used x-ray analysis for quantitative determinations of iron, manganese and carbonates in soils. The study of this literature indicated that further improvement of the analytical technique was desirable and seemed plausible in view of several instrumental developments and theoretical considerations.

Consideration of the nature of soil-cement reactions leads to the conclusion that the amounts of metallic elements should not change when hydration occurs. When the primary beam from an x-ray tube irradiates a sample it excites each chemical element to emit its secondary (fluorescent) radiation, each element having its own characteristic wavelength. The emitted radiation intensity is related to an element's concentration in the sample; thus, both qualitative and quantitative analyses can be made.

The analytical method to determine the weight percentage of cement in an unknown soil-cement mixture is based on the premise that certain types of soil and cement have practically constant calcium and iron contents. If the percentages of calcium, for example, are S in soil, C in cement and M in soil-cement mixture, the weight percentage X (based on total dry weight of the mix) of the cement in the soil-cement can be determined from the relation:

$$X = \frac{S - M}{X - C} \cdot 100$$

X-ray properties and principles of secondary emission require, for quantitative analysis, the knowledge of possibly interfering absorption edges causing enhancement and absorption effects. Therefore, one must have cognizance of the elements that are present in relatively rich concentrations. The scanned x-ray fluorescence spectrum of our soils and cement (Fig. 1) shows the relatively rich elements are iron in the soil and calcium in the cement. The atomic numbers (26 for iron, 20 for calcium) are six numbers apart; no essential matrix interference effects are expected in investigating cement content of the soil-cements.

In establishing working curves or parameters from prepared soil-cement specimens, it is preferable to relate element concentration to the ratio of characteristic radiation intensity from the specimens to the intensity from a standard rather than from peak intensities only of the element of interest. The use of intensity ratios compensates for a number of error sources such as voltage-tube combination instabilities and drift in detection efficiency.

Paper sponsored by Committee on Soil-Portland Cement Stabilization.

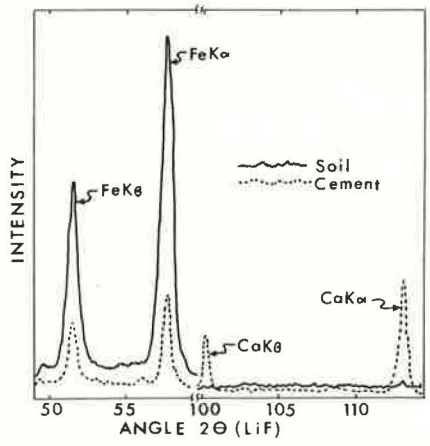

Figure 1. X-ray fluorescence spectrum of soil and cement.

In practice, peak intensities can be measured at the proper angular positions by the counting rate or, for improved statistical accuracy, by accumulating fixed counts and measuring the elapsed time. Background correction intensities are measured on both sides of the element lines.

The forms of intensity ratios used in this study were: the peak to background ratio, I_p/I_b, and the net peak intensity ratio, I_x/I_s. I_p is the peak intensity of an element in the sample, I_b is the background intensity adjacent to the peak for the sample, I_{sp} and I_{sb} are the corresponding intensities from the standard, I_x is $I_p - I_b$, and I_s is $I_{sp} - I_{sb}$.

All intensity measurements must be made under identical conditions of sample preparation, of x-ray excitation, and of instrumentation.

MATERIALS

Soils

Ten soil samples were obtained from the base and subbase at selected locations in a cement-stabilized roadway just prior to incorporation of cement during construction. The soils were used for preparation of test specimens of precisely known cement/soil ratios. These were then analyzed by x-ray fluorescence to establish the parameters used for determination of cement contents of soil-cement samples. The soils ranged from A-2-4 to A-4(3); the physical properties of a typical soil of the group are given in Table 1.

Soil-Cements

The soil-cements analyzed in this study were from Proctor size compression samples of the described soils proportioned, mixed and molded in the laboratory, and samples from the same locations molded after incorporation of cement and mixing of the material on the road. Samples broken after 7 days' curing were set aside for cement content determinations by the ASTM procedure (ASTM Designation: D 806-57), and by x-ray fluorescence analysis.

Portland Cement

The type I cement used in the study was obtained during construction of the stabilized road. The chemical composition of the cement is given in Table 2. As received, the cement had 80 to 85 percent passing the No. 200 sieve. To meet the requirements of the present method of analysis, cement used in standards and "known" samples was reduced so 100 percent passed the No. 200 sieve.

TABLE 1

PHYSICAL PROPERTIES OF SOIL NO. 10

Textural composition:	
Gravel (>2.00 mm), %	20.5
Sand (2.00 to 0.074 mm), %	29.5
Silt (0.074 to 0.005 mm), %	46.0
Clay (<0.005 mm), %	4.0
Consistency limits:	
Liquid limit, %	21.2
Plastic limit, %	NP
Classification	
Textural	Gravelly silt-loam
AASHO	A-4(3)

TABLE 2

CHEMICAL COMPOSITION OF TYPE I CEMENT[a]

Chemical	Percent (by wt)	Chemical	Percent (by wt)
SiO_2	21.3	MgO	3.5
Al_2O_3	4.6	SO_3	2.3
Fe_2O_3	2.3	Na_2O	0.67
CaO	64.0		

[a]Atlantic Cement Co.

TESTING PROCEDURE

The procedure for determining cement content of soil-cements involves specimen preparation, x-ray intensity measurements, and data evaluation. A detailed description of the procedure is given elsewhere (10).

Specimen Preparation

To prepare specimens of known cement-soil composition for establishment of the working curves or equations, a 200-gm representative oven-dry soil sample was first crushed so all passed a No. 40 sieve and was then thoroughly blended. About 20 gm of this material were further reduced in a blender mill so all passed a No. 200 sieve; cement was also reduced to pass a No. 200 sieve. Soil and cement to give a mix of known composition were thoroughly mixed and a 4.000-gm sample placed in a briquetting assembly (as customarily used for specimen mounting in metallography) and compressed under 5000-psi pressure. The sample was then placed in a desiccator to await analysis.

Preparation of "unknown" soil-cement test samples was very similar. Oven-dry soil-cement (in our case the entire broken compression sample) was reduced to pass the No. 40 sieve and thoroughly mixed. About 20 gm were reduced to minus No. 200, and a 4.000-gm sample was compressed as above.

X-Ray Intensity Measurements

The intensities of the characteristic K-alpha radiation of calcium and iron were made with a General Electric XRD/S-5 X-ray Spectrometer with an AEG-50-S tungsten tube operated at a stabilized voltage of 50 KVP and a current of 16 mA. A pulse height selector was used to isolate background noises. X-ray detection was accomplished (by tandem operation) with a scintillation counter and a P-10 gas flow proportional counter. A lithium fluoride analyzing crystal was used.

The LiF analyzing crystal (2d = 4.0267Å) was aligned to the correct angle 2θ for a desired wavelength and peak intensities (cps) were obtained by a fixed-count technique. Four fixed counts of 100,000 for FeKα and 1000 for CaKα were taken and two background counts of 1000 were taken on each side of the peaks.

Data Evaluation

The fixed counts were divided by collection time to give x-ray intensities, I_p and I_b, in counts per second (cps). Background corrections were made to obtain the net peak intensities I_x and I_s, and the intensity ratios I_p/I_b and I_x/I_s were computed. In most cases plots of I_p/I_b or I_s/I_x vs cement content gave very good linear relationships for data from "known" samples. The least squares method was used to find the best fit, or "working curve," and the corresponding equation. Cement contents of "unknown" soil-cements can be obtained directly from the plot (Figs. 5 and 6) or the equation.

For analysis of large quantities of data, a FORTRAN computer program is available which plots the working curve, gives the algebraic equation, and which also gives cement contents of the unknowns (10).

FACTORS IN INTENSITY MEASUREMENTS

Effects of Particle Size

In materials having constituents of various absorption coefficients, a rough surface causes partial shielding resulting in variations of intensities from specimen to specimen. Mixtures containing light and heavy elements, e.g., calcium and iron, require particular care in preparing a homogeneous sample with a smooth surface. Taylor (11) suggested that for powder samples in general, a uniform particle size of 76 microns is sufficient. However, our experiments and calculations show that maximum intensities may be obtained with a maximum particle size as large as 268 microns.

Jenkins and Hurley (12) expressed the effects of shielding due to surface roughness in terms of the linear absorption coefficient, μ, and the coarsest finish, X_{max} (average peak to trough of surface), permissible without significantly decreasing radiation intensity, as:

$$X_{max} \leq 30(46100/\mu)^{1/3} \text{ microns}$$

Applying this relationship to soil-cement, the approximate maximum trough depth, X_{max}, necessary to avoid shielding effects are 141 microns for CaKα radiation and 134 for FeKα.

Figure 2 shows the influence of particle size on FeKα intensity from soil-cement specimens compressed at 5000 psi. Nearly maximum intensity is obtained at a maximum particle size of 254 microns but intensity fluctuations are greater than for smaller particle sizes. The 254 microns maximum is close to the calculated maximum size of 268 microns ($2X_{max}$) at which influence of surface roughness on intensity becomes negligible. Reduction of particle sizes to values below 74 microns becomes increasingly difficult; on the basis of our results 74 microns (No. 200 sieve) was taken as the maximum allowable particle size.

On considering the mass absorption coefficient, depth of x-ray penetration and emitted fluorescence intensity, it seems more reliable results are obtained if the trough depth is smaller than penetration depth. The intensity of emitted radiation is a function of the concentration of the element and of the absorption characteristics of the material. This assumes the output of the x-ray tube is constant, there is no mutual excitation, and the soil-cement sample is infinitely thick. Taylor and Parrish (13) report that 0.10 mm is essentially "infinite" for most common metallic elements.

X-ray emission intensity for CaKα and FeKα from a cement sample may be approximated by

$$I = I_{max}(1 - e^{-a\rho x})$$

where I is intensity of radiation; I_{max} is intensity with an infinitely thick sample; a is $\frac{\mu_1}{\rho} \csc \theta_1 + \frac{\mu_2}{\rho} \csc \theta_2$; θ_1 and θ_2 are the incident and emergent beam angles with the surface; $\frac{\mu_1}{\rho}$ is the mass absorption coefficient of incident radiation; $\frac{\mu_2}{\rho}$ is the mass absorption coefficient of emitted radiation; ρ is the density of cement (3.15 g/cc assuming zero voids); and x is penetration depth (cm).

Results of calculations are plotted in Figure 3, and show that for calcium and iron a depth of 51 microns yields 99 percent of the maximum intensity. The maximum trough depth of our soil-cement samples is 37 microns (one-half maximum particle size) which is less than the 51 microns penetration depth. This confirms our experimental finding that, for our specimen conditions, the influence of surface roughness has been minimized to an extent where it is negligible.

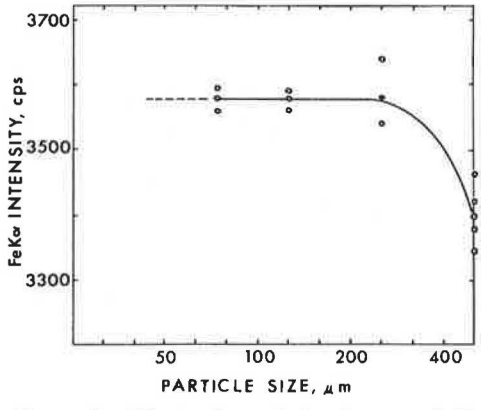

Figure 2. Effect of particle size on FeKα radiation intensity.

Effect of Compression Stress

Compression of powder samples reduces overall intensity variations from one specimen to another and facilitates storage of specimens for future reference.

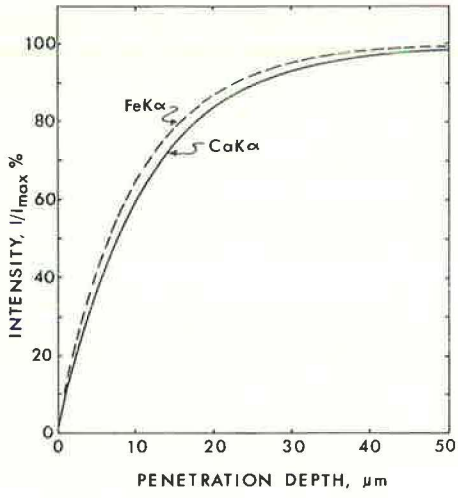

Figure 3. Variation of emitted x-ray intensity with x-ray penetration depth.

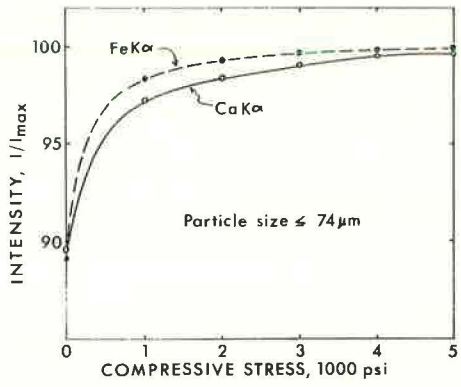

Figure 4. Effect of sample compression on emitted x-ray intensities.

Figure 4 shows the influence of compression stress on the characteristic radiation intensities for cement samples having a maximum particle size of 74 microns. A pressure of 5000 psi was enough for optimizing intensity for both FeKα and CaKα radiation.

Other Factors in X-Ray Measurement

In quantitative x-ray spectroscopy, the influence of matrix composition on peak intensities by enhancement and self-absorption effects must be considered. Of two chemical elements adjacent in the periodic system, the one having the smaller atomic number, Z, will partially absorb radiation of the heavier element, Z + 1, and in turn will emit a stronger characteristic radiation of its own. In our system no elements of adjacent numbers are involved (Fig. 1), and interference due to absorption and enhancement may be considered negligible.

In this study, it was found that the background intensities, I_b, for FeKα and CaKα radiation decrease with increasing cement content of the material. The reason for this cannot be explained at this time. The differences in background intensities averages about 6 cps for FeKα and 1 cps for CaKα in the cement content range of 0 to 20 percent. These are too small to affect the total FeKα intensity but must be considered for CaKα if one strives for better precision.

Error in Measurement

In the measurement of radiation intensity, a scatter of data is caused by the random nature of x-ray production. The probable error of a fixed count is $E_n = 67.5\% \sqrt{N}$, and the standard deviation is $S = \sqrt{N}$, where N is the total number of counts (14, 15). In our case, therefore, for each FeKα fixed count $E_n = 0.21\%$ and S = 316 counts; for CaKα $E_n = 2.12\%$ and S = 31.6 counts. The limit of detectability requires a minimum peak height of at least 3S above the background (15). This requirement is met in all cases, and the difference is considerably greater than 3S in the cement content range in question.

Four fixed counts were taken for each intensity measurement. Typical values of the mean intensity, standard deviation and probable error for each set of readings is given in Table 3 (for sample No. 10—subbase). The relatively weak CaKα radiation can be determined with greater precision by increasing the total number of counts; however, this would require more time.

The precision of the method may also be increased by increasing the intensity of the characteristic radiation. Intensity of CaKα radiation would be increased by using a

TABLE 3

X-RAY INTENSITY DATA FOR SOIL-CEMENT MIXTURES
(Sample No. 10—Subbase)

Cement Content (% total dry wt)		Mean Peak Intensity, I_p (cps)	Standard Deviation, S (cps)	Probable Error, E (%)	Mean Background Int., I_b (cps)
0	Fe	5248	29.1	0.37	48.0
	Ca	26.1	0.47	1.21	22.0
5	Fe	4857	4.0	0.06	46.9
	Ca	47.5	2.78	3.95	22.3
10	Fe	4544	17.6	0.26	45.2
	Ca	67.5	1.10	1.10	22.0
15	Fe	4211	3.3	0.05	44.0
	Ca	86.1	2.76	2.16	22.0
20	Fe	3904	58.3	1.01	41.9
	Ca	109.2	2.76	1.70	22.0
Cement Standard, 100	Fe	1162	0.5	0.03	32.3
	Ca	479.7	7.90	1.11	19.9
Lab Sample, ?	Fe	4723	10.0	0.14	46.9
	Ca	48.1	0.99	1.39	22.0
Field Sample, ?	Fe	4777	12.8	0.18	46.8
	Ca	49.1	1.46	2.01	22.0

chromium rather than tungsten x-ray tube (15). A great increase in intensity would be obtained by using a curved focusing crystal analyzer rather than a flat crystal (16). Also, discriminate selection of a specific tube excitation voltage for a particular element would yield the maximum ratio of peak to background intensities.

RESULTS

Discussion of Data

As an example of the data obtained for establishing working curves and equations and determining cement contents of unknowns, Table 3 gives results for a typical soil (No. 10—subbase, Table 1), with known and unknown cement contents. The ratios I_p/I_b and I_x/I_s were obtained from the peak and background intensities and the working curves established by least squares fitting. Figures 5 and 6 show the curves for this typical example. For this material, compressed at 5000 psi, the curves obtained from

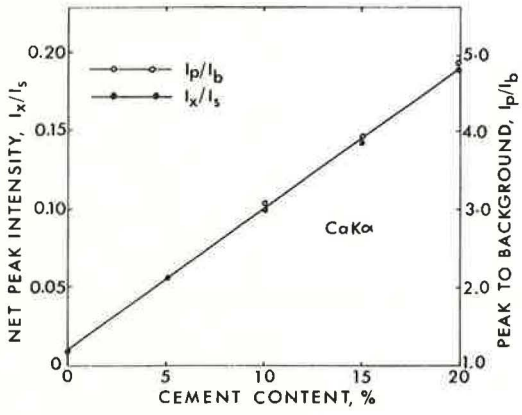

Figure 5. Relation between cement content and CaKα radiation (Sample No. 10—subbase).

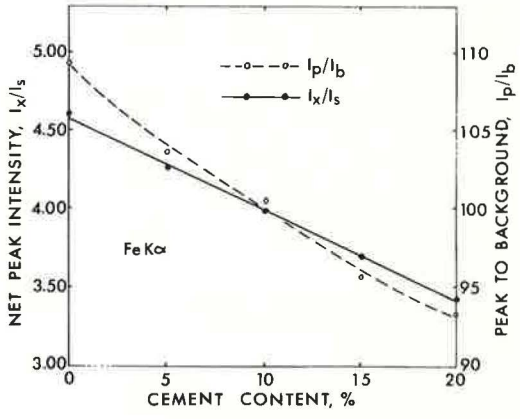

Figure 6. Relation between cement content and FeKα radiation (Sample No. 10—subbase).

TABLE 4

CEMENT CONTENT OF "UNKNOWN" SOIL-CEMENT MIXTURES

Specimen No.		Cement Content (% total dry wt)			
		Based on FeKα		Based on CaKα	
		I_p/I_b	I_x/I_s	I_p/I_b	I_x/I_s
8 Subbase	Lab.	9.36	6.41	5.02	5.48
	Field	13.96	13.91	12.12	12.71
9 Subbase	Lab.	12.73	6.99	5.48	5.49
	Field	12.66	8.02	7.05	7.00
10 Subbase	Lab.	9.08	7.25	5.41	5.38
	Field	7.91	6.46	5.64	5.63
8 Base	Lab.	6.00	7.40	5.41	5.59
	Field	12.13	10.80	7.83	8.11
9 Base	Lab.	13.34	13.82	8.77	9.06
	Field	24.89	20.19	13.41	13.73
10 Base	Lab.	10.64	8.04	9.43	9.67
	Field	13.38	10.00	10.61	10.79

I_p/I_b and I_x/I_s coincide for CaKα data while those for FeKα show considerable deviation.

Three different kinds of standards were used during this study: (a) solid standards, an iron plate and a calcite plate for samples No. 1 and 2, (b) cement powder standard compacted at 1000 psi for samples No. 3 through 7, and (c) cement powder standard compacted at 5000 psi for samples No. 8 through 10. The powder standards were subjected to the same pressure as their corresponding soil-cement samples.

Table 4 gives results of cement content determinations for unknown soil-cements compressed under 5000 psi and cement powder standards. Data for the remaining samples (compressed at 1000 psi) for CaKα radiation show, in general, considerably greater differences between cement contents calculated from I_p/I_b and I_x/I_s (10). The effect of compaction pressures on radiation intensity has been discussed earlier. Although the solid standards were not used with any of the materials compressed under 5000 psi, it is felt that the cement powder standard should be used; i. e., the standard should be of the same nature as the test specimens and be prepared under identical conditions.

Cement contents based on FeKα radiation data are considerably different depending on whether I_p/I_b or I_x/I_s was used for calculation even though, for all samples presented, the compacting pressure was 5000 psi. The erratic results are possibly due to iron contamination during specimen preparation; e. g., the steel blades of the rotary mixer used for field mixing wear rapidly, and the crusher used to reduce particles to pass the No. 40 sieve has steel rollers. On the basis of the results, it is concluded that the CaKα data gives a much better indication of actual cement contents for the soils tested.

Comparison of ASTM and X-Ray Methods

Table 5 compares cement contents (based on the dry soil weight) determined by the standard ASTM procedure, D 806-

TABLE 5

CEMENT CONTENTS BY THE ASTM AND X-RAY FLUORESCENCE METHODS

Specimen No.		Cement Content (% dry wt soil)			
		Nominal	ASTM	X-Ray Fluor. (CaKα)	
				I_p/I_b	I_x/I_s
8 Subbase	Lab.	5.0	5.2	5.3	5.8
	Field	5.0	11.2	13.8	14.5
9 Subbase	Lab.	5.0	5.2	5.7	5.8
	Field	5.0	6.8	7.6	7.5
10 Subbase	Lab.	5.0	5.4	5.7	5.7
	Field	5.0	5.8	5.9	5.9
8 Base	Lab.	6.0	5.6	5.7	5.9
	Field	6.0	7.6	8.5	8.8
9 Base	Lab.	10.0	9.1	9.5	9.9
	Field	10.0	14.5	15.5	15.9
10 Base	Lab.	10.0	9.1	10.4	10.7
	Field	10.0	9.6	11.8	12.1

57, and the present method. The results for x-ray analysis are those for CaKα radiation and samples compressed at 5000 psi, the most reliable conditions as discussed earlier. The data show that the results from the x-ray fluorescence method are consistently higher than those from the ASTM method. Both methods require small quantities of material, 5 gm for the ASTM and 4 gm for the x-ray procedure. Although the x-ray procedure requires greater reduction in particle size, the probability of sampling and sample preparation errors are probably about the same for both methods. The accuracy of the ASTM method is much more dependent on the experience and technique of the operator than is the x-ray analysis.

More research is needed to determine the relative accuracy of the two methods. Enough data are needed from samples of various soil types with precisely known cement contents to make possible a valid statistical analysis of accuracy. The same samples should be analyzed by both methods, first by the nondestructive x-ray fluorescence method and then by the ASTM method.

Curtis and Forbes (17) investigated various methods of determining cement contents of soil-cements; methods employed were ASTM, California, Versene, flame photometer, conductivity, and chemical analysis. Their study shows that, in general, results by the ASTM method are lower than those by the Versene, chemical analysis and conductivity methods. Although no direct comparison can be made, the values obtained by these methods would seem to compare favorably with those by the x-ray procedure. The California method yields results closer to those from ASTM (17).

Application to Field Control

With the recent introduction of portable x-ray spectrometer units, the present method should be applicable for field control. Other basic equipment required for a field laboratory are grinder mills, analytic balance, hydraulic press and a desk calculator. Once working curves have been established for a given soil and cement, the cement content of soil-cement mixes can be quite quickly determined.

CONCLUSIONS

The following conclusions are made on the basis of the results obtained and for the type of soil used:

1. X-ray fluorescence determination of cement content of soil-cement is nondestructive, fairly rapid, simple, and should be sufficiently accurate. The method is relatively insensitive to operator experience and technique.
2. Corrections for background intensities are necessary. The net peak intensity ratio, I_X/I_S, appears to give the most reliable results.
3. The known and unknown soil-cements, and the standards should be of the same nature; i. e., powder specimens of similar particle size distribution and identical preparation conditions.
4. The most reliable results are obtained when maximum particle size in the samples is 74 microns, samples are compressed under 5000 psi, and CaKα radiation intensities are used.
5. Cement contents determined by x-ray fluorescence are generally higher than those by the ASTM method, but seem to compare favorably with those by other methods.

ACKNOWLEDGMENTS

This investigation was conducted at the University of Rhode Island while the authors were associated with that institution. The authors wish to express their thanks to Dr. Anton F. Mohrnheim, Professor of Chemical Engineering, for his guidance and help in the study.

REFERENCES

1. Croke, J. F., and Kiley, W. R. The Determination of Iron, Calcium, Silicon, Aluminum and Magnesium in Finished and Raw Mix Cement Samples Using the the Norelco Autrometer. Norelco Reporter, 6, p. 29-33, 1959.

2. Frank, G. Modern Physical Methods in the Lime and Cement Industry. Zement-Kalk-Gips, Vol. 13, p. 270-274, 1960.
3. Schloemer, H. The Use of X-Ray Fluorescence Analysis in the Cement Industry. Zement-Kalk-Gips, Vol. 13, p. 522-530, 1960.
4. Bens, J. Adaption of X-Ray Spectrometry to an Analysis of Hydraulic Binders. Silicate Industry, Vol. 26, p. 526-534, 1961.
5. Uchikawa, H., Inomata, Y., and Inoue, T. Fluorescence X-Ray Spectrometric Determination of Sulfur Trioxide and Magnesium Oxides in Cements. Bunseki Kagaku, Vol. 11, p. 182-188, 1962.
6. Rabot, R., and Alegre, R. X-Ray Spectrometry Application in Cement Manufacturing. Silicate Industry, Vol. 27, p. 181-191, 305-309, 1962.
7. Andermann, G., and Allen, T. D. The Evaluation and Improvement of X-Ray Emission Analysis of Raw-Mix and Finished Cement. Advances in X-Ray Analysis, Vol. 4, p. 4-32, 1962.
8. Handy, R. L., and Rosauer, E. A. X-Ray Fluorescence Analysis of Total Iron and Manganese in Soils. Iowa Engr. Exp. Sta. Bulletin, 192, p. 126-136, 1959.
9. Handy, R. L., and Demirel, T. Notes on Determination of Carbonates in Soils by Chemical Means, D. T. A., and X-Ray. Iowa Engr. Exp. Sta. Bulletin, 192, p. 153-166, 1959.
10. Huang, R. J. W. Determination of Cement Content in Soil-Cement by X-Ray Fluorescence Analysis. Unpublished M. S. Thesis, University of Rhode Island, 1968.
11. Taylor, A. X-Ray Metallography. New York, John Wiley and Sons, 1961.
12. Jenkins, R., and Hurley, P. W. Analysis of Copper Based Alloys by X-Ray Fluorescence Spectroscopy. Proc. XIIth International Spectroscopy Colloquium, 1965.
13. Taylor, J., and Parrish, W. Absorption and Counting-Efficiency Data for X-Ray Detectors. Review of Scientific Instruments, Vol. 26, p. 367, 1955.
14. Cullity, B. D. Elements of X-Ray Diffraction. Addison-Wesley Publishing Co. 1959.
15. Rich, C. I., and Kunze, G. W. Soil Clay Mineralogy—A Symposium. Univ. of North Carolina Press, 1964.
16. Garett, H. J., and Lipsill, H. A. Die Forming Doubly Focusing X-Ray Monochromators. Review of Scientific Instruments, Vol. 32, p. 942, 1961.
17. Curtis, W. E., and Forbes, A. J. Determination of Cement Content of Soil-Cement Mixtures. Highway Research Record 36, p. 123-132, 1963.

The Effect of Admixtures on Layered Systems Constructed With Soil-Cement

ARA ARMAN and TERRY J. DANTIN, Louisiana State University

The highway design engineer is primarily interested in the loads that are applied upon a layered system and the transmission of these loads through this layered system. The lack of bond between adjacent layers of soil-cement has prevented its use in more than one layer of a layered system. Since soil-cement construction frequently allows the use of on-site materials, construction costs can be reduced by its use.

It is the purpose of this study to present a method for the analysis and design of a layered soil-cement system with the use of a set retarding agent as an admixture. Results for this analysis are obtained from tests of more than 2,000 specimens molded with Louisiana soils from 26 different locations. The tests show that there is a definite increase produced in the shear strength of the layered system by developing a bond between adjacent layers of a soil-cement stabilized system with the addition of calcium lignosulfonate and hydroxylated carboxylic acid for soils of low plasticity with the exception of pure silts.

•THE PRESENT placement practices of soil-cement stabilized base and subbase courses do not lend themselves to the construction of compacted layers exceeding 10 in. Whenever pavements thicker than 10 in. are required, it is common practice to use material other than cement-stabilized soil to avoid "lamination" of the pavement structure caused by the lack of bond between subsequent layers. It is practically impossible to create bond between two layers of conventionally constructed soil-cement bases and subbases because the initial setting time of the soil-cement mixture is approximately 2 hours and the field construction procedure requires 2 hours or longer for the mixing, compacting, and grading of each layer. A method of construction using two or more layers of compacted soil-cement mixtures can create weak interfaces (even when "roughened" surfaces are used at the interface), which may cause failures of a flexible pavement system under loads well below the design loads. These failures may be due to slippage of the two layers or they may be due to tensile cracking and consequent failure of the top layer of the system.

Flexible pavement design theories are based on the assumption that there is perfect bond between subsequent layers. Without the presence of this bond, individual layers would be expected to carry the load by so-called "beam action" at a higher intensity than if they were bonded.

The scope of the study was to investigate the effect of dispersant additives on the physical characteristics of soil-cement mixes and layered pavement systems. These additives are industrial byproducts and chemicals that can impart special characteristics to concrete and masonry. They have been used successfully for more than 25 years in improving structural concrete by reducing cracking and increasing shear strength. Their function is to control the rate of cement hydration by retarding the setting and reducing the thickness of the cement gel. Commercially available admixtures are hydroxylated carboxylic acid and calcium lignosulfonate. In this study the effects of these additives were studied in three major areas:

Paper sponsored by Committee on Soil-Portland Cement Stabilization.

1. Increases in the shear strength of individual layers;
2. Increases in the durability; and
3. Production of bond at the interface, which considerably increases the shear strength of the layered system.

LITERATURE SURVEY

Only limited data have been published on the theoretical and experimental measurements of stresses induced by static loads applied on flexible layered systems. Publications on design methods differ in choosing between strength and deflection as criteria. In some cases, the supporters of the deflection theory tend to disagree about the fact that pure deflection tends to minimize the importance of shear strength. A compacted deposit or organic material may deflect several inches without tensile failure under certain conditions. It may even obey Hooke's law verbatim; however, it will never resist shear forces applied by roadway or airport runway loads. On the other hand, a thin semi-rigid pavement designed to resist pure shear forces will not resist the tensile stresses induced at the interface of the base and subbase as a result of very minute deflections, or shear stresses induced within the layer will easily exceed the shear strength of the material.

Most materials used for flexible pavement construction do not possess any tensile strength to resist the tensile stresses that will be developed, especially where E_1, the modulus of elasticity of the top layer, is much larger than E_2, the modulus of elasticity of the bottom layer. As indicated by Casagrande (1) in his discussion of Burmister's two-layer theory, ". . . if no tension cracks develop, the computed result will be on the unsafe side because the 'modulus of elasticity' for tension is much smaller than for compression, which is another way of saying that the material for practical purposes can not take tension." According to Sowers and Vesic (2): "An analysis of lateral stresses in an ideal two-layer system shows that the upper layer . . . will have tension at the interface as soon as $E_1/E_2 > 1.5$ and that, in the cases tested, tension should be of the order of 30 psi in the flexible bases and of the order of 60 psi in the soil-cement base. The tensile strength of the flexible bases was most likely not higher than 5 psi." A tensile test of a soil specimen will never produce a shear failure, but only a tensile failure. An unconfined compression test is likely to result in a bulging of the specimen, accompanied by the opening of tension cracks, but the soil in the ground is unable to fail in this manner since it is laterally confined. Although tension failures will sometimes take place in the laboratory, the reliable strength of a soil is its shear strength.

In 1959 the Highway Research Board Committee on Soil-Cement Stabilization prepared a comprehensive questionnaire to determine the state of the art of soil-cement stabilization. The questionnaire was sent to 50 states and 25 foreign countries.

Fifty-two of the agencies reported that they use soil-cement stabilization for roads, shoulders, and airfields. Out of the 52 states and countries, only three—Virginia, Australia, and England—reported to be using soil-cement stabilized layers thicker than 10 in. Australia indicated that 12 in. of soil-cement base were used for airfield construction, the commonwealth of Virginia reported using 12 in. of base stabilized with 14 percent portland cement, and England reported using 18 in. of stabilized base with 10 to 15 percent portland cement. All replies to the question, "In your experience, what is the maximum compacted thickness of soil-cement that can be constructed in one lift?", showed that the maximum thickness recommended was 8 in.

Fifteen of the 52 replies indicated that two-layered construction was used while the rest reported that two-layered construction was not used in their areas. Nine out of the latter group of 15 showed satisfactory results obtained with two-layered construction, one indicated "apparent" satisfaction while four indicated unsatisfactory or poor results. None of the statements made as "satisfactory" or "unsatisfactory" results were qualified except the one by France, which indicated that the results of two-layered construction were unsatisfactory because bad bonding between layers occurred (3).

TESTING PROCEDURES

At the outset of this study the physical characteristics and the classification of each soil were determined according to standard procedures of AASHO. The study began with the use of two admixtures, namely, calcium lignosulfonate and hydroxylated carboxylic acid. Initially, the effect of the admixtures on a layered soil-cement base course was to be investigated in the major areas of (a) unconfined compressive strength, (b) durability, and (c) production of bond at the interface of two layers.

Preliminary tests on the first five soil samples were performed to establish test schedules in the areas mentioned. According to these schedules (both admixtures were used), it was found that the results produced did not vary to any major extent between the two admixtures. Therefore, it was decided to use only calcium lignosulfonate for the remainder of the study.

Cement contents were determined in the manner suggested by the Portland Cement Association for the usual range in cement requirements for subsurface soils of the various AASHO soil groups. The cement was mixed thoroughly with the dry soil, and the admixture was mixed thoroughly with the water. The water and admixture were then poured on the soil-cement and mixed until the mixture became uniformly moistened. The soil-cement mixture was then placed in the Proctor mold and immediately compacted in three layers of approximately equal thickness.

Compressive strength test specimens were molded at optimum moisture content to a maximum density as determined by the standard Proctor test. After compaction, specimens were placed in the 100 percent humidity chamber for scheduled periods of curing before testing.

Upon reaching its designated curing time, the specimen was removed from the moisture chamber and submerged in water and allowed to soak for 4 hours prior to testing. The test specimen was removed from the water and tested to failure in compression.

The initial program, using soils D-1, D-2, and D-3, consisted of molding five sets of 21 specimens each for 1, 2, 7, 14, and 28-day periods. Each set was accompanied by three pilot specimens (no admixture), nine specimens with hydroxylated carboxylic acid, and nine specimens with calcium lignosulfonate. Each soil specimen contained the same amount of portland cement. The amounts of admixture used were 0.50, 1.00, and 1.50 lb of admixture per bag of cement. Three cylinders were molded for each amount of admixture.

After reviewing the results of soils D-1, D-2, and D-3, the amounts of admixture used with soils D-4 and D-5 were changed to 0.25, 0.50, and 1.00 lb of admixture per bag of portland cement, and specimens were molded for 7, 14, and 28-day periods.

The testing of these specimens yielded results indicating that both admixtures reacted similarly; therefore, only one of them, calcium lignosulfonate, was used for the remainder of the study. It was also observed that a smaller quantity of admixture gave the most favorable results; thus it was decided to use 0.25 and 0.50 lb of admixture per bag of portland cement. Changes were also made whereby four sets of specimens were molded for 1, 7, 14, and 28-day periods, since no appreciable difference in the characteristics of the specimens were noted after the 1- and 2-day curing periods.

For soils D-6 through D-26 a group of specimens was molded, and each was tested at 1, 7, 14, and 28-day periods. Each group consisted of nine specimens: three pilot samples (no admixture), three with 0.25 lb of calcium lignosulfonate per bag of portland cement, and three with 0.50 lb of calcium lignosulfonate per bag of portland cement. The cement content used was held constant for each soil.

Wet-Dry Test

Wet-dry test specimens were prepared in an identical manner as those for the unconfined compression test. All wet-dry test specimens were cured for 7 days in the 100 percent humidity chamber. At the end of 7 days, specimens were removed from the humidity chamber and submerged in tap water at room temperature. They were

allowed to soak for 5 hours and then removed. The specimens were placed in a drying oven at 71 C for 42 hours, after which the standard brush test was run.

The soaking, drying, and brushing constituted one cycle (48 hours) of the wet-dry test. This procedure was repeated for 12 cycles.

Wet-dry test specimens were molded in sets of six for soils D-1 through D-5. Each set consisted of two pilot specimens, two specimens with 0.50 lb of hydroxylated carboxylic acid per bag of portland cement and specimens with 0.50 lb of calcium lignosulfonate per bag of portland cement.

For each soil type, D-6 through D-26, a set of specimens was molded containing two pilot specimens, two specimens with 0.25 lb and two specimens with 0.50 lb of calcium lignosulfonate per bag of portland cement.

Soil-Cement Admixture Layer Bond Test (LSU Bond Test)

During the attempt to determine the effect of soil-cement and soil-cement with admixtures when they were compacted in two layers (with some time lapse between the compaction of the first layer and the compaction of the second layer), the LSU bond test method was developed. In developing this method, the apparatus used were the standard Proctor compaction mold and the standard Proctor compaction hammer. In addition, a finishing head (Fig. 1) was fabricated with its face machined with a 20-deg angle from horizontal to fit into the compaction mold (Fig. 2).

The bond test specimen was molded in two layers. The mold was filled with enough soil to produce approximately half the height of a compacted specimen. The finishing head was placed in the compaction mold and the bottom half of the specimen was compacted by 60 blows with the compaction hammer. The finished compaction plane had a 20-deg angle with the horizontal and a density figure equivalent to the standard Proctor density (Fig. 3).

A damp cloth was placed on the compaction plane to keep the top moist. Detention periods (elapsed time between molding of the first layer and molding of the second layer) of 0, 4, 7, and 16 hours were observed before the top layer of the specimen was molded. The damp cloth was removed and the compaction plane was scratched prior to compaction of the top layer. The top layer was then compacted by 35 blows with the compaction hammer. The specimen was removed from the mold and cured for 7 days in the moisture chamber. Then it was tested in compression to determine if failure occurred along the compaction plane because of lack of bond or through a shear plane (Fig. 4).

The number of blows applied to each layer of the bond test specimen was obtained by trial and error in order to determine the number of blows that would produce maximum density in both layers. It was found that nearly double the number of blows applied

Figure 1. Finishing head used in molding bottom layer of bond test specimen.

Figure 2. Finishing head fabricated to fit inside the compaction mold.

Figure 3. Bottom layer of a bond test specimen.

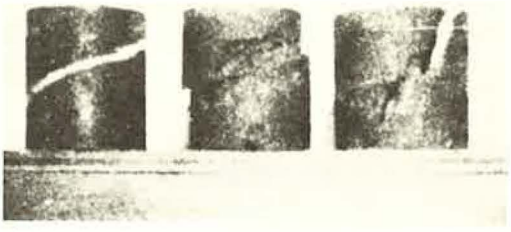

Figure 4. The chalk mark on the untested specimen on the left depicts the 20-deg angle of the compacted plane. The middle specimen failed in bond, which is synonymous to slippage along the 20-deg compaction plane. The specimen on the right is typical of a shear failure, for which the angle of failure can be seen to be about 60 deg.

to the top layer was required on the bottom layer. This was attributed to the fact that part of the effort applied was being absorbed by the mass of the finishing head.

For the bond test a group of specimens was molded for each soil containing two different cement-admixture ratios: two specimens with 0.25 and two specimens with 0.50 lb of calcium lignosulfonate per bag of portland cement. Four sets of bond test specimens were molded for each soil: one set for each of 0, 4, 7, and 16-hour detention time.

RESULTS

There are a limited number of works available on the effects of admixtures on soil-cement mixtures; however, in order to benefit from the research of others, a comprehensive study of the literature in this and other related areas was made, the highlights of which have been discussed.

Earlier studies performed have indicated that certain improvements occur in the physical properties of soil-cement mixes when hydroxylated carboxylic acid or calcium lignosulfonate are used. The published reports contain test results of a few specimens; however, considering the number of probabilities of statistically nonconforming results, it is difficult to draw a valid conclusion from these reports. It should be noted that early researchers in this field made substantial contributions by introducing the idea of admixtures for improving the physical characteristics of soil-cement mixtures and by establishing guidelines for further research.

Frequent mention of the necessity for bond has been made in the literature concerning studies of stress distribution within the layers of a flexible pavement system; however, no research has been found on the use of admixtures to create bond between soil-cement layers. The analytical work indicates that continuity conditions with perfect contact and perfect bond between subsequent layers are required in determining stress at different levels of a layered system.

At an earlier date, Palmer and Barber used an approach similar to Burmister's in which the numerical results obtained are approximately the same (4). When comparing two systems (based on Burmister's and other solutions) with similar material of equal thickness, it can be concluded that the strength of a layered system composed of unbonded, frictionless, and semi-flexible layers is a function of the tensile strength of the top layer and a constant that is dependent on the bearing capacity of the lower layer; however, the strength of a bonded and semi-flexible system is a function of the cumulative strength of the system as a whole and a constant that is dependent on the bearing capacity of the lower layer. In the frictionless and unbonded layered system, the Westergaard approach to stress distribution is more applicable than the Boussinesq, Burmister, or other similar theories. Applying the Westergaard theory of stress distribution to an 8- or 10-in. layered soil system shows that the tensile stresses developed at the interface may cause failure of the layer immediately above the interface.

Consider the following example. Suppose a layered system is constructed having a base composed of two layers of soil-cement with the following characteristics:

Load	10,000 lb
Modulus of elasticity	E = 300,000 psi
Modulus of subgrade	k = 300 psi
Poisson's ratio	μ = 0.30
Layer thickness	h = 8 in.
Radius of contact area	a = 6 in.
Radius of relative stiffness	L = 14.71 in.

In analyzing the condition when bond does not exist between layers 1 and 2 (Fig. 5a), it is seen that, without bond, continuity does not exist. Since continuity is assumed in the Burmister and Boussinesq solutions, the stress at the interface can best be represented by the Westergaard solution:

$$L = \sqrt[4]{\frac{Eh^3}{12(1-\mu^2)k}} = \sqrt[4]{\frac{(300000)\,(8)^3}{12(1-0.09)\,300}} = 14.71 \text{ in.}$$

$$\sigma_A = \frac{3(1+N)\,P}{2\,\pi h^2}\left(\log_e \frac{L}{a} + 0.6159\right)$$

$$= \frac{3(1+0.3)\,(10000)}{2\pi(8)^2}\left(\log_e \frac{14.71}{6} + 0.6159\right)$$

$$\sigma_A = 147 \text{ psi (stress at point A without bond)}$$

When bond does exist (Fig. 5b), there is continuity and the stress at point A can be determined from Burmister's (5) influence curves:

$$\frac{z}{a} = \frac{8 \text{ in.}}{6 \text{ in.}} = 1.33$$

$$\frac{E_1}{E_2} = 1$$

$$\text{Influence coefficient} = \sigma_{zp} = 0.5$$

$$p = \frac{P}{\pi r^2} = \frac{10000}{\pi(36)} = 88.4 \text{ psi}$$

$$\sigma_A = 0.5\,(88)$$

$$\sigma_A = 44 \text{ psi (stress at point A with bond)}$$

Therefore the stress produced at point A is reduced by 70 percent when bonded.

At point B the stresses are 37 psi for the unbonded condition and 16 psi for the bonded condition. It is concluded that bond is not critical at this section.

At point C, z/a is greater than 3. In both the bonded and unbonded conditions, the stresses are greatly reduced, and they are approaching approximately the same stress (Fig. 6).

The results of this study indicate that where bond does not exist between layers, the normal stresses induce slippage of the top layer before the shear strength of the material is reached. Wherever bond is created by the use of admixtures, the specimen representing a two-layered system under severe conditions fails in internal shear. Since failure in each case occurs on a different inclination, stress analysis is based on the

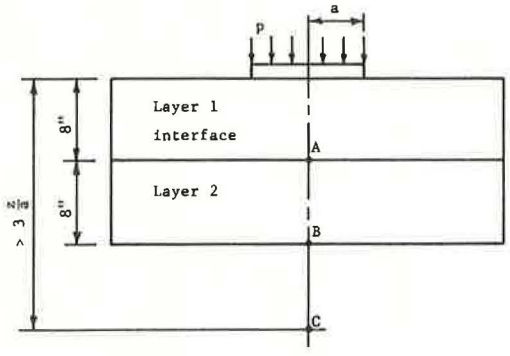

Figure 5a. Unbonded condition.

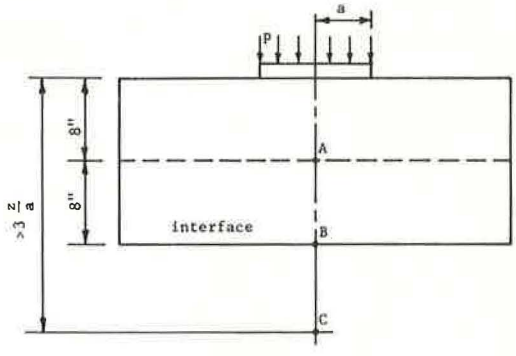

Figure 5b. Bonded condition.

shear strength developed on the plane of failure rather than the compressive strength required to produce failure.

Shear stress and normal stress for each soil are computed using Mohr's circle of stress diagram and are given in Tables 1 and 2. When admixture is added to the soil-cement specimen (excluding silts) a considerable increase in strength is apparent, and failure occurs in shear rather than bond.

In order to correlate the results of the change in the shear strength of mixes using lignosulfonate admixtures with those of the soil-cement mixes without admixtures, a shear factor (S_f) is established (Table 3) defined as the ratio of percent clay to the sum of the percent silt and percent sand. When shear factors are plotted as the abscissa and the change in shear strength as the ordinate (Fig. 7), it is seen that there are two general zones where the test results fall. Zone 1, where lignosulfonate admixtures do not react or the reaction decreases the strength, is called the "silt zone." It should be noted that Louisiana silts are considered highly undesirable for stabilization with cement because of their low strength and low durability characteristics. Zone 2, the "integrated zone," represents all other types of soil tested. Test results plotted in this zone are shown as a smooth curve that indicates a definite trend in the reaction of lignosulfonate. Results indicate increases in the shear strength of the system ranging from 70 to 180 percent. The equation of the curve of best fit for these points is obtained by

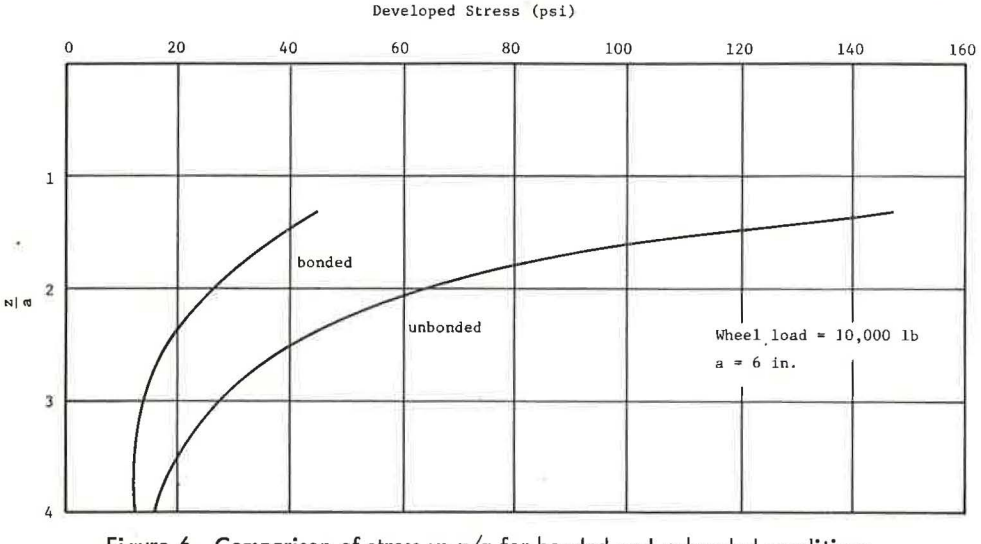

Figure 6. Comparison of stress vs z/a for bonded and unbonded conditions.

TABLE 1

SHEAR STRENGTH

Soil No.	Type Soil	Shear Strength				Percent Increase
		Without Admixture		With Admixture		
		psi	Failure	psi	Failure	
		(a) Integrated Zone				
D-3	Silty loam	35	Bond	96	Shear	+174
D-4*	Sandy clay loam	55	Bond	105	Shear	+ 91
D-6	Silty loam	163	Shear	149	Shear	- 9
D-7	Silty loam	75	Bond	180	Shear	+140
D-8	Silty loam	85	Bond	206	Shear	+142
D-11	Silty loam	40	Bond	100	Shear	+150
D-12	Silty loam	65	Bond	115	Shear	+ 77
D-14	Silty clay	45	Bond	76	Shear	+ 69
D-15	Silty clay	50	Bond	90	Shear	+ 80
D-17	Silty clay loam	77	Bond	144	Shear	+ 87
D-19	Sandy clay loam	122	Bond	259	Shear	+112
D-23	Sandy loam	No results after 4 hours detection				
D-24	Silty clay loam	102	Bond	180	Shear	+ 76
		(b) Silt Zone				
D-5	Silt	70	Shear	70	Shear	0
D-10	Silt	40	Bond	42	Bond	+ 5
D-13	Silt	159	Shear	130	Shear	- 18
D-16	Silt	96	Shear	99	Shear	+ 3
D-18	Silt	65	Bond	61	Bond	- 8
D-20	Silt	100	Shear	100	Shear	0
D-21	Silt	120	Shear	111	Shear	- 8
D-22	Silt	96	Bond	96	Bond	0
D-25	Silt	128	Shear	131	Shear	+ 2
D-26	Silt	123	Shear	122	Shear	0

*All cylinders were molded with 7 hours detention between layers and tested after 7 days cure except D-4, which was molded with 16 hours detention.

TABLE 2

NORMAL STRENGTH

Soil	Type Soil	Normal Strength				Percent Increase
		Without Admixture		With Admixture		
		psi	Failure	psi	Failure	
		(a) Integrated Zone				
D-3	Silty loam	98	Bond	192	Shear	+96
D-4*	Sandy clay loam	178	Bond	210	Shear	+18
D-6	Silty loam	325	Shear	298	Shear	- 8
D-7	Silty loam	231	Bond	348	Shear	+51
D-8	Silty loam	253	Bond	411	Shear	+62
D-11	Silty loam	126	Bond	190	Shear	+51
D-12	Silty loam	198	Bond	228	Shear	+15
D-14	Silty clay	123	Bond	153	Shear	+24
D-15	Silty clay	143	Bond	179	Shear	+25
D-17	Silty clay loam	248	Bond	287	Shear	+16
D-19	Sandy clay loam	378	Bond	517	Shear	+37
D-23	Sandy loam	No results after 4 hours detention				
D-24	Silty clay loam	337	Bond	410	Shear	+22
		(b) Silt Zone				
D-5	Silt	140	Shear	138	Shear	0
D-10	Silt	122	Bond	130	Bond	+ 7
D-13	Silt	318	Shear	260	Shear	-18
D-16	Silt	191	Shear	198	Shear	+ 4
D-18	Silt	214	Bond	190	Bond	-11
D-20	Silt	200	Shear	202	Shear	0
D-21	Silt	240	Shear	221	Shear	- 8
D-22	Silt	218	Bond	219	Bond	0
D-25	Silt	256	Shear	261	Shear	+ 2
D-26	Silt	245	Shear	243	Shear	0

*All cylinders were molded with 7 hours detention between layers and tested after 7 days cure except D-4, which was molded with 16 hours detention.

TABLE 3

SHEAR FACTORS

Soil No.	Percent Silt	Percent Sand	Percent Clay	Soil	Shear Factor, $S_f = \frac{\% \text{ Clay}}{\% \text{ Sand} + \% \text{ Silt}}$
D-1	57	40	7	Loam	0.070
D-2	83	2	15	Silt	0.176
D-3	80	4	16	Silty loam	0.179
D-4	23	58	19	Sandy clay loam	0.235
D-5	84	5	11	Silt	0.124
D-6	70	12	18	Silty loam	0.220
D-7	68	16	16	Silty loam	0.190
D-8	77	6	17	Silty loam	0.205
D-10	83	0	17	Silt	0.205
D-11	64	20	16	Silty loam	0.190
D-12	75	8	17	Silty loam	0.205
D-13	80	1	19	Silt	0.235
D-14	60	9	31	Silty clay	0.449
D-15	55	12	33	Silty clay	0.493
D-16	86	0	14	Silt	0.163
D-17	61	19	20	Silty clay loam	0.250
D-18	80	4	16	Silt	0.190
D-19	12	68	20	Sandy clay loam	0.250
D-20	80	1	19	Silt	0.235
D-21	81	1	18	Silt	0.220
D-22	82	2	16	Silt	0.191
D-23	21	62	12	Sandy loam	0.014
D-24	50	28	22	Silty clay loam	0.282
D-25	85	0	15	Silt	0.176
D-26	86	0	14	Silt	0.163

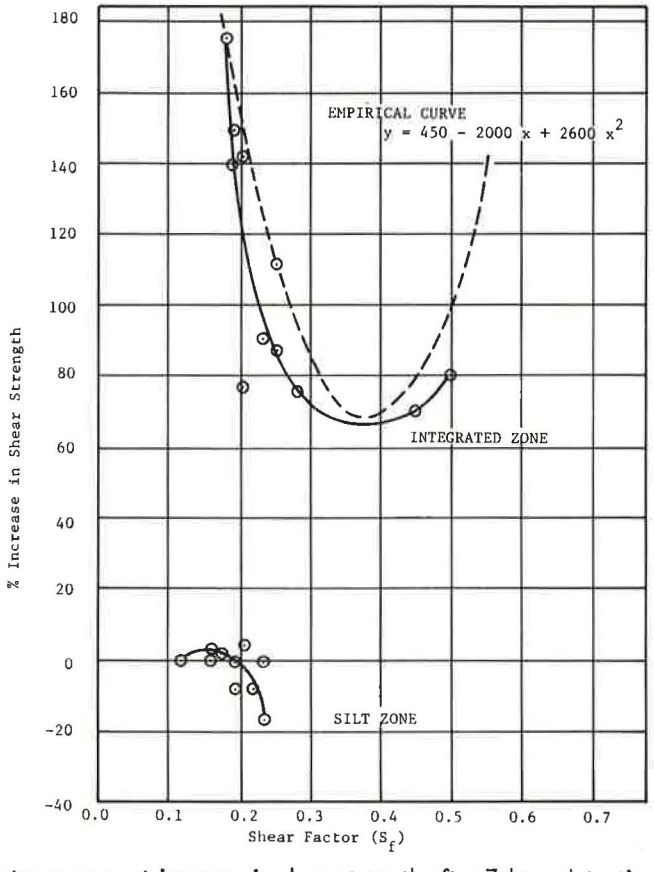

Figure 7. Shear factor vs percent increase in shear strength after 7-hour detention, 0.25 lb admixture per bag of cement.

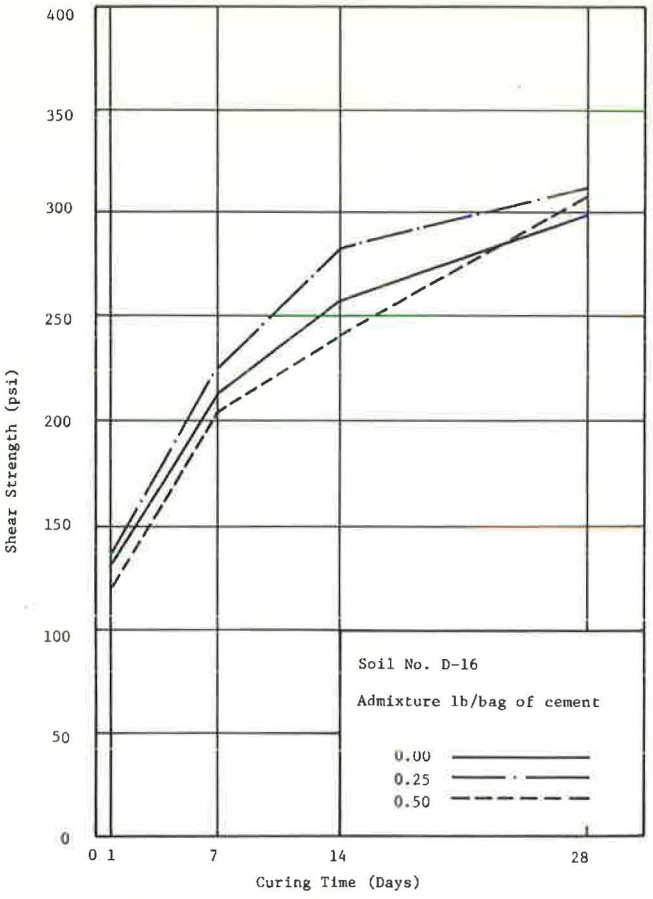

Figure 8. Shear strength vs curing time for Soil No. D-16.

TABLE 4

DURABILITY

Soil No.	Without Admixture	With Admixture			
		0.25 lb/bag		0.50 lb/bag	
	Percent Loss	Percent Loss	Percent Effective*	Percent Loss	Percent Effective*
D-1	13.9	12.9	+ 7	15.9	-14
D-2	5.7	5.5	+ 4	6.0	- 5
D-3	6.4	7.6	-19	6.7	- 5
D-4	11.0	10.6	+ 4	11.0	0
D-5	5.1	5.4	- 6	5.1	0
D-6	7.5	5.1	+32	7.0	+ 7
D-7	6.1	4.5	+26	4.7	+23
D-8	4.4	3.1	+30	3.2	+27
D-10	4.1	2.2	+46	2.9	+29
D-11	5.1	5.6	-10	4.3	+16
D-12	5.3	4.8	+ 9	4.3	+19
D-13	7.5	5.8	+29	5.1	+32
D-14	11.9	7.8	+34	7.2	+39
D-15	8.4	10.6	-26	7.9	+ 6
D-16	5.6	4.7	+16	4.8	+14
D-17	6.3	5.7	+10	4.7	+25
D-18	5.8	3.6	+38	6.0	- 3
D-19	5.7	6.0	- 5	5.1	+11
D-20	5.0	6.3	-26	4.9	+ 2
D-21	5.5	5.0	+10	5.8	- 5
D-22	4.8	4.8	0	4.0	+16
D-23	6.6	5.4	+18	5.3	+19
D-24	7.9	7.7	+ 2	10.0	-26
D-25	5.7	4.8	+15	4.4	+22
D-26	5.9	5.6	+ 5	8.2	+38

*Percent Effective = $\frac{\text{\% Loss Without Admixture - \% Loss With Admixture}}{\text{\% Loss With Admixture}}$

using the curve-fitting method of least squares and is shown in Figure 7. These curves graphically demonstrate the benefits of lignosulfonate admixtures when a routine gradation test is run and the values for shear factor are entered in this graph. The results are reproducible, and they can be correlated with the shear factor.

Curves were plotted for all soils with shear strength in psi as the ordinate and curing time in days as the abscissa. Of 30 curves studied, 22 showed increase in shear strength after the 28-day curing period; 16 showed a greater than 10 percent increase in shear strength above that of the pilot samples. Dispersion of the cement within the first 2 to 7 days (Fig. 8) was instrumental in retarding the hydration process of the soil-cement mixture, thus preventing it from gaining full strength. This effect should not be considered detrimental unless calcium lignosulfonate and soil-cement mixtures remain below the design stresses during this period of curing. The results indicated that the strength of the material, in any case, did not drop below 250 psi, which is well within design stress requirements for a soil-cement base. Furthermore, by the time the base is completed and covered with a protective wearing surface and opened to traffic, the base will have developed strength well above its allowable strength. In Table 4 the results of the durability tests are summarized. The durability of the specimens indicates an improvement in most cases; however, they could not be correlated with the shear strength results. Based on the conclusions drawn from pertinent literature and on the results shown in Table 4, it is the authors' opinion that the durability of those mixtures containing an admixture will increase with time.

CONCLUSIONS

From the preceding analysis it is concluded that:

1. When the thickness of the overlaying layer of a two-layered soil-cement base system is less than $2\frac{1}{2}$ times the radius of contact area, bond between the subsequent layers of soil-cement is necessary to prevent tensile failure at the interface in the top layer.
2. Bond is also necessary at the interface of multiple-layered soil-cement pavement structures to overcome slipping tendencies of the top layer induced by the tangential components of the normal stresses at intensities below the internal shear strength of the material.
3. Calcium lignosulfonate and hydroxylated carboxylic acid are effective in creating bond between subsequent layers of soil-cement.
4. The use of the admixtures in the underlying layer of a two-layered soil-cement system is recommended at a concentration of 0.25 lb per bag of portland cement. The time lapse between mixing of the first layer and placing of the second layer is not to exceed 7 hours.
5. The admixture is to be premixed with the water prior to mixing with the soil-cement mixture.
6. No reduction should be made in optimum water content when the admixture is used.
7. Although silts tested in this study did not show any improvements, it is quite possible that silts with electrochemical and shape characteristics different from those existing in Louisiana may show an improvement. This should be investigated.
8. The terminal shear strength of the individual layers of soils favorably reacting with admixtures, besides that of the layered system, is improved by the introduction of the admixtures in the amount specified.
9. Admixtures used in this study generally improved the durability of the stabilized material.
10. The shear factor values obtained by the authors should be duplicated for different geographical locations and an attempt to correlate them to the percent increase in the shear strength should be made before these results are used.

REFERENCES

1. Casagrande, A. Discussion of: Burmister, D. M. The Theory of Stresses and Displacements in Layered Systems and Applications to the Design of Airport Runways. HRB Proc., Vol. 23, p. 147, 1943.

2. Sowers, G. F., and Vesic, A. B. Vertical Stresses in Subgrades Beneath Statically Loaded Flexible Pavements. HRB Bull. 342, p. 122, 1962.
3. Souers, W. A. Report on Soil-Portland Cement Stabilization Practices. HRB Bull. 292, p. 145-212, 1961.
4. Palmer, L. A., and Barber, E. S. Soil Displacement Under a Circular Loaded Area. HRB Proc., Vol. 20, p. 279-286, 1940.
5. Burmister, D. M. The Theory of Stresses and Displacements in Layered Systems and Applications to the Design of Airport Runways. HRB Proc., Vol. 23, p. 126-148, 1943.